Dr. HANS D. OSTHOFF
Associate Professor, Department of Chemistry
University of Calgary, Faculty of Science
2500 University Drive NW, Calgary, AB, Canada T2N 1N4, Canada
phone: 403-220-8689; e-mail: hosthoff@ucalgary.ca
http://homepages.ucalgary.ca/~hosthoff/

September 17, 2018

Re: manuscript ACP-2017-1026

Dear Dr. Russell:

Enclosed, please find a revised manuscript, titled "Principal component analysis of summertime ground site measurements in the Athabasca oil sands with a focus on analytically unresolved intermediate volatility organic compounds" for your consideration.

In our detailed rebuttal, we have outlined additional changes made to the manuscript.

Summarizing the main points: We have developed and described a new way to measure something indicative of the illusive total IVOC, which many, including Liggio et al. (2016), have shown to be important. Previous studies have only poorly captured the gas phase constituents contributing to SOA formation in this volatility bin. We sustained our new measurement for several weeks, creating a unique time series close to the sources, enabling a first look at where the IVOCs may originate. We have capitalized on a large suite of advanced concurrent measurements to help narrow down where IVOCs are coming from, using PCA and polar plots. We have tentatively identified some of its likely sources through PCA. This information is important for understanding this large contributor to PM mass associated with the oil sands mining operation found by Liggio et al. (2016), in terms of helping to determine the extent to which IVOCs emissions could be controlled to reduce oil sands impacts.

We hope that you will find the revised manuscript acceptable for publication and of interest to your readership.

Sincerely,

Dr. Hans D. Osthoff

We thank both reviewers and editor for their time and effort reviewing this manuscript. All reviewer comments are reproduced below in ***bold, italicized font***. Our responses are shown in regular font. Changes to the text are indicated as underlined text for insertions or are ~~crossed-out~~ for deletions. Line numbers given below are for the revised version with all markups shown. We numbered the reviewer comments for easier cross-referencing.

Co-Editor (Lynn M. Russell) received and published July 27, 2018
I agree with Reviewer 1 and the new Reviewer that more revisions to the manuscript are needed to fully address the previous comments.

In the text below, we have responded to each of the concerns carefully and have made changes to the manuscript, where we believe they are warranted.

Anonymous Referee #1 received and published June 25, 2018:
The authors have addressed most of my comments on the previous version. However, I still have major concern on the identification of IVOC source in the revised manuscript though I noted that it was impossible for them to resolve the IVOCs on the chromatographic column for the measurement campaign.

On one hand, in their response to me (Points 1d and 6), they claimed that "Table 5 suggests that the IVOCs in this study originated mainly from a standalone component (#5), were not associated with a biogenic source (#3) and only very weakly with vehicular sources (#2)", and "It is possible that the IVOCs included species formed by secondary processes.
However, given the close proximity to sources (and a bias of the measurement towards non-oxygenated hydrocarbons), it is reasonable to assume that most of what was observed in this study was primary".
In their response to reviewer #2 (point 2), the replied that "bitumen contains very little oxygen (Yoon et al., 2009) and the extent of oxidative processing was assumed to be negligible".
In their response to reviewer #3 (point 2), they responded that "there could have been other IVOC sources, which we don't believe to be significant at this site, however".
Based on their responses to all reviewers, the authors are quite confident that bitumen vapors dominate the IVOCs in this study though none of IVOC species was identified in this study.

On the other hand, the authors admitted in the response to reviewer #2 (point 2) that "oxygenated compounds will likely not elute from the analytical column. They are, therefore, not included in the IVOC signature detected".
In other word, the GC-ITMS technique cannot provide complete elution of oxygenated IVOCs from the GC column or bitumen indeed does not contain oxygenated compounds.

However, In Table 5, though IVOCs originated from a standalone component (#5) with factor loading of 0.74, the LO-OOA also had strong correlation with component #5 (0.72) while HOA had poor correlation with component #5, indicating that IVOCs were more related oxygenated organic aerosols (OOA) rather than hydrogen-like OA (HOA).
As such, it is not convincing that the IVOCs identified in this study were definitely caused by bitumen vapors.

The reviewer is correct that we believe that the analytically unresolved IVOC feature is due to bitumen vapors. At the same time, one cannot be 100% certain in a receptor-based analysis but can only present the evidence and draw a conclusion, with caveats noted. Our opinion is based on the similar response of the lab head space analysis to what was observed in ambient air (e.g., Figure 2 and Figure S-1) and that no other source that produces such a response is known to us, nor is a credible alternate source suggested by the reviewer. We have also never observed an unresolved IVOC feature at locations other than the AB oil sands region, where bitumen is mined. At the same time, an unresolved hydrocarbon signal as we observed in this work will have multiple contributing sources. This does not, preclude, however, that one source dominates. We believe this to be bitumen vapors, as stated above.

In contrast, the reviewer's suggestion that the IVOC signature is not caused by bitumen vapors is less likely. The reviewer suggests that the association of IVOCs with the organic aerosol fractions LO-OOA and HOA is somehow in contradiction to bitumen vapors being the dominant source of IVOCs. We do not agree, as such correlations could arise from a fraction of IVOCs partitioning to the aerosol phase, perhaps assisted by oxidation. Furthermore, there are many heavy haulers emitting HOA driving all over the ground covered in bitumen that is dug up and carrying fresh bitumen. It would hence be surprising to not see a correlation between bitumen vapors and HOA. The fact that we do not see oxidation products in the GC-MS is irrelevant in this context.

However, we recognize that our line of reasoning is circumstantial and have made the following change to the text on lines 518-522:

"One possible explanation for t~~T~~he association of IVOCs with tailings ponds vapor ~~can be explained by~~ is the presence of bitumen in the ponds that was not separated from the sand during the separation stage (Holowenko et al., 2000). This semi-processed bitumen would be expected to emit similar IVOC vapors to those that were observed in the lab (Fig. 2)."

Since the focus of this manuscript was about IVOC sources, it is important to make robust and reliable identification of IVOC sources. So far, it is still not certain.

The identification of IVOC sources was indeed the goal of this work. Hence, as we stated on lines 93-95, "PCA was chosen ... as an exploratory tool for identification of components without a priori constraints." We agree with the reviewer that we fell somewhat short of this goal since there remains considerable uncertainty regarding the exact identification of sources, though we identified several classes of sources (i.e., components of the PCA analysis that are associated with IVOCs). The manuscript reflects this, as we qualified identifications as "hypothesized" (lines 366 and 390) and sources as "potential" (line 100) but we strengthened this point by adding "tentative" to assignments, e.g., on line 450: " ~~The~~ Tentative assignments of these components to source types in the oil sands are given in Table 6 and are discussed below. " and on line 754: "Three components correlated with the IVOC signature and were tentatively assigned to ...".

Having said this, the PCA presented in this paper clearly shows that the IVOCs are associated with emissions from anthropogenic activities, i.e., oil sands mining and upgrading operations. In the conclusion section on line 768 we state that further studies will be needed to pinpoint the exact sources:

"Direct measurements of emissions throughout the processing of raw bitumen are needed to pinpoint source contributions more accurately and aid in the development of potential mitigation strategies. "

In response to the reviewer's concern we have altered the title of the paper, de-emphasizing the source identification:

"Principal component analysis of summertime ground site measurements in the Athabasca oil sands~~: Sources of~~with a focus on analytically unresolved intermediate volatility organic compounds~~IVOCs~~"

In addition, we have replaced "Sources" with "Components" in the titles of subsection 4.1 (line 469) and 4.2 (line 632) and on line 663 and changed the title of section 3.3 (line 417) from "~~Spatial distribution of IVOC sources~~" to "Bivariate polar plots".

Question on the response 2a about PAC results: could the authors share the raw data for PCA analysis? We often encounter the problems of "collocated factors" when using PCA/APCS though we have many years experience using this tool.

We have added the raw data as a supplemental file as requested.

We are not sure what "problems of collocated factors" are that the reviewer is referring to, since this is not standard terminology in the PCA literature. Perhaps the reviewer is referring to the general issue with a receptor analysis that different sources/mixtures in the same direction relative to the observing site are usually observed together and are hence challenging to separate. This is acknowledged on lines 772-773:

"Further, the receptor nature of PCA did not always discern between large source areas that may have many individual point sources coming together at the point of observation."

Clarification:

My questions in the previous version from #13a to #17 in your response were related to the "Supplementary" file (not the "manuscript"). Hence, your replies are not relevant.

We apologize for the earlier misunderstanding. We believe that our responses were relevant, with exception of question 13a (which we misunderstood) and question 14 (which referred to an empty line). We have restated the reviewer's questions and our responses below, making further clarifications as needed.

13a. Lines 54-55. Again, what are the selection criteria for these specific VOCs?

~~We are not sure what specific lines the reviewer is referring to.~~ Lines 55-57 in the supplemental states that the GC-ITMS quantified " o-xylene, decane, undecane, 1,2,3- and 1,2,4-trimethylbenzene (TMB), and several monoterpenes (i.e., α-pinene, ß-pinene and limonene)." As stated in our response to minor question #3, "we included all quantified non-methane hydrocarbons in the analysis".

In response to the reviewer's question, we added the following to line 57 of the supplemental: "The GC-ITMS primary responsibility was the quantification of monoterpenes. The remaining VOCs quantified were chosen because (a) they sufficiently resolved on the analytical column, and (b) response factors could be determined, either because the compounds of interest were part of the VOC standard used in the field (such as the aromatics o-xylene, 1,2,3- and 1,2,4-TMB, see below) or relative response factors were determined post-campaign."

13b. Can GC-ITMS measure more VOCs such as C2-C10 HCs and so on for better source identification?

In principle, yes. However, the GC-ITMS was on site to quantify monoterpenes and set up for measurements of C9 and higher hydrocarbons. Hydrocarbons up to an approximate volatility of toluene did not resolve on our column. It may be possible with column cooling, a different column and longer adsorption times that we might be able to see compounds as low as C2. However, this would be at the expense of C9 and higher time resolution and at the time of measurement was not feasible.

No changes were made to the manuscript in response to the reviewer's comment.

14. Line 330. No solid evidence for this.

It is still not clear what the reviewer is referring to here. In the version uploaded Jan 19 and published Jan 25, 2018, line 330 of the supplemental is an empty line. The preceding section deals with NH_3, the following section with CO.

We added a reference to the sentence on lines 326-329 "The lack of association of ammonia with other variables in this component and the bivariate polar plots (Figure S-9) are consistent with an NH_3-specific source profile, such as fugitive emissions from one or more point sources that emit independently from other activities (i.e., ammonia storage tanks) and natural emissions from soil and trees (Whaley et al., 2018)."

Line 331 was changed as follows in response to an earlier reviewer comment:
"Component 9: ~~Background CO from VOC oxidation~~ Incomplete hydrocarbon oxidation"

15. Figs S2-S4, S7-S11 caption: Table 4 should be Table 5 in the text?

Thank you for noticing this. All captions have been corrected.

16. Figure S5 caption: Table 4 should be other Table in the text?

We believe the reviewer is referring to Table 7 in the main text. The following correction has been made: "Bivariate polar plots associated with component 4 for the optimum secondary~~primary~~ pollutant solution (Table 74)"

17. Figure S6 caption: Table 4 should be Table 5 in the text?

We believe the reviewer is referring to Table 7 in the main text. The following correction has been made: "Bivariate polar plots associated with component 5 for the optimum secondary~~primary~~ pollutant solution (Table 74)"

Anonymous Referee #4 received and published July 27, 2018:
I have been asked to review this manuscript at this late stage as I understand that two of the initial reviewers were not available to review the revisions.

We greatly appreciate referee #4's efforts, thank you.

I find the authors have done a good job of responding to many specific comments, but that a number of issues were not addressed. While I also have some new suggestions/comments, I think the most important thing for the authors to do is more fully address the first round of comments, especially the more general comments of Reviewer 3 for which no changes were made in the manuscript (some of which I repeat and rephrase below).

1. Given the limitations on source sampling:

a. Is the subtitle "Sources of IVOCs" really appropriate? I suggest that if the main source is not really verifiable, it's not appropriate.

We thank the reviewer for this constructive comment and have changed the title to the following:

"Principal component analysis of summertime ground site measurements in the Athabasca oil sands~~:~~ ~~Sources of~~with a focus on analytically unresolved intermediate volatility organic compounds~~IVOCs~~"

b. Are there GCMS profiles of similar operations available in the literature that could be compared to, providing also a more substantial review of the relevant literature, and comparison of the results of this work to that? This is not that onerous and seems a minimum that the authors can do to provide appropriate context.

This is an excellent suggestion. We found a handful of relevant papers (Stout and Wang, 2016; Payzant et al., 1980; Yang et al., 2011; Boczkaj et al., 2014; Stout and Wang, 2017) . One of them, Boczkaj et al.

(2014) state that a "literature search revealed that the information on volatile chemical compounds present in bitumen fumes is scarce."

The literature papers all extracted bitumen heavy crude oil and injected their extracts (usually after a clean-up step) via syringe. We did not find anything in the literature regarding direct air injection of bitumen (the method used in our work). Thus, the literature results are not directly comparable to our work since, for example, some components may be extracted into a solution but may not be volatile enough to be detected in a headspace analysis.

Having said this, Yang et al. (2011) report that "a large chromatographic hump of unresolved complex mixtures (UCMs) eluting between n-C10 to n-C40 is pronounced in all oil sands extracts and bitumen samples." in their analysis of AB oil sands samples, which is qualitatively similar to what we report. We have added the following to the main text on lines 147-149:

"The observed unresolved hydrocarbon feature is qualitatively similar to the "large chromatographic hump of unresolved complex mixtures" reported by Yang et al. (2011) during their analysis of bitumen extracts."

2. Correlations:

a. I suggest using the scale and nomenclature of a standard stat reference rather than making one up.

We're not certain which reference text to consider a standard, and there is no consensus in the literature as to what scale to use (and nomenclature varies somewhat between authors). For example, Henry and Hidy (1979) defined values of near zero -0.2 to +0.2 as "almost no correlation or dependence", < -0.9 and >+0.9 as "strong correlation", and intermediates values (0.2 to 0.9, or -0.2 to -0.9) as a "proportionally less strong correlation". Guo et al. (2004) chose to present only loadings with r > 0.3 in their PCA, whereas Harrison et al. (1996) present only loadings r > 0.23.

In response to this comment, since we found the lowest correlation in the literature that was interpreted being ±0.2, we have altered our criteria on line 365 as follows:

"Associations with r>0.7, r>0.3, and r>0.2~~r>0.1~~ are referred to as "strong", "weak", and "poor", respectively." and have updated the descriptions for the few instances where 0.2>r>0.1 from "poor correlation" to "no correlation" throughout the manuscript (lines 373, 376, 575, 583, 588, 603, 666, 668, 670, and 684) and in the supplement, noting that this change did not affect any of the conclusions. For the remaining associations, we note that the r value does give a quantitative measure of the degree of correlation, which supersedes the labels "strong", "weak", and "poor" anyhow.

b. Have the authors investigated the degree of autocorrelation in the measurements?

We had not investigated autocorrelation and thank the reviewer for bringing this issue to our attention. In any PCA, it is assumed that the data are independent and not autocorrelated. Autocorrelation, i.e., successive observations are serially correlated, can adversely affect a PCA if present (Vanhatalo and Kulahci, 2016). In a recent paper on this subject, Vanhatalo and Kulahci (2016) state that "the impact of

autocorrelation on PCA ... is neither well understood nor properly documented in the literature" and that "there is no clear-cut recommendation on how to deal with autocorrelated data".

We do not believe that autocorrelation significantly affected our analysis. The measurements are independent (see the next question below), are spaced 60 min apart, and the data vary considerable in time (see the time series shown in Figure 3 in the main manuscript). Furthermore, the data were normalized ("standardized") in the PCA to remove relatively constant and large background present for, for example, CO_2, CH_4, and CO.

Since the reviewer has asked, we calculated the autocorrelation functions of the variables after normalization. In all cases, the autocorrelation function drops roughly exponentially from a value of 1 at lag 0 with a time constant of between 1 and 4 (hrs), with the only exceptions being TRS (time constant of <1) and CO (time constant of 5). At longer time constants, the autocorrelations appear random and show little trend. The only exception is SO_2 (and TS), whose autocorrelation function increases to 0.379 with a 7-day period, for reasons unknown though it may suggest a S-related process that is performed weekly at the source facility or facilities.

We found no mention of auto-correlation in any of the PCA papers in the literature and, as non-experts in chemometrics, decided not to comment on the degree of autocorrelation in this paper.

Is each measurement independent? If so, the low r values are more meaningful.

Yes, the measurements (Table 2) are independent, with two exceptions. The 22 variables were quantified by 12 independent instruments. Some instruments reported multiple variables, though quantified these variables independently (e.g., by resolving peaks in a chromatogram, or using different wavelengths to quantify CO, CH_4, and CO_2). The only exceptions are TRS, which is calculated by subtracting TS and SO_2, and (perhaps) the apportionment of organic aerosol by the AMS into HOA and LO-OOA.

3. Is the paper new and interesting? (See general comments from Reviewer 3.)

a. I realize these are not specific comments that can be addressed easily, but I believe the authors can do a better job of more explicitly telling readers what is interesting and new about their work. Is it really the sources? If no, don't emphasize that in title. If yes, support it with any available literature.

We thank the reviewer for this constructive suggestion. There are many interesting aspects of this new and unique data set that we can emphasize more. For instance, there are few independent data sets collected in the Athabasca oil sands region, one of the largest emitters of pollutants in Canada (NPRI, 2013). Further, the measurement suite encompassed the largest variety of collocated analytical instruments close to oil sands mining and upgrading operations to date and included a first, direct observation of airborne IVOCs, that is unique to this area and we have not observed elsewhere where we have made GC-ITMS measurements, i.e., in Calgary and on Vancouver Island (Tokarek et al., 2017). This paper presents this unique data set as a whole, which is analyzed by PCA with Varimax rotation. We show that the integrated IVOC signal is indeed associated with components that include known primary emissions, as suspected by Liggio et al., but not verified with direct IVOC measurements near the sources, as presented in this paper.

There are few source apportionment studies investigating pollution in the Athabasca oil sands (and none that include IVOCs) in the current literature. Existing studies usually had a fairly narrow focus: for example, Cho et al. investigated ground level O_3 and $PM_{2.5}$ (Cho et al., 2012), and VOCs (Bari and Kindzierski, 2018; Bari et al., 2016) and $PM_{2.5}$ (Bari and Kindzierski, 2017; Landis et al., 2017) impacting the nearby communities of Ft. McKay and Ft. McMurray were examined. Other studies included source apportionments of pollutants such as PAHs as they affect sediments (Jautzy et al., 2013) or lichens (Landis et al., 2012). Two recent papers based in part on data collected during JOSM focused on CH_4 (Baray et al., 2018) and metals (Phillips-Smith et al., 2017).

We have modified three paragraphs in the introduction, starting on line 64:

"In August 2013, a comprehensive air quality study as a part of the Joint Oil Sands Monitoring (JOSM) plan (JOSM, 2012), referred to here as the 2013 JOSM intensive study was conducted. This study was performed in northern Alberta at two ground sites in and near Fort McKay in close proximity (as close as 3.5 km) to oil sands mining operations and from a National Research Council of Canada (NRC) Convair 580 research aircraft to characterize oil sands emissions and their downwind physical and chemical transformations (Gordon et al., 2015; Liggio et al., 2016; Li et al., 2017).
One ground site, located at the Wood Buffalo Environmental Association (WBEA) air monitoring station (AMS) 13 (Fig. 1), was equipped with a comprehensive set of instrumentation to measure concentrations of a wide range of trace gases and aerosols (Table 1), yielding a unique and new data set, parts of which are presented in this paper for the first time. As part of this effort, a gas chromatograph equipped with an ion trap mass spectrometer (GC-ITMS) was deployed ..."

Continuing on line 86:

"In this paper, concurrent measurements of air pollutants at the AMS 13 ground site during the 2013 JOSM intensive study are presented. ~~The~~An analytically unresolved hydrocarbon signal was successfully integrated and quantified and is presented as a time series here for the first time. This independent measurement, which represents an important source of SOA (Liggio et al.) is included directly in ~~and used as an input variable in a analyzed using~~ principal component analysis (PCA), along with a large number of other measurements, to ~~elucidate~~ gain new insight into the possible origins of the ~~the~~ IVOCs in the Athabasca oil sands ~~by association~~."

On line 436 at the beginning of the introduction, we added the following:

"This work has added to the relatively few data sets of pollutants in the Athabasca oil sands region, one of the largest emitters of airborne pollutants in Canada (NPRI, 2013), that are available in the open literature. Earlier source apportionment studies in the region investigated ground level O_3 and $PM_{2.5}$ (Cho et al., 2012), examined VOCs (Bari and Kindzierski, 2018; Bari et al., 2016) and $PM_{2.5}$ (Bari and Kindzierski, 2017; Landis et al., 2017) impacting the nearby communities of Fort McKay and Fort McMurray, or investigated pollutants such as PAHs as they affect sediments (Jautzy et al., 2013) or lichens (Landis et al., 2012). The measurement suite in this work encompassed a larger variety of collocated analytical instruments closer to oil sands mining and upgrading operations than these earlier studies and included a first, direct observation of airborne IVOCs, that is unique to this area and we have not observed elsewhere where we have made GC-ITMS measurements, i.e., in Calgary and on Vancouver Island (Tokarek et al., 2017). "

b. For example, additional and specific discussion in response to Reviewer 2 Comment 7 could add some depth to the information presented.

We appreciate the suggestion. In comment 7, reviewer 2 asked for more discussion on the link between IVOCs and SOA production several hours downwind of the oil sands region.

"***7. Liggio et al. (2016) finds that the evaporation and atmospheric oxidation of low-volatility organic vapors from mined oil sands is directly responsible for the majority of observed SOA mass. Does this mean that the contribution of the component 2 to IVOCs shall be small given that this component is likely related to "Mine fleet and vehicle emissions". More discussion is needed."***

Our response was:

> "The transformation of IVOCs to organic aerosol mass is outside the scope of this paper, considering that we were close to sources and oxygenated IVOCs were not quantified. The aircraft study, in contrast, focused on the atmospheric oxidation of IVOC emissions that were entrained aloft, transported several hours downwind, at which time emissions from different sources would have merged into a single plume. At our ground site, the extent of oxidative processing is less, and more components are distinguishable. Our analysis indicates that IVOCs ~~emitted~~ loaded onto~~in~~ component 2 were qualitatively different from those ~~emitted by~~loaded on components 1 and 5, in that they were less associated with the LO-OOA organic aerosol mass loading, but we do not have sufficient information to comment on how IVOCs from these compounds transform and add to aerosol mass downwind. No changes were made to the manuscript in response to this comment."

We would like to add that there is already some discussion of this subject in the paper, e.g., on line 738:

"The analysis indicates that the component with the strongest IVOC source (Component 5) also has the highest association with PM_1 ($r = 0.70$; Table 7). Aircraft measurements combined with a modelling study have required a group of IVOC hydrocarbons to explain the significant SOA formation and growth downwind of the oil sands region (Liggio et al., 2016). The association of IVOCs with PM_1 volume is consistent with the hypothesis that oxidation of IVOCs observed at AMS 13 leads to SOA generation and appears to have a significant impact on the variation in PM_1 mass. "

and on line 762:

"Liggio et al. (2016) showed that these hydrocarbons constitute a group of IVOCs in the saturation vapor concentration (C^*) range 10^5 µg $m^{-3} < C^* < 10^7$ µg m^{-3} that contribute significantly to secondary organic aerosol formation and growth downwind of the oil sands facilities. The correlation of LO-OOA with two of the three IVOC components in the main PCA ~~analysis~~ and with PM_1 in the extended analysis ~~corroborates~~ is consistent with the high SOA formation potential of IVOCs and suggests that further differentiation may be needed and stresses the need for IVOCs to be routinely monitored."

Literature cited

Baray, S., Darlington, A., Gordon, M., Hayden, K. L., Leithead, A., Li, S. M., Liu, P. S. K., Mittermeier, R. L., Moussa, S. G., O'Brien, J., Staebler, R., Wolde, M., Worthy, D., and McLaren, R.: Quantification of methane sources in the Athabasca Oil Sands Region of Alberta by aircraft mass balance, Atmos. Chem. Phys., 18, 7361-7378, 10.5194/acp-18-7361-2018, 2018.

Bari, M. A., Kindzierski, W. B., and Spink, D.: Twelve-year trends in ambient concentrations of volatile organic compounds in a community of the Alberta Oil Sands Region, Canada, Environ. Int., 91, 40-50, 10.1016/j.envint.2016.02.015, 2016.

Bari, M. A., and Kindzierski, W. B.: Ambient fine particulate matter (PM2.5) in Canadian oil sands communities: Levels, sources and potential human health risk, Sci. Tot. Environm., 595, 828-838, 10.1016/j.scitotenv.2017.04.023, 2017.

Bari, M. A., and Kindzierski, W. B.: Ambient volatile organic compounds (VOCs) in communities of the Athabasca oil sands region: Sources and screening health risk assessment, Environ. Pollut., 235, 602-614, 10.1016/j.envpol.2017.12.065, 2018.

Boczkaj, G., Przyjazny, A., and Kamiński, M.: Characteristics of volatile organic compounds emission profiles from hot road bitumens, Chemosphere, 107, 23-30, 10.1016/j.chemosphere.2014.02.070, 2014.

Cho, S., Morris, R., McEachern, P., Shah, T., Johnson, J., and Nopmongcol, U.: Emission sources sensitivity study for ground-level ozone and PM2.5 due to oil sands development using air quality modelling system: Part II – Source apportionment modelling, Atmos. Environm., 55, 542-556, 10.1016/j.atmosenv.2012.02.025, 2012.

Gordon, M., Li, S. M., Staebler, R., Darlington, A., Hayden, K., O'Brien, J., and Wolde, M.: Determining air pollutant emission rates based on mass balance using airborne measurement data over the Alberta oil sands operations, Atmos. Meas. Tech., 8, 3745-3765, 10.5194/amt-8-3745-2015, 2015.

Guo, H., Wang, T., and Louie, P. K. K.: Source apportionment of ambient non-methane hydrocarbons in Hong Kong: Application of a principal component analysis/absolute principal component scores (PCA/APCS) receptor model, Environ. Pollut., 129, 489-498, 10.1016/j.envpol.2003.11.006, 2004.

Harrison, R. M., Smith, D. J. T., and Luhana, L.: Source Apportionment of Atmospheric Polycyclic Aromatic Hydrocarbons Collected from an Urban Location in Birmingham, U.K, Environm. Sci. Technol., 30, 825-832, 10.1021/es950252d, 1996.

Henry, R. C., and Hidy, G. M.: Multivariate analysis of particulate sulfate and other air quality variables by principal components-Part I: Annual data from Los Angeles and New York, Atmos.Environm. (1967), 13, 1581-1596, 10.1016/0004-6981(79)90068-4, 1979.

Jautzy, J., Ahad, J. M. E., Gobeil, C., and Savard, M. M.: Century-Long Source Apportionment of PAHs in Athabasca Oil Sands Region Lakes Using Diagnostic Ratios and Compound-Specific Carbon Isotope Signatures, Environm. Sci. Technol., 47, 6155-6163, 10.1021/es400642e, 2013.

Landis, M. S., Pancras, J. P., Graney, J. R., Stevens, R. K., Percy, K. E., and Krupa, S.: Chapter 18 - Receptor Modeling of Epiphytic Lichens to Elucidate the Sources and Spatial Distribution of Inorganic Air Pollution in the Athabasca Oil Sands Region, in: Developments in Environmental Science, edited by: Percy, K. E., Elsevier, 427-467, 2012.

Landis, M. S., Pancras, J. P., Graney, J. R., White, E. M., Edgerton, E. S., Legge, A., and Percy, K. E.: Source apportionment of ambient fine and coarse particulate matter at the Fort McKay community site, in the Athabasca Oil Sands Region, Alberta, Canada, Sci. Tot. Environm., 584, 105-117, 10.1016/j.scitotenv.2017.01.110, 2017.

Li, S.-M., Leithead, A., Moussa, S. G., Liggio, J., Moran, M. D., Wang, D., Hayden, K., Darlington, A., Gordon, M., Staebler, R., Makar, P. A., Stroud, C. A., McLaren, R., Liu, P. S. K., Oâ€™Brien, J., Mittermeier, R. L., Zhang, J., Marson, G., Cober, S. G., Wolde, M., and Wentzell, J. J. B.: Differences

between measured and reported volatile organic compound emissions from oil sands facilities in Alberta, Canada, Proceedings of the National Academy of Sciences, 114, E3756-E3765, 10.1073/pnas.1617862114, 2017.

Liggio, J., Li, S.-M., Hayden, K., Taha, Y. M., Stroud, C., Darlington, A., Drollette, B. D., Gordon, M., Lee, P., Liu, P., Leithead, A., Moussa, S. G., Wang, D., O'Brien, J., Mittermeier, R. L., Brook, J., Lu, G., Staebler, R., Han, Y., Tokarek, T. W., Osthoff, H. D., Makar, P. A., Zhang, J., Plata, D., and Gentner, D. R.: Oil Sands Operations as a Large Source of Secondary Organic Aerosols, Nature, 534, 91-94, 10.1038/nature17646, 2016.

NPRI: Detailed facility information: http://www.ec.gc.ca/inrp-npri/donnees-data/index.cfm?do=facility_information&lang=En&opt_npri_id=0000002274&opt_report_year=2013, access: April 13, 2017, 2013.

Payzant, J. D., Rubinstein, I., Hogg, A. M., and Strausz, O. P.: Analysis of Cold Lake bitumen hydrocarbons by combined GLC-field ionization mass spectrometry and GLC-electron impact mass spectrometry, Chemical Geology, 29, 73-88, 10.1016/0009-2541(80)90006-6, 1980.

Phillips-Smith, C., Jeong, C. H., Healy, R. M., Dabek-Zlotorzynska, E., Celo, V., Brook, J. R., and Evans, G.: Sources of particulate matter components in the Athabasca oil sands region: investigation through a comparison of trace element measurement methodologies, Atmos. Chem. Phys., 17, 9435-9449, 10.5194/acp-17-9435-2017, 2017.

Stout, S., and Wang, Z.: Oil Spill Environmental Forensics: Fingerprinting and Source Identification, San Diego: Elsevier Science & Technology, San Diego, 10.1016/b978-0-12-369523-9.x5000-9, 2016.

Stout, S., and Wang, Z.: Oil Spill Environmental Forensics Case Studies, Elsevier Science, 2017.

Tokarek, T. W., Brownsey, D. K., Jordan, N., Garner, N. M., Ye, C. Z., Assad, F. V., Peace, A., Schiller, C. L., Mason, R. H., Vingarzan, R., and Osthoff, H. D.: Biogenic emissions and nocturnal ozone depletion events at the Amphitrite Point Observatory on Vancouver Island, Atmosphere-Ocean, 55, 121-132, 10.1080/07055900.2017.1306687, 2017.

Vanhatalo, E., and Kulahci, M.: Impact of Autocorrelation on Principal Components and Their Use in Statistical Process Control, Quality and Reliability Engineering International, 32, 1483-1500, doi:10.1002/qre.1858, 2016.

Whaley, C. H., Makar, P. A., Shephard, M. W., Zhang, L., Zhang, J., Zheng, Q., Akingunola, A., Wentworth, G. R., Murphy, J. G., Kharol, S. K., and Cady-Pereira, K. E.: Contributions of natural and anthropogenic sources to ambient ammonia in the Athabasca Oil Sands and north-western Canada, Atmos. Chem. Phys., 18, 2011-2034, 10.5194/acp-18-2011-2018, 2018.

Yang, C., Wang, Z., Yang, Z., Hollebone, B., Brown, C. E., Landriault, M., and Fieldhouse, B.: Chemical Fingerprints of Alberta Oil Sands and Related Petroleum Products, Environmental Forensics, 12, 173-188, 10.1080/15275922.2011.574312, 2011.

Principal component analysis of summertime ground site measurements in the Athabasca oil sands~~:~~ ~~Sources of~~ with a focus on analytically unresolved intermediate volatility organic compounds ~~IVOCs~~

Travis W. Tokarek[1], Charles A. Odame-Ankrah[1], Jennifer A. Huo[1], Robert McLaren[2], Alex K. Y. Lee[3, 4], Max G. Adam[4], Megan D. Willis[5], Jonathan P. D. Abbatt[5], Cristian Mihele[6], Andrea Darlington[6], Richard L. Mittermeier[6], Kevin Strawbridge[6], Katherine L. Hayden[6], Jason S. Olfert[7], Elijah. G. Schnitzler[8], Duncan K. Brownsey[1], Faisal V. Assad[1], Gregory R. Wentworth[5, a], Alex G. Tevlin[5], Douglas E. J. Worthy[6], Shao-Meng Li[6], John Liggio[6], Jeffrey R. Brook[6], and Hans D. Osthoff[1*]

[1] Department of Chemistry, University of Calgary, Calgary, Alberta, T2N 1N4, Canada

[2] Centre for Atmospheric Chemistry, York University, Toronto, Ontario, M3J 1P3, Canada

[3] Department of Civil and Environmental Engineering, National University of Singapore, Singapore 117576, Singapore

[4] NUS Environmental Research Institute, National University of Singapore, Singapore

[5] Department of Chemistry, University of Toronto, Toronto, Ontario, M5S 3H6, Canada

[6] Air Quality Research Division, Environment and Climate Change Canada, Toronto, Ontario, M3H 5T4, Canada

[7] Department of Mechanical Engineering, University of Alberta, Edmonton, Alberta, T6G 1H9, Canada

[8] Department of Chemistry, University of Alberta, Edmonton, Alberta, T6G 2G2, Canada

[a] Now at: Environmental Monitoring and Science Division, Alberta Environment and Parks, Edmonton, Alberta, T5J 5C6, Canada

* Corresponding author

for Atmos. Chem. Phys.

Abstract

In this paper, measurements of air pollutants made at a ground site near Fort McKay in the Athabasca oil sands region as part of a multi-platform campaign in the summer of 2013 are presented. The observations included measurements of selected volatile organic compounds (VOCs) by a gas chromatograph – ion trap mass spectrometer (GC-ITMS). This instrument observed a large, analytically unresolved hydrocarbon peak (with retention index between 1100 and 1700) associated with intermediate volatility organic compounds (IVOCs). However, the activities or processes that contribute to the release of these IVOCs in the oil sands region remain unclear.

Principal component analysis (PCA) with Varimax rotation was applied to elucidate major source types impacting the sampling site in the summer of 2013. The analysis included 28 variables, including concentrations of total odd nitrogen (NO_y), carbon dioxide (CO_2), methane (CH_4), ammonia (NH_3), carbon monoxide (CO), sulfur dioxide (SO_2), total reduced sulfur compounds (TRS), speciated monoterpenes (including α- and β-pinene and limonene), particle volume calculated from measured size distributions of particles less than 10 μm and 1 μm in diameter (PM_{10-1} and PM_1), particle-surface bound polycyclic aromatic hydrocarbons (pPAH), and aerosol mass spectrometer composition measurements, including refractory black carbon (rBC) and organic aerosol components. The PCA was complemented by bivariate polar plots showing the joint wind speed and direction dependence of air pollutant concentrations to illustrate the spatial distribution of sources in the area. Using the 95% cumulative percentage of variance criterion, ten components were identified and categorized by source type. These included emissions by wet tailings ponds, vegetation, open pit mining operations, upgrader facilities, and surface dust. Three components correlated with IVOCs, with the largest associated with surface mining and is likely caused by the unearthing and processing of raw bitumen.

1. Introduction

The Athabasca oil sands region of Northern Alberta, Canada, has seen extraordinary expansion of its oil sands production and processing facilities (CAPP, 2016) and associated emissions of air pollutants over the last several decades (Englander et al., 2013; Bari and Kindzierski, 2015). Air emissions from these facilities have been impacting surrounding communities, including the city of Fort McMurray and the community of Fort McKay (WBEA, 2013). To assess the impact of these emissions on human health, visibility, climate, and the ecosystems downwind, it is critical to obtain an understanding of the source types from all activities associated with oil sands operations (ECCC, 2016).

Prior to 2013, there had been only a single industry-independent study of trace gas emissions from the Athabasca oil sands mining operations (Simpson et al., 2010; Howell et al., 2014). The data showed elevated concentrations in n-alkanes (30% of the total quantified hydrocarbon emissions), cycloalkanes (49%), and aromatics (15%) in plumes from an oil sands surface mining facility intercepted from a single aircraft flight. These compounds are associated with oil and gas developments including mining, upgrading, and transportation of bitumen (Siddique et al., 2006). Specifically, these activities involve the use of naphtha, a complex mixture of aliphatic and aromatic hydrocarbons in the range of C_3 to C_{14} containing n-alkanes (e.g., n-heptane, n-octane, and n-nonane) and benzene, toluene, ethylbenzene, and xylenes (BTEX).

In August 2013, a comprehensive air quality study as a part of the Joint Oil Sands Monitoring (JOSM) plan (JOSM, 2012), referred to here as the 2013 JOSM intensive study was conducted. This study was performed in northern Alberta at two ground sites in and near Fort McKay in close proximity (as close as 3.5 km) to oil sands mining operations and from a National Research Council of Canada (NRC) Convair 580 research aircraft to characterize oil sands emissions and their downwind physical and chemical transformations (Gordon et al., 2015; Liggio et al., 2016; Li et al., 2017).

One ground site, located at the Wood Buffalo Environmental Association (WBEA) air monitoring station (AMS) 13 (Fig. 1), was equipped with a comprehensive set of instrumentation to measure concentrations of a wide range of trace gases and aerosols (Table 1), yielding a unique and new data set, parts of which are presented in this paper for the first time. As part of this effort, a gas chromatograph equipped with an ion trap mass spectrometer (GC-ITMS) was deployed at AMS 13. When air masses passing over regions with industrial activities were observed (as judged from a combination of local wind direction and tracer measurements), the total ion chromatogram showed an analytically unresolved hydrocarbon signal associated with intermediate volatile organic compounds (IVOCs) with saturation concentration (C^*) in the range 10^5 µg m^{-3}< C^* < 10^7 µg m^{-3} (Liggio et al., 2016).

Emission estimates for analytically unresolved hydrocarbons range from 5×10^6 kg $year^{-1}$ to 14×10^6 kg $year^{-1}$ for the two facilities that reported such emissions (Li et al., 2017). Using aircraft measurements during the 2013 study, Liggio et al. (2016) showed that IVOCs contributed to the majority of the observed secondary organic aerosol (SOA) mass production in a similar fashion as anthropogenic VOCs contributed to SOA production during the Deepwater Horizon oil spill (de Gouw et al., 2011) and rivaling the magnitude of SOA formation observed downwind of megacities (Liggio et al., 2016), though ultimately it has remained unclear which activities are associated with IVOC emissions.

In this paper, concurrent measurements of air pollutants at the AMS 13 ground site during the 2013 JOSM intensive study are presented. The analytically unresolved hydrocarbon signal was integrated and is presented as a time series and ~~analyzed~~ used as an input variable in a ~~using~~ principal component analysis (PCA) to elucidate the origin of ~~the~~ IVOCs in the Athabasca oil sands by association. The analysis presented here is a receptor analysis focusing on the normalized variability of pollutants impacting the AMS 13 ground site and hence does not constitute a comprehensive emission profile analysis of the oil sands facilities as a whole, for which aircraft-based measurements and/or direct plume or stack measurements are more suitable. PCA was chosen over the more popular positive matrix factorization

(PMF) method (Paatero and Tapper, 1994) because it yields a unique solution and is particularly suited as an exploratory tool for identification of components without *a priori* constraints (Jolliffe and Cadima, 2016). The PCA was complemented by bivariate polar plots (Carslaw and Ropkins, 2012; Carslaw and Beevers, 2013) to show the spatial distribution of sources in the region as a function of locally measured wind direction and speed. A second PCA was performed to investigate which components correlate with (and generate) secondary pollutants, i.e., pollutants that are formed by atmospheric processes. Potential sources and processes contributing to each of the components identified by PCA are discussed.

2. Experimental

2.1 Measurement location

Measurements of air pollutants were made at AMS 13 routine air monitoring station (Fig. 1), which is operated by WBEA. The site is located at 111.6423° W longitude and 57.1492° N latitude about 3 km from the southern edge of the community of Fort McKay, 300 m west from a public road, and 1 km west of the Athabasca river. The immediate vicinity of the site consisted of mixed-leaf boreal forest with a variety of tree species, including poplar, aspen, pine and spruce trees (Smreciu et al., 2013). The site was accessible via a gravel road; traffic on this road was restricted during the study period (August - September, 2013).

The site is impacted by emissions from nearby oil sands facilities (Table 1 and Fig. 1), including a large surface mining site operated by Syncrude Canada whose northeastern corner is located 3.5 km to the south of AMS 13 (and which is adjacent to the 5 km long Syncrude – Mildred Lake (SML) tailings pond) and from a large upgrader stack facility operated by Suncor Energy Inc. located to the Southeast. There are additional oil sands facilities operated (during the study period) by Canadian Natural Resources Limited, Imperial Oil, and Shell Canada to the North and Northeast.

Table 1. Oil sands facilities located within 30 km of AMS 13. Distances were estimated using coordinates provided in the National Pollutant Release Inventory (NPRI, 2013) and do not account for the size of each facility whose boundaries may be considerably closer to (or further away from) AMS 13. PACPRM = Petroleum and coal products refining and manufacturing; OGPS = Oil and gas pipelines and storage.

Company	Name	Type	Direction	Distance (km)
Syncrude Canada Ltd.	Mildred Lake Plant Site	PACPRM	S	12.2
Athabasca Minerals Inc.	Susan Lake Gravel Pit	Mining and Quarrying	N	15.5
Syncrude Canada Ltd.	Aurora North Mine Site	PACPRM	NE	18.7
Suncor Energy	Suncor Energy Inc. Oil Sands	PACPRM	SE	19.4
Enbridge Pipelines Inc.	MacKay River Terminal	OGPS	WSW	19.7
Suncor Energy	MacKay River, In-Situ, Oil Sands Plant	PACPRM	WSW	19.9
Enbridge Pipelines Inc.	Athabasca Terminal	OGPS	SE	21.2
Williams Energy	Fort McMurray Hydrocarbon Liquids Extraction Facility	Conventional oil and gas extraction	SE	21.6
Canadian Natural Resources Limited	Horizon Oil Sands Processing Plant and Mine	PACPRM	NNW	21.8
Shell Canada Energy	Muskeg River Mine and Jackpine Mine	PACPRM	NNE	23.7

123 **Figure 1**. Map of oil sands facilities showing locations of surface mines and tailings ponds, downloaded

124 from the Oil Sands Information Portal (Alberta, 2017). The red star indicates the location of AMS 13.

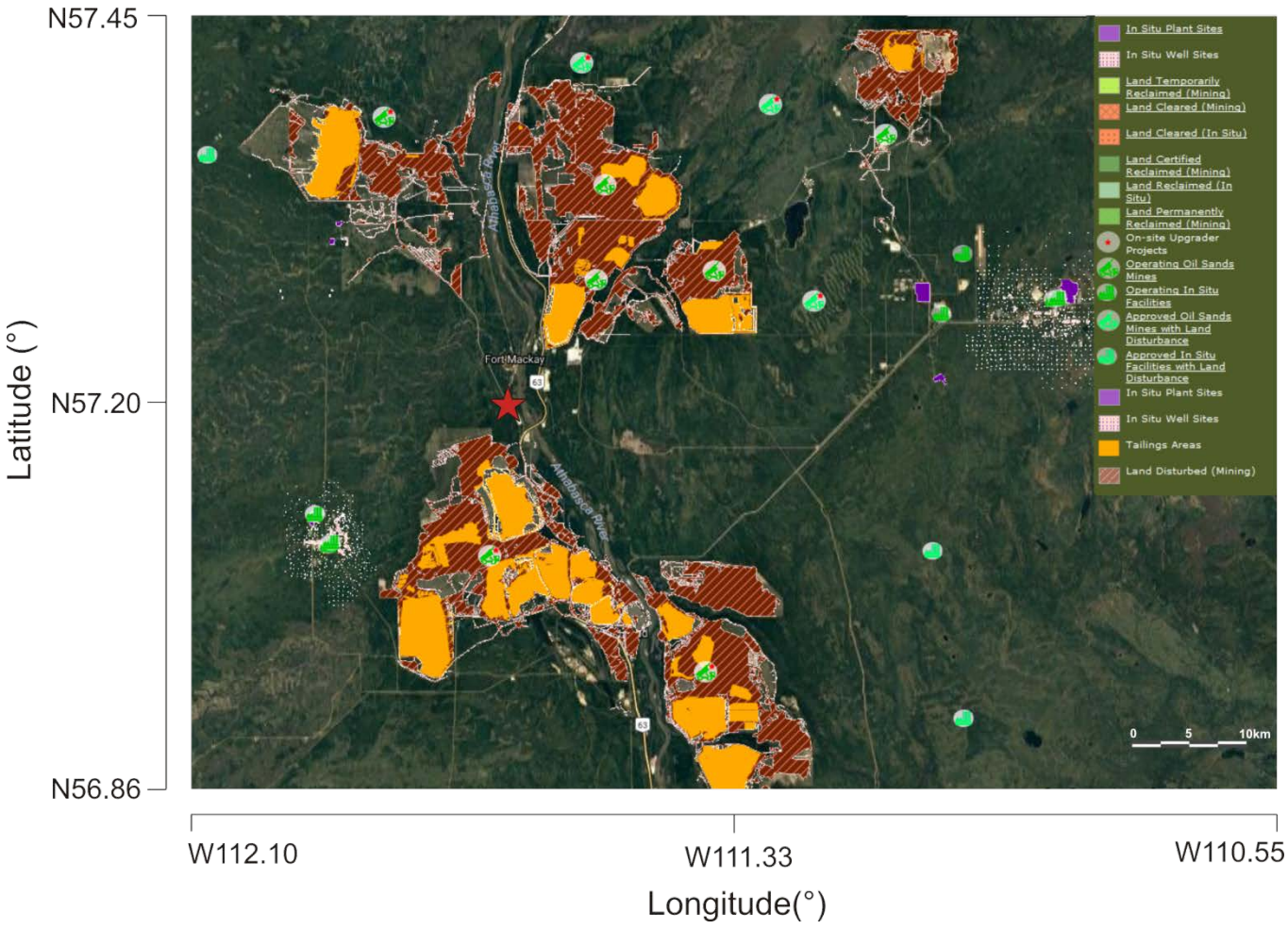

125

126 **2.2 Instrumentation**

127 A large number of instruments was deployed for this study; a partial list whose data were utilized in this

128 manuscript is given in Table 2. Detailed descriptions of these instruments and operational aspects such

129 as calibrations are given in the S.I. Sample observations of analytically unresolved hydrocarbons by GC-

130 ITMS and how these data were used in the analysis are described in section 2.2.1 below.

131 **Table 2**. Instruments used to measure ambient gas-phase and aerosol species during the 2013 JOSM

132 intensive study at AMS 13.

Instrument and Model	Species measured	Time resolution	Reference
Picarro CRDS G2401	CO, CO_2, CH_4	1 min	(Chen et al., 2013; Nara et al., 2012)
Thermo Scientific, Model 42i	NO_y	10 s	(Tokarek et al., 2014; Odame-Ankrah, 2015)
Blue diode cavity ring-down spectroscopy	NO_2	1 s	(Paul and Osthoff, 2010; Odame-Ankrah, 2015)
Thermo Scientific Model 49i	O_3	10 s	(Tokarek et al., 2014; Odame-Ankrah, 2015)
Griffin/FLIR, model 450 GC-ITMS	VOCs	1 hr	(Tokarek et al., 2017b; Liggio et al., 2016)
Thermo Scientific CON101	TS	1 min	n/a
Thermo Scientific 43iTLE	SO_2	1 min	n/a
AIM-IC	$NH_{3(g)}$, $NH_4^+{}_{(p)}$	1 hr	(Markovic et al., 2012)
Aerodyne SP-AMS	rBC, $NH_4^+{}_{(p)}$, $SO_4^{2-}{}_{(p)}$, $NO_3^-{}_{(p)}$, $Cl^-{}_{(p)}$, organics	1-5 min (variable)	(Onasch et al., 2012)
TSI APS 3321	PM_{10-1} size distribution	5-6 min (variable)	(Peters and Leith, 2003)
TSI SMPS (3081 DMA, 3776 CPC)	PM_1 size distribution	6 min	(Wang and Flagan, 1990)
EcoChem Analytics PAS 2000CE	pPAH	1 min	(Wilson et al., 1994; Burtscher et al., 1982)

133

2.2.1 Analytically unresolved hydrocarbon signature

As previously reported (Liggio et al., 2016), the total ion chromatogram of the GC-ITMS occasionally showed elevated and analytically unresolved hydrocarbons in the volatility range of C_{11} – C_{17} with saturation vapor concentration (C^*) from 10^5 µg m^{-3}< C^* < 10^7 µg m^{-3}. An example is shown in Fig. 2.

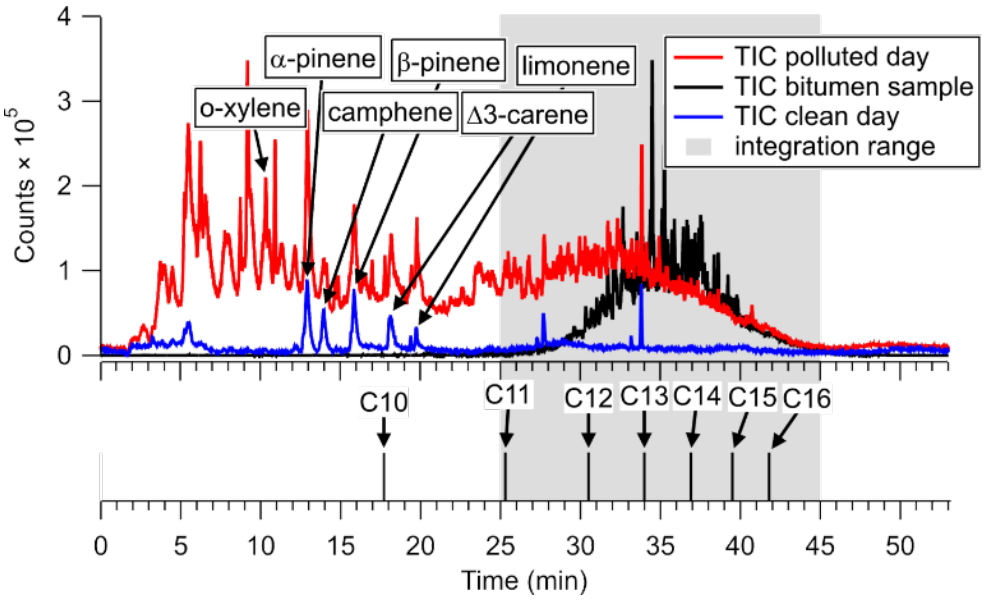

Figure 2. (**Top**) Total ion chromatograms of air samples collected on August 27, 2013 from 18:04 to 18:14 UTC (red) and on August 28, 2013 from 13:43 to 13:53 UTC (blue). The TIC of a head space sample of ground-up bitumen collected post-campaign is superimposed (black). The gray area indicates the range over which IVOC signal was integrated. (**Bottom**) Retention times of n-alkanes, determined after the measurement intensive by sampling a VOC mixture containing a C_{10} – C_{16} n-alkane ladder.

An offline analysis of the headspace above ground-up bitumen gave a similarly unresolved hydrocarbon signal (Fig. 2, black trace). In this particular case, the ambient air chromatogram also shows enhancements of lower molecular weight hydrocarbons (possibly from naphtha) that were not observed in the bitumen sample**.** The observed unresolved hydrocarbon feature is qualitatively similar to the "large chromatographic hump of unresolved complex mixtures" reported by Yang et al. (2011) during

their analysis of bitumen extracts.

The major ions contributing to the unresolved signals in Figure 2 are associated with alkanes (i.e., *m/z* 55, 57, 67, 69, etc. – see Fig. S-1). In contrast, counts at masses associated with aromatics (i.e., *m/z* 115, $C_9H_7^+$, and *m/z* 91, $C_7H_7^+$) as reported by Cross et al. (2013) were negligible in both the bitumen head space and polluted day samples. The strong resemblance of the unresolved hydrocarbon feature in ambient air with the bitumen head space sample both in terms of volatility (i.e., elution time) and electron impact mass fragmentation is consistent with bitumen as the source of IVOCs at this site.

In the interpretation of the integrated IVOC signal, it is assumed that it is of primary origin, i.e., emitted directly from point sources in the vicinity of the measurement site. For the PCA ~~analysis~~, the unresolved signal was integrated from a retention time of 25 min to 45 min (gray area in Fig. 2) in all ambient air chromatograms.

The IVOCs observed in this work likely encompass a portion of the total that is emitted. For example, IVOCs generated by combustion processes, such as aircraft engine exhaust, are comprised of alkanes, aromatics and oxygenated compounds (Cross et al., 2013). The use of a chromatographic column in this work biases the IVOC signal towards hydrocarbon-IVOCs, since oxygenated compounds (i.e., alcohols and acids) will not elute from the analytical column. Furthermore, the recovery of VOCs from the pre-concentration unit, while reproducible and likely complete for n-alkanes which bracket the bulk of IVOC emitted and whose calibration curves were linear, is not known for late-eluting compounds, but is assumed to be sufficiently reproducible to yield a semi-quantitative signal.

2.3 Principal Component Analysis

The PCA was carried out using the "Statistical Analysis System" (SAS™) Studio 3.4 software (SAS, 2015)

using a method similar to that described by Thurston et al. (2011; 1985). The source-related components and their associated profiles are derived from the correlation matrix of the input trace constituents. This approach assumes that the total concentration of each "observable" (i.e., input variable) is made up of the sum of contributions from each of a smaller number of pollution sources and that variables are conserved between the points of emission and observation.

2.3.1 Selection of variables

22 variables whose ambient concentrations are dominated by primary emissions or which are formed very shortly after emission (such as the less oxidized oxygenated organic aerosol (LO-OOA) factor observed by the SP-AMS, see below) were included in the PCA (Table 3). These variables included CO_2, CH_4, NO_y, CO, and SO_2, which are known to be emitted in the oil sands region from stacks, the mine fleet and faces, tailings ponds, and by fugitive emissions (Percy, 2013). The median NO_x (= NO + NO_2) to NO_y ratio was 0.85, consistent with the close proximity of the measurement site to emission sources and limited chemical processing. Because NO_x constituted a large fraction of NO_y, its temporal variation was captured by the latter, and it was not included as a separate variable in the PCA ~~analysis~~.

For this work, mixing ratios of all non-methane hydrocarbons (NMHCs) that were quantified (i.e., o-xylene, the n-alkanes decane and undecane, the aromatics 1, 2, 3- and 1, 2, 4-TMB, as well as limonene and α- and β-pinene) were included as variables. In addition, the aforementioned unresolved signal associated with IVOCs was included as a variable by integrating total GC-ITMS ion counts (*m/z* 50 –425) over a retention time range of 25-45 min (retention index range of 1100 to 1700).

Gas-phase ammonia was included as a variable because elevated reduced nitrogen concentrations have been observed in the region and were linked to the use of ammonia on an industrial scale, for example as a floating agent and for hydrotreating (Bytnerowicz et al., 2010). Total sulfur and total reduced sulfur

were added as tracers of upgrader stack SO_2 emissions and of "odours", believed to be emitted from oil sands tailings ponds which continue to be of concern in surrounding communities (Small et al., 2015; Percy, 2013; Holowenko et al., 2000).

Refractory black carbon was added as a variable since it is present in diesel truck exhaust and in biomass burning plumes and, hence, a combustion tracer (Wang et al., 2016; Briggs and Long). pPAHs were included because of their association with facility stack emissions and combustion particles in the area (Allen, 2008; Grimmer et al., 1987). Hydrocarbon-like organic aerosol (HOA) was included as a surrogate for fossil fuel combustion by vehicles (Jimenez et al., 2009). The LO-OOA factor was included as it is unique to the Alberta oil sands and appears to form rapidly after emission of precursors (Lee et al., 2018). Supermicron aerosol volume (PM_{10-1}, i.e., the volume of particles between PM_{10} and PM_1) was also included as a tracer of coarse particles from primary sources, which are expected to be dominated by dust emissions.

207 **Table 3.** Variables observed at the AMS 13 ground site during the 2013 JOSM campaign used for PCA.

Variable	Unit	Median[a]	Average[a,b]	Standard deviation[a,b]	LOD[e]	Min.[a]	Max.[a]	Fraction <LOD
Anthropogenic VOCs								
o-xylene	pptv[f]	5	30	69	1	< LOD	635	10%
1,2,3 - TMB	pptv	1.7	4.3	7.9	0.2	< LOD	67	27%
1,2,4 - TMB	pptv	2.1	7.7	14.7	0.2	< LOD	107	8%
decane	pptv	0.5	8.5	18.2	0.1	< LOD	125	44%
undecane	pptv	0.4	3.0	6.3	0.1	< LOD	37	39%
Biogenic VOCs								
α-pinene	pptv	477	542	401	1	19	1916	0%
ß-pinene	pptv	390	467	334	1	18	1594	0%
limonene	pptv	150	179	158	2	< LOD	711	1%
Combustion tracers								
NO_y	ppbv	1.79	4.00	5.44	0.01	0.13	41.6	0%
rBC	μg m^{-3}	0.13	0.20	0.10	0.02	< LOD	0.90	40%
CO	ppbv	117.6	120.0	18.2	5.7[h]	90.9	241.2	0%
CO_2	ppmv	420.2	433.2	39.5	0.4[h]	386.0	577.7	0%
Aerosol species								
pPAH	ng m^{-3}	1	2	2	1[c]	< LOD	14	39%
PM_{10-1}	μm^3 cm^{-3}	11.2	14.4	12.9	0.003	1.0	79.5	0%
HOA	μg m^{-3}	0.31	0.43	0.35	N/A[g]	0.04	2.32	N/A
LO-OOA	μg m^{-3}	1.19	2.00	2.26	N/A[g]	0.11	15.6	N/A
Sulfur species								
Total sulfur (TS)	ppbv	0.22	1.41	4.27	0.13	< LOD	33.3	35%
SO_2	ppbv	< LOD	1.0	4.0	0.2	< LOD	33.5	81%
Total reduced sulfur (TRS)	ppbv	0.26	0.38	1.05	0.2	< LOD	14.8	81%
Other								
IVOCs	Counts × min	1.8×10^7	3.4×10^7	4.2×10^7	N/A[g]	1.4×10^6	2.5×10^8	N/A
CH_4	ppbv	1999.2	2065.5	169.6	1.8[h]	1880	2959	0%
NH_3	μg m^{-3}	0.79	1.10	1.03	0.05	0.06	5.75	39%

[a] Values were determined only from data points included in the PCA ~~analysis~~, not from entire campaign.

[b] Average and standard deviation were calculated before zeros were replaced with 0.5×LOD.

[c] Estimated.

[e] LOD = limit of detection.

[f] parts-per-trillion by volume (10^{-12})

[g] N/A = data not available

[h] calculated using 3 × standard deviation at ambient background levels

208

To assess which components have the greatest impact on secondary product formation, a second PCA was performed which included variables mainly formed through atmospheric chemical processes and whose concentrations more strongly depend on air mass chemical age than those variables selected initially. In this PCA, odd oxygen ($O_x = O_3 + NO_2$), submicron aerosol $SO_4^{2-}{}_{(p)}$, $NO_3^-{}_{(p)}$, $NH_4^+{}_{(p)}$, a second, more-oxidized OOA factor (MO-OOA), and PM_1 volume were included, increasing the total number of variables to 28 (Table 4).

Table 4. Variables added in the second PCA. Particle-phase concentrations, i.e., $SO_4^{2-}{}_{(p)}$, $NO_3^-{}_{(p)}$, $NH_4^+{}_{(p)}$ and MO-OOA were made by aerosol mass spectrometry and account for PM_1 only.

Variable	Unit	Median	Average	Standard deviation	LOD	Min.	Max.
O_x	ppbv	7.35	11.1	10.6	1	<LOD	41.1
$SO_4^{2-}{}_{(p)}$	μg m^{-3}	0.3	0.8	1.1	0.1	<LOD	6.6
$NO_3^-{}_{(p)}$	μg m^{-3}	0.08	0.13	0.13	0.01	0.01	0.72
$NH_4^+{}_{(p)}$	μg m^{-3}	0.13	0.28	0.37	0.05	<LOD	2.21
MO-OOA	μg m^{-3}	1.65	1.83	0.960	N/A	1.41×10^{-6}	4.65
PM_1 volume	μm^3 cm^{-3}	2.48	3.77	3.72	N/A	0.35	20.9

2.3.2 Treatment of input data

Data used in the PCA ~~analysis~~ were averaged to match the time resolution of the GC-ITMS VOC and IVOC measurements, i.e. over 10 minute long periods (spaced ~ 1 hr apart) set by the start and stop times of the GC-ITMS pre-concentration period. When concentrations were below their respective limit of detection (LOD; values are given in Table 3), half the reported LOD was used to minimize bias (Harrison et al., 1996; Buhamra et al., 1998). Prior to PCA, input variables were standardized to eliminate unit differences by subtracting the mean concentration $\overline{C_i}$ of pollutant *i* from the concentration of sample *k* ($C_{i,k}$) and dividing by the standard deviation (s_i) of all samples included in the PCA ~~analysis~~.

$$Z_{i,k} = \frac{C_{i,k} - \overline{C_i}}{s_i} \quad (1)$$

Here, $Z_{i,k}$ is the standardized pollutant concentration. In total, 218 data points from all identified species over the period of the campaign were used for the main PCA ~~analysis~~.

2.3.3 PCA solutions

In this work, the Varimax method (Kaiser, 1958) was used to rotate the loading matrix. This method is an orthogonal rotation (i.e., components are not expected to correlate) which minimizes the impact of high loadings, making the results easier to interpret (Kaiser, 1958). Several criteria (Table S-10) were considered for component selection: the latent root criterion, i.e., on the basis that rotated eigenvalues must be greater than unity, the (cumulative) percentage of variance criterion, where the extracted components accounts for >95% of the variance, and the Scree test (Fig. S-2) (Thurston and Spengler, 1985; Guo et al., 2004; Hair et al., 1998; Cattell, 1966). For the optimal solution presented in the main manuscript, the 95% variance criterion was chosen, providing a 10-component solution for the PCA with

only primary variables and an 11-component solution for the PCA with both primary and secondary variables. Components 1 through 4 were consistent regardless of the number of components retained. Solutions with fewer and more components are presented in the supplemental material section.

Time series of each of the components were calculated by multiplying the original standardized matrix by the rotated loading matrix and were used to generate bivariate polar plots (section 2.4).

2.4 Bivariate polar plots

The PCA was complemented by bivariate polar plots showing the wind speed and direction dependence of air pollutant concentrations. The use of these representations implies a linear relationship between local wind conditions and air mass origin, which may not be always the case (for example, during or after stagnation periods). In addition, local topography, such as the Athabasca river valley, complicates regional air flow patterns and limit the interpretability of polar plots in general and in particular to the E of AMS 13, where the river valley is located. The plots were generated with the Openair software package (Carslaw and Ropkins, 2012; Carslaw and Beevers, 2013) using the R programming language and the open-source software "RStudio: Integrated development environment for R" (RStudio Boston, 2017). The default setting (100) was used as the smoothing function.

3. Results

3.1. Overview of the data set

Time series of the 22 pollution tracers chosen for PCA ~~analysis~~ are presented in Fig. 3~~2~~, grouped approximately by source type. Statistics of the data (i.e., median, average, maxima, minima, etc.) are summarized in Table 3.

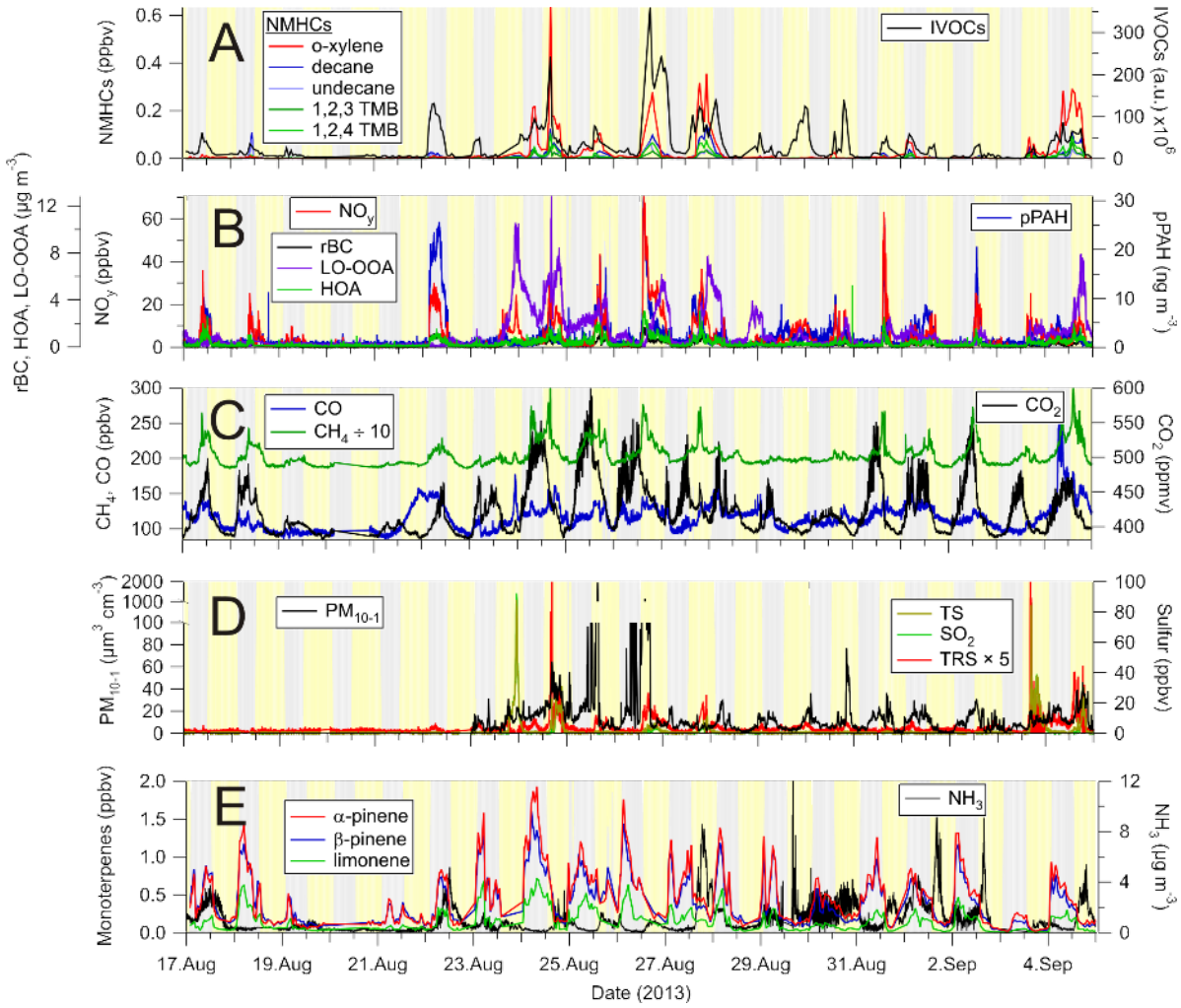

Figure 3. Time series of selected pollution tracers observed at the AMS 13 ground site in the Athabasca oil sands during the 2013 JOSM measurement intensive. The gray and yellow backgrounds represent night and day, respectively. (**A**) Selected non-methane hydrocarbons (NMHCs) and IVOCs. (**B**) Combustion product tracers: refractory black carbon (rBC), total odd nitrogen (NO_y) and particle surface bound polycyclic aromatic hydrocarbons (pPAH), and organic aerosol components: hydrocarbon-like organic aerosol (HOA) and less oxidized oxygenated organic aerosol (LO-OOA). (**C**) Methane (CH_4), carbon dioxide (CO_2) and monoxide (CO). (**D**) Total sulfur (TS), sulfur dioxide (SO_2), and total reduced sulfur (TRS) and PM_{10} particle volume. (**E**) Biogenic VOCs (α-pinene, ß-pinene and limonene) and ammonia (NH_3).

Time series of VOCs of primarily anthropogenic origin (i.e., o-xylene, 1, 2, 3- and 1, 2, 4-TMB, etc.) as well as the IVOC signature are shown in Fig. 3A. The abundances of these species, as well as the other compounds, were highly variable and varied as a function of time of day (i.e., boundary layer mixing height) and air mass origin, with higher VOC concentrations generally observed during daytime. The VOC concentrations varied between nearly pristine, remote conditions, with concentrations below detectable limits, to mixing ratios of aromatic species exceeding 100 pptv. The concentration range of o-xylene is within the extremes reported by WBEA in their 2013 annual report (WBEA, 2013), exemplifying that the data set is representative of typical pollutant levels in this region.

While there is some obvious covariance between variables (i.e., when the mixing ratios of one particular VOC increases, so do others), the ratios of hydrocarbons varied considerably. For example, on August 18, 10:50 UTC, the n-decane to o-xylene ratio was ~22:1, whereas on August 24, 07:40 UTC it was ~1:5.7. The IVOC magnitude also varied greatly and often increased and decreased in tandem with the other VOCs (e.g., on Aug 24, 16:30 UTC) but also increased independently from the other VOC abundances (e.g., on Aug 30, 01:20 UTC, and on the night of Aug 22). This behaviour suggests the presence of multiple sources with distinct signatures that are being sampled to a varying extent at different times. This, coupled with the intermittency of the highly elevated signals, presents an analysis problem frequently encountered in environmental analysis that is usually investigated through a factor or principal component analysis (Thurston et al., 2011; Guo et al., 2004).

Presented in Fig. 3B are the time series of NO_y, rBC and pPAH abundances, all of which are combustion byproducts. For example, rBC is emitted from combustion of fossil fuels, biofuels, open biomass burning, and burning of urban waste (Bond et al., 2004). Similar to the VOCs, the abundances of these species varied greatly, from very low, continental background levels (i.e., <100 pptv of NO_y, < LOD for rBC and pPAHs) to polluted concentrations (i.e., > 60 ppbv of NO_y, > 1 μg m^{-3} rBC, > 10 ng m^{-3} pPAHs) characteristic of polluted urban and industrial areas. When high concentrations of NO_y were observed,

its main component was NO_x (data not shown), which is a combustion byproduct usually associated with automobile exhaust. In the Alberta oil sands, emissions from off-road mining trucks as well as the upgrading processes are the main contributors to the NO_y burden (Percy, 2013; Watson et al., 2013).

Shown in Fig. 3C are the mixing ratios of the greenhouse gases CH_4 and CO_2 along with CO. Abundances of CO_2 were clearly attenuated by photosynthesis and respiration of the vegetation near the measurement site, as judged from the strong diurnal cycle in its concentration (not shown). Maxima typically occurred shortly after sunrise, coincident with the expected break-up of the nocturnal boundary layer. In addition to biogenic emissions from vegetation and soil, CO_2 originates from a variety of point and mobile sources in this region, including off-road mining trucks (Watson et al., 2013) and the extraction, upgrading, and refining of bitumen and on-road vehicle sources in the area (Nimana et al., 2015a, b). Concentrations of CO_2 spiked whenever these emissions were transported to the measurement site.

Concentrations of CH_4 also exhibit a diurnal cycle, with higher concentrations generally observed at night and peaking in the early morning hours. While CH_4 and CO_2 mixing ratios frequently correlated in plumes, their ratios were variable overall, suggesting they often originated from distinct sources. Potential methane point sources in the region include microbial production in tailings ponds (Siddique et al., 2012) and fugitive emissions associated with the mining and processing of bitumen (Johnson et al., 2016). Indeed, a recent analysis shows tailings ponds and open pit mining sources to be the largest sources of CH_4 in the region (Baray et al., 2018).

Similar to the anthropogenic VOCs, the abundances of CH_4 and CO_2 were highly variable and ranged from minima of 1.88 and 384 ppmv to maxima of 2.96 and 578 ppmv, corresponding to maximum enhancements of 1.63 and 1.47 relative to tropospheric global monthly means of 1.806±0.001 and 394.3±0.1 ppmv for July, 2013 (Dlugokencky, 2017b, a), respectively.

Mixing ratios of CO also varied with time but generally were not elevated greatly (median 118 ppbv) above background levels (minimum 91 ppbv), except for occasional spikes in concentration (Fig. 3C). Carbon monoxide is a tracer of biomass burning and fossil fuel combustion, in particular in automobiles with poorly performing or absent catalytic converters, but is also a byproduct of the oxidation of VOCs, in particular of methane and isoprene which are oxidized over a wide area upwind of AMS 13 (Miller et al., 2008).

Time series of sulfur species and PM_{10-1} volume are shown in Fig. 3D. The TS and SO_2 data are dominated by intermittent plumes containing SO_2 mixing ratios exceeding 5 ppbv. The highest mixing ratio observed was 92.5 ppbv (in between the preconcentration periods of the GC-ITMS). Mixing ratios of SO_2 exhibited the most variability of all pollutants, as judged from the standard deviation of each of the measurements (Table 3). TRS levels were generally small (< 1 ppbv) and variable, except for plumes; TRS abundances in plumes, however, are more uncertain since they were calculated by subtraction of two large numbers. When TS and SO_2 abundances were low (< 1 ppbv), TRS abundances were variable and occasionally exhibited spikes that did not show any obvious correlation with other variables, suggesting the presence of one or more distinct TRS sources. PM_{10} volume concentrations varied a lot as well and, just like TRS, did not show an obvious correlation with other variables. Fugitive dust emissions likely contributed to much of the PM_{10} volume in the Athabasca oil sands region (Wang et al., 2015).

Time series of monoterpene mixing ratios are shown in Fig. 3E. α-Pinene was generally the most abundant monoterpene, followed by β-pinene. Their ratio, averaged over the entire campaign was 1:0.85, though occasionally the α- to β-pinene ratio was below 1:2 (e.g., on Aug 28, 14:50 UTC and Sept 5, 12:40 UTC). Terpene mixing ratios were generally higher at night than during the day, with maxima of 1.9 and 1.6 ppbv, respectively, a diurnal pattern consistent with what has been observed at other forest locations (Fuentes et al., 1996). Monoterpenes are emitted by plants via both photosynthetic and non-photosynthetic pathways (Fares et al., 2013; Guenther et al., 2012); at night, their emissions accumulate

in a shallow nocturnal boundary layer, whereas during daytime, they are entrained aloft (above the canopy) and oxidized by the hydroxyl radical (OH) and O_3, which are more abundant during the day than at night (Fuentes et al., 1996). α- and β-pinene mixing ratios were lowest mid-day (median values at noon of 140 and 133 pptv, respectively). The largest daytime concentrations were observed on Aug 25, a cloudy day (as judged from spectral radiometer measurements of the NO_2 photolysis frequency): on this particular day, mixing ratios at noon were 687 and 850 pptv, respectively.

Also shown in Fig. 3E is the time series of ammonia. These data were dominated by spikes which were observed sporadically and did not correlate with other variables, suggesting the presence of nearby ammonia point sources. Ammonia was not as variable as some of the other pollutants (e.g., the anthropogenic VOCs, sulfur species) as judged from its standard deviation (Table 3), which suggests a geographically more disperse source or sources similar to CO or CH_4, which have a "background". This is consistent with a recent study by Whaley et al. (Whaley et al., 2018) that estimated over half (~57%) of the near-surface NH_3 during the study period originated from NH_3 bi-directional exchange (i.e. re-emission of NH_3 from plants and soils), with the remainder being from a mix of anthropogenic sources (~20%) and forest fires (~23%).

3.2. Principal component analysis

3.2.1. PCA ~~analysis~~ with primary variables

The loadings of the optimum solution are presented in Table 5. The 10-component solution accounts for a cumulative variance of 95.5%. The communalities for the analysis, i.e., the fraction of total pollutant observations accounted for by the PCA are all greater than 85%, with the lowest communality obtained for the IVOCs (0.86).

In the following, an overview of the observed components is presented. Associations with r>0.7, r>0.3,

and r>0.~~1~~ 2 are referred to as "strong", "weak", and "poor", respectively. Hypothesized identifications are given in section 4 and are summarized in Table 6 and Fig. 4.

The component accounting for most of the variance of the data, component 1, is strongly associated with the anthropogenic VOCs (r > 0.87), weakly associated with CH_4 (r = 0.59), TRS (r = 0.59), HOA (r = 0.40), LO-OOA (r = 0.45), CO (r = 0.41), and the IVOCs (r = 0.31), and poorly associated with NO_y (r = 0.27) and rBC (r = 0.30). Component 2 is strongly associated with the combustion tracers NO_y (r = 0.82), rBC (r = 0.77), HOA (r = 0.74), and pPAH (r = 0.94), weakly associated with CH_4 (r = 0.39) and IVOCs (r = 0.39), and poorly associated with ammonia (r = 0.20), ~~CO (r = 0.18)~~ and undecane and decane (r = 0.27 and 0.22, respectively). Component 3 is strongly associated (r > 0.9) with the biogenic VOCs and weakly associated with CO_2 (r = 0.48) and shows poor negative correlations with NO_y (r = -0.26) and~~,~~ ammonia (r = -0.24)~~, and SO_2 (r = -0.15)~~. Component 4 is strongly associated with SO_2 and TS (r = 0.97 and 0.93, respectively) and poorly with NO_y (r = 0.21) and LO-OOA (r = 0.28).

Components 1 through 4 emerged regardless of the number of components used to represent the data, whereas the structure of components 5 through 10 only fully emerged in the 10-component solution (see S.I.). Hence, components 6 through 10 are somewhat tentative as many (i.e., 7 – 9) are single variable components and have eigenvalues close to or below unity, i.e., account for less variance than any single variable. As a result, the interpretations of these components are subject to more uncertainty and are more speculative but are presented in the S.I. for the sake of completeness and transparency. For the purpose of this manuscript, this is inconsequential as components 6 – 10 are not associated with IVOCs.

Table 5. Loadings for the 10-factor, optimal solution (primary variables only). Coefficients with Pearson correlation coefficients r>0.3 are shown in bold font.

	1	2	3	4	5	6	7	8	9	10	Commu-nalities
Anthropogenic VOCs											
o-xylene	**0.88**	0.08	0.02	0.10	0.14	0.13	0.07	-0.04	0.16	**0.32**	0.95
1,2,3 - TMB	**0.93**	0.16	0.07	0.05	0.05	0.11	0.04	-0.02	0.18	-0.01	0.95
1,2,4 - TMB	**0.94**	0.14	0.01	0.10	0.11	0.08	0.07	-0.03	0.18	0.13	0.98
decane	**0.92**	0.22	-0.02	0.15	0.23	0.01	0.05	0.04	0.04	0.03	0.97
undecane	**0.87**	0.27	-0.08	0.23	0.20	-0.06	0.12	0.07	-0.04	-0.10	0.96
Biogenic VOCs											
α-pinene	-0.03	-0.08	**0.98**	-0.11	0.02	0.04	0.01	-0.08	0.02	0.01	0.98
ß-pinene	-0.02	-0.08	**0.98**	-0.12	0.02	0.03	0.02	-0.07	0.00	0.01	0.98
limonene	0.07	-0.03	**0.92**	-0.08	0.12	0.24	0.05	-0.11	0.03	-0.05	0.95
Combustion tracers											
NO_y	0.27	**0.82**	-0.26	0.21	0.22	-0.04	0.02	0.10	-0.08	0.01	0.92
rBC	**0.30**	**0.77**	0.03	0.05	**0.44**	0.10	0.09	0.13	0.12	-0.10	0.94
CO	**0.41**	0.18	0.04	0.02	0.09	0.09	0.08	0.06	**0.87**	-0.01	0.99
CO_2	0.09	0.08	**0.48**	-0.12	-0.03	**0.77**	0.25	-0.14	0.05	-0.08	0.95
Aerosol species											
pPAH	0.06	**0.94**	-0.07	-0.13	-0.11	0.07	0.01	0.13	0.10	0.04	0.95
PM_{10-1}	0.18	0.14	0.08	0.09	0.11	0.17	**0.93**	-0.03	0.07	0.08	0.98
HOA	**0.40**	**0.74**	0.02	0.12	0.25	0.15	0.23	-0.06	0.16	0.09	0.90
LO-OOA	**0.45**	0.11	0.12	0.28	**0.72**	0.05	0.25	0.00	0.10	0.04	0.91
Sulfur											
TS	0.25	0.04	-0.16	**0.93**	0.08	-0.05	0.07	-0.02	0.01	0.12	1.00
SO_2	0.12	0.03	-0.15	**0.97**	0.02	-0.04	0.03	-0.03	0.01	-0.05	0.99
TRS	**0.59**	0.04	-0.08	0.11	0.26	-0.04	0.16	0.04	-0.04	**0.71**	0.96
Other											
IVOCs	**0.31**	**0.39**	0.12	-0.08	**0.74**	-0.02	-0.02	-0.06	0.02	0.20	0.86
NH_3	0.01	0.20	-0.24	-0.05	-0.02	-0.08	-0.03	**0.94**	0.04	0.02	0.99
CH_4	**0.59**	**0.39**	0.10	-0.05	0.12	**0.59**	0.11	0.00	0.17	0.14	0.93
Eigenvalues	5.72	3.32	3.23	2.16	1.64	1.13	1.13	0.99	0.96	0.74	
% of variance	25.99	15.08	14.69	9.80	7.46	5.14	5.13	4.51	4.36	3.35	
Cumulative variance	25.99	41.07	55.76	65.56	73.02	78.16	83.30	87.81	92.17	95.52	

390 **Table 6**. Hypothesized identifications of principal components.

Component	Key observations	Possible source(s)	Relevant references
1	Enhancements of aromatics, n-alkanes, TRS, NO_y, rBC, HOA, LO-OOA, CO and CH_4	Wet tailings ponds and associated facilities	(Simpson et al., 2010; Small et al., 2015; Percy, 2013; Holowenko et al., 2000; Howell et al., 2014)
2	Enhancements of NO_y, rBC, pPAH and HOA due to engine exhaust	Mine fleet and operations	(Wang et al., 2016; Grimmer et al., 1987; Allen, 2008; Briggs and Long, 2016)
3	Enhancements of monoterpenes and CO_2, poor anticorrelation with NO_y and absence of anthropogenic VOCs	Biogenic emission and respiration	(Guenther et al., 2012; Helmig et al., 1999)
4	Enhancements of SO_2 and TS, poor correlation with NO_y and LO-OOA	Upgrader facilities	(Simpson et al., 2010; Kindzierski and Ranganathan, 2006)
5	Enhancements of IVOCs, rBC, LO-OOA, NO_y, and TRS	Surface exposed bitumen and hot-water based bitumen extraction	this work
6	Enhancements of CO_2 and CH_4, absence of combustion tracers	Mine face and soil	(Johnson et al., 2016; Rooney et al., 2012)
7	Enhancement of PM_{10-1}	Wind-blown dust	(Wang et al., 2015)
8	Enhancement of ammonia	Fugitive emissions from storage tanks and natural soil/plant emissions	(Bytnerowicz et al., 2010; Whaley et al., 2018)
9	Enhancement of CO	Incomplete hydrocarbon oxidation	(Marey et al., 2015)
10	Enhancements of TRS and o-xylene, poor association with CH_4	Composite tailings	(Small et al., 2015; Warren et al., 2016)

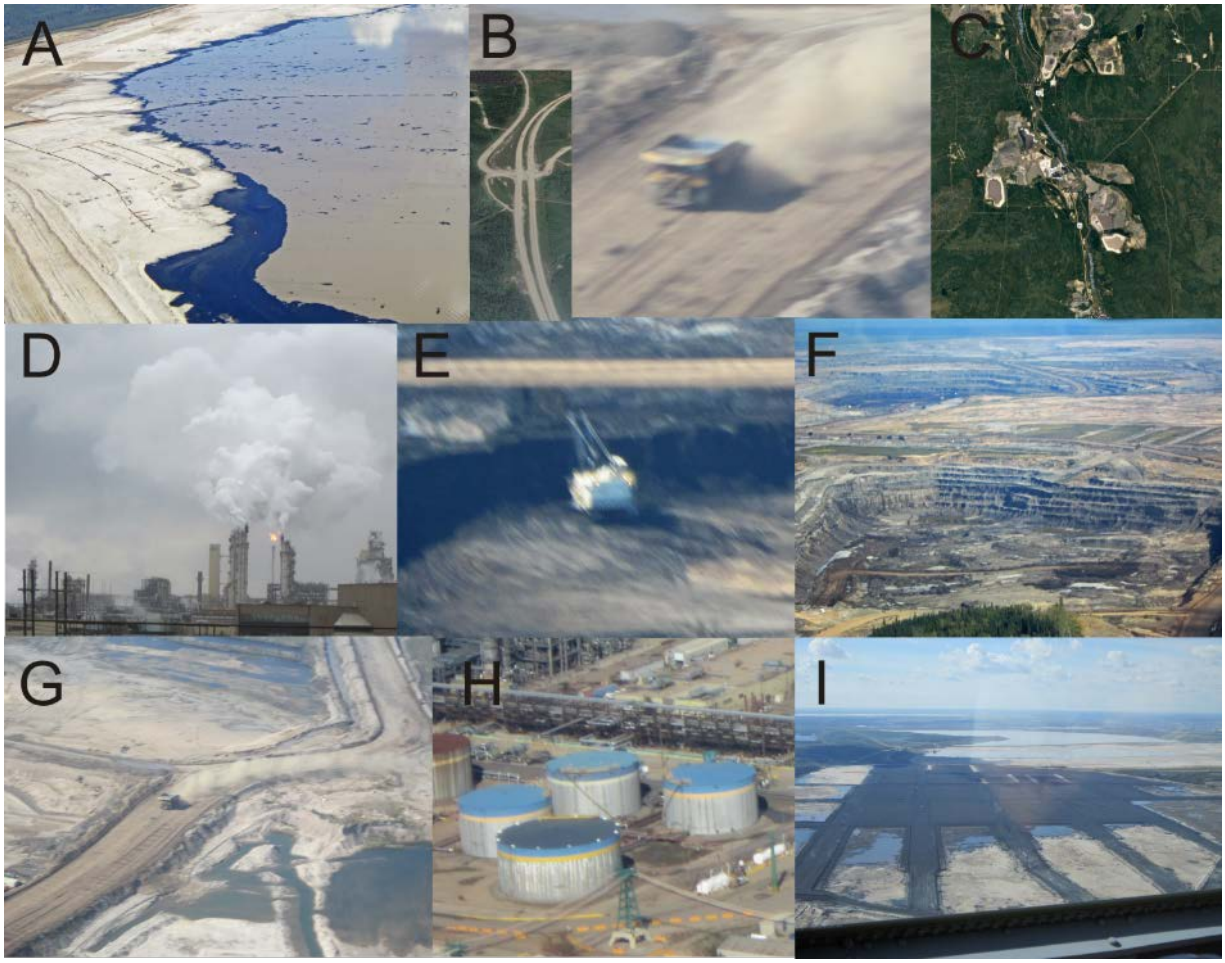

Figure 4. Images of likely sources associated with each of the principal components. From top left to bottom: **(A)** Wet tailings ponds (component 1). **(B)** Mine truck fleet and highway traffic emissions (component 2). **(C)** Biogenic emissions from vegetation (component 3). **(D)** Upgrader facilities (component 4). **(E)** Exposed bitumen on mined surfaces (component 5). **(F)** Fugitive greenhouse gas emissions from mine faces (component 6). **(G)** Wind-blown dust from exposed sand (component 7). **(H)** Fugitive emissions of ammonia from storage tanks (Component 8). **(I)** Composite (dry) tailings (component 10). No image is shown for production CO from oxidation of VOCs (component 9).

3.2.2. Extended PCA ~~analysis~~ with added secondary variables

The loadings of the optimum solution that includes primary and secondary variables are shown in Table 7. In this 11-component solution, the 10 components originally identified were preserved, though their relative order was changed, with the upgrader component moving from the 4th to 2nd position. There was one new component (#6), which encompassed only secondary species, including MO-OOA (r = 0.92), O_x (r = 0.33), $NO_{3(p)}^-$ (r = 0.36), PM_1 (r = 0.31) and LO-OOA (r = 0.31).

$NH_{4(p)}^+$, $SO_{4(p)}^{2-}$, and $NO_{3(p)}^-$ are associated with the stack emissions component (#2, with r = 0.84, 0.84 and 0.44, respectively), which also weakly correlated with PM_1 (r = 0.44) and O_x (r = 0.36). The association of secondary variables with the primary components suggests rapid formation of these secondary products on a time scale that is similar to the transit time of the pollutants to the measurement site. PM_1 correlated strongly with the major IVOC component (component 5, r = 0.80), which also weakly associated with LO-OOA (r=0.66) and $NO_{3(p)}^-$ (r = 0.59), as well as $NH_{4(p)}^+$ and $SO_{4(p)}^{2-}$ (r = 0.32 and 0.33, respectively).

Table 7. Loadings for the 11-component solution with the inclusion of variables associated with secondary processes.

	1	2	3	4	5	6	7	8	9	10	11	Commu-nalities
Anthropogenic VOCs												
o-xylene	**0.89**	0.16	0.04	0.04	0.15	0.00	0.10	0.07	-0.04	0.17	0.24	0.94
1,2,3 - TMB	**0.91**	0.13	0.10	0.16	0.09	0.07	0.11	0.03	-0.03	0.16	-0.08	0.95
1,2,4 - TMB	**0.93**	0.19	0.02	0.13	0.13	0.05	0.06	0.07	-0.03	0.17	0.06	0.99
decane	**0.89**	0.25	0.00	0.22	0.26	0.05	-0.01	0.05	0.01	0.00	0.01	0.98
undecane	**0.81**	**0.35**	-0.08	0.27	0.21	0.15	-0.07	0.08	0.04	-0.12	-0.10	0.96
Biogenic VOCs												
α-pinene	0.00	-0.08	**0.98**	-0.07	0.05	0.03	0.01	0.01	-0.07	0.02	0.01	0.98
ß-pinene	0.01	-0.08	**0.98**	-0.08	0.05	0.05	0.01	0.03	-0.06	0.01	0.02	0.98
limonene	0.11	-0.02	**0.92**	-0.02	0.14	0.09	0.21	0.02	-0.10	0.02	-0.03	0.95
Combustion tracers												
NO_y	0.23	0.20	-0.27	**0.82**	0.21	-0.06	-0.07	0.03	0.10	-0.10	0.01	0.92
rBC	0.22	0.15	0.05	**0.80**	**0.43**	0.15	0.10	0.05	0.09	0.07	0.00	0.95
CO	**0.40**	0.09	0.08	0.20	0.09	0.22	0.08	0.06	0.03	**0.83**	-0.02	0.97
CO_2	0.12	-0.07	**0.50**	0.08	-0.03	0.09	**0.75**	0.28	-0.12	0.03	-0.08	0.95
Aerosol species												
pPAH	0.06	-0.10	-0.06	**0.93**	-0.07	-0.06	0.07	0.03	0.15	0.13	-0.05	0.94
PM_{10-1}	0.19	0.16	0.08	0.16	0.13	0.08	0.18	**0.91**	-0.03	0.05	0.07	0.99
PM_1	0.24	**0.44**	0.00	0.17	**0.70**	**0.31**	-0.06	0.11	-0.04	0.07	-0.14	0.90
$NH_4^+{}_{(p)}$	0.28	**0.84**	0.02	0.12	**0.32**	0.22	0.06	0.07	-0.04	0.14	-0.04	0.97
$SO_4^{2-}{}_{(p)}$	0.29	**0.84**	0.03	0.12	**0.33**	0.19	0.06	0.06	-0.05	0.12	-0.05	0.97
$NO_3^-{}_{(p)}$	**0.30**	**0.44**	0.09	0.23	**0.59**	**0.36**	0.08	0.15	-0.13	0.02	0.24	0.92
HOA	**0.37**	0.18	0.02	**0.77**	0.25	0.10	0.10	0.18	-0.08	0.13	0.14	0.93
LO-OOA	**0.37**	**0.40**	0.12	0.16	**0.66**	**0.31**	0.03	0.12	-0.06	0.00	0.27	0.97
MO-OOA	0.10	0.15	0.09	0.00	0.10	**0.92**	0.05	0.07	0.10	0.16	-0.03	0.95
Sulfur												
TS	0.27	**0.90**	-0.20	0.03	0.04	-0.04	-0.09	0.07	0.00	-0.04	0.18	0.98
SO_2	0.09	**0.96**	-0.19	0.02	-0.03	-0.01	-0.08	0.03	-0.02	-0.03	0.00	0.98
TRS	**0.65**	0.14	-0.10	0.05	0.23	-0.08	-0.07	0.17	0.06	-0.04	**0.63**	0.95
Other												
IVOCs	**0.34**	-0.01	0.12	**0.33**	**0.80**	-0.23	-0.02	0.02	0.02	0.06	0.06	0.94
NH_3	-0.03	-0.08	-0.22	0.21	-0.04	0.09	-0.07	-0.03	**0.93**	0.02	0.02	0.99
O_x	0.07	**0.36**	**-0.62**	0.01	0.27	**0.33**	**-0.41**	-0.07	-0.03	-0.14	0.12	0.91
CH_4	**0.60**	0.00	0.14	**0.42**	0.10	0.08	**0.57**	0.08	-0.04	0.13	0.16	0.94
Eigenvalues	5.85	4.30	3.71	3.51	2.78	1.58	1.24	1.09	1.01	0.94	0.75	
% of variance	20.90	15.34	13.25	12.52	9.92	5.65	4.43	3.88	3.59	3.37	2.66	
Cumulative variance	20.90	36.24	49.49	62.02	71.94	77.59	82.03	85.90	89.50	92.87	95.53	

3.3 ~~Spatial distribution of IVOC sources~~Bivariate polar plots

Bivariate polar plots were generated for all components and their dominant, associated variables and are shown in the supplemental material section (Figs. S2-S11). Winds were predominantly from the SW but were also observed often from the S and N. Fig. 5A shows the plot for IVOCs. The highest concentrations were observed when the local wind direction was from the NE, where several facilities including the Aurora North, Musket River and Jackpine mines and large swaths of disturbed and cleared land are located in close proximity to each other (Table 1 and Fig. 1). The second highest IVOC signal intensity was observed when local wind direction was from the SSE.

The bivariate polar plots of the 3 components associated with IVOCs are shown in Fig. 5B-D. These components are associated with winds from the NE, E, SE and S at low to moderate speeds (1-3 m s^{-1}). Component 5 (Fig. 5B) was the most strongly correlated with IVOCs and shows the most spatial overlap with the distribution of the IVOC source; however, the intensities differ owing to the association of component 5 with other variables such rBC and LO-OOA.

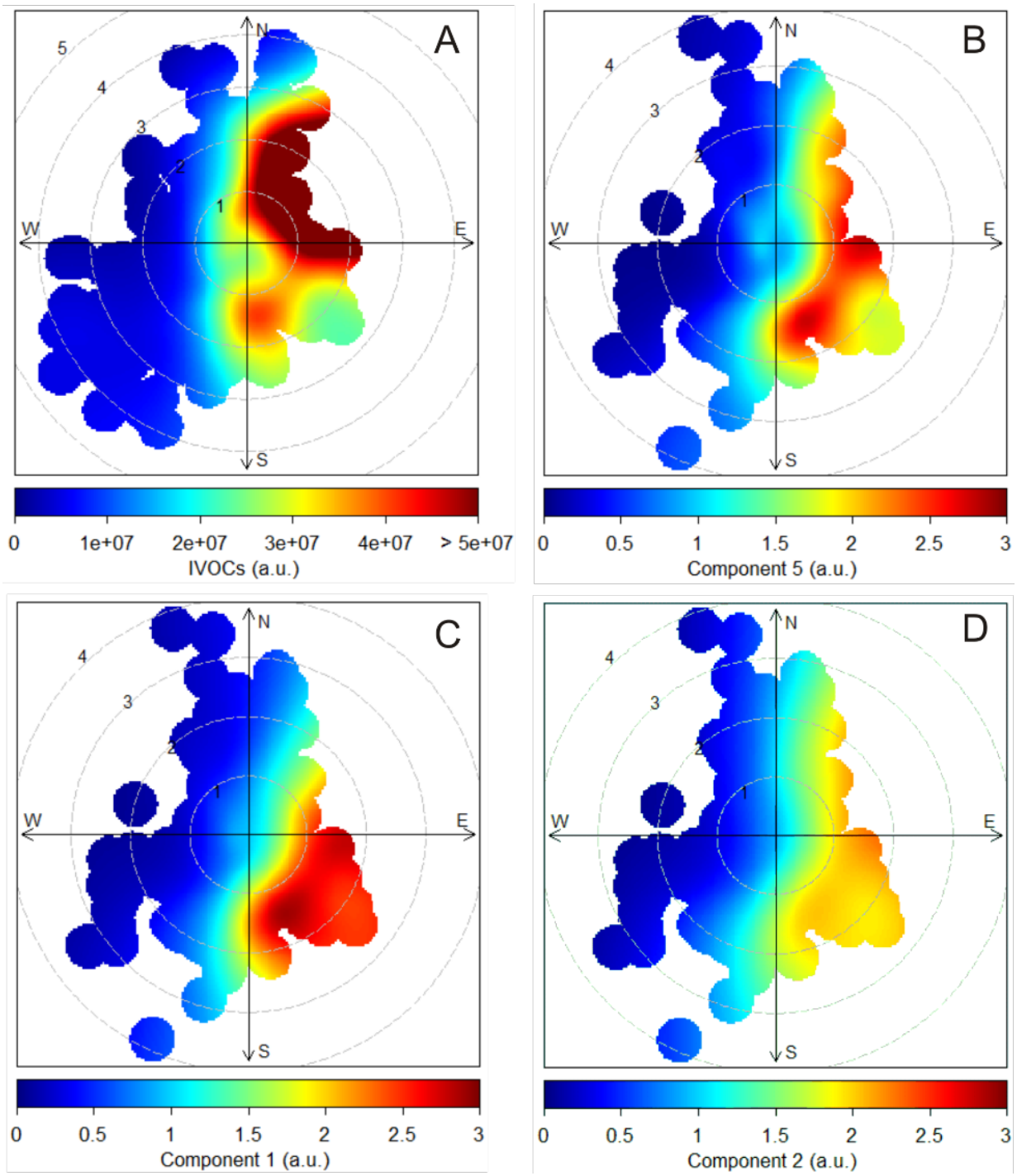

430

431 **Figure 5.** Bivariate polar plots related to IVOCs: **(A)** IVOCs from the complete data set. **(B)** Component 5

432 extracted from the main PCA (Table 5). **(C)** Component 1 extracted from the main PCA. **(D)** Component 2

433 extracted from the main PCA ~~analysis~~. Wind direction is binned into 10° intervals and wind direction into

434 30° intervals. The polar axis indicates wind speed (m s^{-1}). a.u. = arbitrary units.

4. Discussion

This work has added to the relatively few data sets of pollutants in the Athabasca oil sands region, one of the largest emitters of airborne pollutants in Canada (NPRI, 2013), that are available in the open literature. Earlier source apportionment studies in the region investigated ground level O_3 and $PM_{2.5}$ (Cho et al., 2012), examined VOCs (Bari and Kindzierski, 2018; Bari et al., 2016) and $PM_{2.5}$ (Bari and Kindzierski, 2017; Landis et al., 2017) impacting the nearby communities of Fort McKay and Fort McMurray, or investigated pollutants such as PAHs as they affect sediments (Jautzy et al., 2013) or lichens (Landis et al., 2012). The measurement suite in this work encompassed a larger variety of collocated analytical instruments closer to oil sands mining operations than these earlier studies and included a first, direct observation of airborne IVOCs, that is unique to this area and we have not observed elsewhere where we have made GC-ITMS measurements, i.e., in Calgary and on Vancouver Island (Tokarek et al., 2017a).

The main objective of this work ~~is~~ was to elucidate the origin of the IVOC signature observed at the AMS 13 ground site downwind from the AB oil sands mining operations (Fig. 2) through a ~~principal component analysis~~PCA. The optimum ~~PCA~~ solution identified 10 components, of which three were associated with the IVOC signature: 1, 2, and 5 (Table 5). ~~The~~ Tentative assignments of these components to source types in the oil sands are given in Table 6 and are discussed below.

Emission inventories show that the facilities that process the mined bitumen are by far the largest anthropogenic point sources in the oil sands region (NPRI, 2013), consistent with recent aircraft measurements (Baray et al., 2018; Howell et al., 2014; Li et al., 2017; Simpson et al., 2010) which have shown substantial emissions of NO_y, SO_2, CO, VOCs, CO_2, and CH_4, from these facilities and associated mining activities. No single component correlates with all of these variables, suggesting that the PCA is able to distinguish between source types within the facilities such as tailings ponds (component 1), stack

emissions (component 4), and mining (component 2).

Close-up overflights (Howell et al., 2014; Li et al., 2017; Baray et al., 2018) were able to spatially resolve various oil sands facility emission sources (i.e., tailings ponds from upgraders, fluid coking reactors, hydrocrackers and –treaters); the PCA presented in this manuscript is not expected to do this in all cases because some emissions would have frequently merged into a single plume by the time of observation at AMS 13; unless their emissions vary considerably in time, these sources could be interpreted as originating from a single source in the PCA.

The discussion below focuses on components that are associated with IVOCs (section 4.1), followed by those that are not (section 4.2). The PCA ~~analysis~~ that included 6 secondary products is discussed in section 4.3. Components which are not associated with IVOCs and have only tentatively been identified (i.e., components 6 – 10) are discussed in the S.I.

4.1 ~~Sources~~ Components associated with IVOCs

4.1.1. Component 1: Tailings ponds (wet tailings)

Component 1 is strongly associated with anthropogenic VOCs ($r > 0.87$) and weakly with TRS ($r = 0.59$), and CH_4 ($r = 0.59$). These pollutants originate from tailings ponds (Small et al., 2015), though it is unclear from this analysis how large a source tailings ponds are compared to fugitive emissions of these pollutants from the nearby processing (e.g., bitumen separation and mining) facilities.

Tailings ponds cover large areas of land and are used to slowly (on a time scale of years to decades) separate solid components, or tailings, from water used in bitumen extraction. Residual bitumen often floats to the top of the settling basins. Most tailings ponds are "wet" (as they contain residual naphtha that is used as a diluent during the transfer of tailings to the ponds) and emit VOCs, CH_4, and CO_2 (Small et al., 2015). The presence of o-xylene, TMB and the n-alkanes in component 1 is consistent with the

480 fugitive release of VOCs from residual naphtha, which contains these compounds (Siddique et al., 2008;
481 Siddique et al., 2011; Small et al., 2015). Furthermore, the observation of TRS and CH_4 from this source is
482 consistent with the presence of anaerobic sulfur reducing bacteria and methanogens within the ponds,
483 which degrade not only the residual bitumen (Holowenko et al., 2000; Percy, 2013; Quagraine et al.,
484 2005) but also the various components of naphtha (Shahimin and Siddique, 2017; Small et al., 2015).
485 Overall, tailings ponds emissions explain much of the TRS and CH_4 concentration variability in this data
486 set (Table 5) and in a recent aircraft study (Baray et al., 2018).

487 While component 1 correlates with CH_4 ($r = 0.59$), it does not correlate with CO_2 ($r = 0.09$). Emissions of
488 CH_4 from tailings ponds due to methanogenic bacterial activity are well-documented (Small et al., 2015;
489 Yeh et al., 2010) and hence the correlation with CH_4 is not unexpected. On the other hand, the lack of
490 correlation with CO_2 seems inconsistent with emission inventories that generally present tailings ponds
491 as large CO_2 sources (Small et al., 2015). One plausible explanation is that tailings ponds are a relatively
492 small CO_2 source overall in the region and that other, larger CO_2 sources and sinks (such as
493 photosynthesis and respiration by the vegetation surrounding the site) dominate the variance impacting
494 the PCA results. It may also indicate that, at least on aggregate and for the particular ponds detected in
495 this work, the emissions are in a regime where the release of CH_4 dominates over CO_2, i.e., the ponds
496 have, perhaps, become more anoxic than believed to be the case in previous studies and hence emit
497 more CH_4 (Holowenko et al., 2000). For example, Small et al. (2015) showed that older tailings ponds
498 (those without the addition of fresh froth or thickening treatments) tended to emit more CH_4, while
499 newer ponds are associated with higher VOC emissions. It is likely that component 1 is dominated by the
500 nearest pond (the Mildred Lake settling basin, 6 – 11 km SSE of AMS 13) and other tailings in the SE
501 where the majority of air samples originated from. The Mildred Lake settling basin is one of the oldest in
502 the region and is still actively being used; the correlation with CH_4 and VOC emissions is hence expected.

503 Component 1 is also associated with NO_y, rBC, CO, and HOA, though these correlations are relatively

modest (r = 0.27, 0.30, 0.41, and 0.40, respectively). These species typically originate from combustion sources, such as generators, motor vehicles, including diesel powered engines powering generators or pumps; it is not obvious if and to what extent these are operated on or near tailings ponds, though. Satellite observations have shown elevated concentrations of NO_2 above on-site upgrader facilities, likely a result of emissions from extraction and transport sources (McLinden et al., 2012). In addition, one of the major highways of the region is located adjacent to the Mildred Lake settling basin and other major ponds in the region; highway traffic emissions (of CO, NO_y, rBC, and HOA) may hence also be partially included in component 1.

The bivariate polar plot shows that component 1 was observed when local wind speeds were from the SE and E of the measurement site (Fig. 5C), which is consistent with the notion that the Mildred Lake settling basin and emissions along Highway 63 and, potentially, more distant facilities are sources contributing to this component.

Component 1 is associated with the IVOC signature, though to a lesser degree than components 2 and 5. The association of the IVOC signal with component 1 is slightly poorer (r = 0.31) than the association with component 2 (r = 0.39), but significantly poorer than component 5 (r = 0.74). One possible explanation for ~~T~~the association of IVOCs with tailings ponds vapor ~~can be explained by~~is the presence of bitumen in the ponds that was not separated from the sand during the separation stage (Holowenko et al., 2000). This semi-processed bitumen would be expected to emit the same IVOC vapors to those that were observed in the lab (Fig. 2). Tailings ponds contain anywhere from 0.5% - 5% residual bitumen by weight (Chalaturnyk et al., 2002; Holowenko et al., 2000; Penner and Foght, 2010). As illustrated in Fig. 4A, some of this material floats on the ponds' surfaces, where IVOCs can partition to the air. Emission of IVOCs from bitumen floating on tailings ponds would be a function of many variables (e.g., diluent composition, extraction methodology, settling rate, temperature, etc.) and is thus not expected to be as persistent as CH_4 partitioning from the ponds to the above air or from exposed bitumen on the

mine surface, leading to a lower overall correlation.

Component 1 is also weakly associated with the less oxidized oxygenated organic aerosol factor, LO-OOA (r = 0.45). Liggio et al. (2016) found that the observed secondary organic aerosol is dominated by an OOA factor whose mass spectrum was similar to those of aerosols formed from oxidized bitumen vapours. The organic aerosol budget in this study was also dominated by an OOA factor, the LO-OOA (Lee et al., 2018). The association of LO-OOA with component 1 is thus consistent with its association with IVOCs.

4.1.2. Component 2: Mine fleet and vehicle emissions

Component 2 strongly correlates with NO_y (r = 0.82), rBC (r = 0.77), pPAH (r = 0.94), and HOA (r = 0.74), which suggests a combustion source such as diesel engines. In the AB oil sands, there is a sizeable off-road mining truck fleet consisting of heavy aggregate haulers. In addition, there are diesel engine sources associated with generators, pumps and land moving equipment, i.e., graders, dozers, hydraulic excavators, and electric rope shovels (Watson et al., 2013; Wang et al., 2016). Most of these non-road applications have been exempt from highway fuel taxes, on-road fuel formulation requirements and after-engine exhaust treatment (Watson et al., 2013). Emissions from the hauler fleet and the stationary sources would fit the profile of component 2. Other diesel engines operated in the region include a commuter bus fleet, pickup and delivery trucks, tractor-trailers, and privately owned diesel powered automobiles used to commute from the work sites to the major residential areas around Fort McMurray, whose emissions are likely captured by component 2 as well, though the magnitude of these relative to the mining truck fleet is not known. Consistent with component 2 being associated with an anthropogenic source is its poor correlation with undecane (r =0.27), likely arising from fugitive fuel emissions.

The bivariate polar plot (Fig. 5D) for component 2 and NO_y in particular (Fig. S-4A) match the location of

Highway 63 which crosses the river to the SE of AMS 13 and bends to the E and is indicative of a line source. At the same time, some of the largest mining operations in the region, the Susan Lake Gravel Pit, Aurora North, Muskeg river, and Millennium mines are located to the NE and SE of AMS 13 as well. NO_y, rBC, and HOA (Fig. S-4A, B and D) all appear to have dominating point sources to the S and E when wind speeds are 1-2 m s^{-1}. These directions are the same as the Fort McKay industrial park to the E and the Syncrude Mildred Lake facility parking lot to the S which would have a higher concentration of vehicles emitting these pollutants in a smaller area, whose emissions would be in addition to those from industrial activities.

Component 2 is associated with the IVOCs signature and CH_4 (both r = 0.39). The mining activities bring bitumen to the surface; similar to what we had observed in lab experiments (Fig. 2, black trace), the surface exposure of bitumen during mining and on-site processing is expected to be associated with fugitive emissions of CH_4 (Johnson et al., 2016) and IVOCs.

Fine-fraction particle-surface bound PAHs (pPAH) are associated strongly with component 2, but no other components. Measurements of individual PAHs in snow and moss downwind from the oil sands facilities have identified multiple sources of PAHs in the Athabasca oil sands, which include wind-blown petroleum coke dust (also referred to as petcoke for short), a carbonaceous residual product from the upgrading of crude petroleum that is stockpiled on mine sites, and emissions from fine tailings, oil sands ore, and naturally exposed bitumen (Zhang et al., 2016; Jautzy et al., 2015; Parajulee and Wania, 2014). Given this diversity of known sources, the associations of PAHs with only a single component is surprising, though indicates that emissions from the mining fleet (which would include diesel and, perhaps, wind-blown emissions from petcoke that is being transported) gave rise to most of the variability in surface-bound PAH concentrations in this data set. The petcoke emissions identified in the studies mentioned above are likely mainly associated with larger, supermicron sized particles, whose PAH content would not be detected by the pPAH measurement in this data set.

Component 2 is not ~~significantly~~ associated with LO-OOA (r = 0.11), even though IVOCs are associated with this component. This feature may indicate that the IVOCs emitted in component 2 are qualitatively different from those emitted by components 1 and 5, in that they are less likely to yield organic aerosol on the time scale of transport from emission to observation. One reason for the difference could be that the bitumen that is transported by the mining fleet is relatively freshly exposed, whereas the IVOCs released by bitumen in tailings ponds has been processed by microbes and that released by mine faces (component 5) may have been photochemically oxidized to a greater extent and hence more prone to rapid aerosol formation.

There is ~~little to~~ no association of component 2 with CO_2 (r = 0.08). This is somewhat unexpected as the trucks are expected to release CO_2 (Wang et al., 2016) but could be due to significantly larger CO_2 sources in the area dominating the observed CO_2 variability at AMS 13 (e.g., components 3 and 6). Furthermore, one would expect an association of non-road mining truck emissions with aromatics and alkanes. Component 2 exhibited only poor correlations with decane (r = 0.22) and undecane (r = 0.27) and ~~negligible~~ no correlation with o-xylene (r = 0.08), suggesting that other components (i.e., component 1) explained most of the variability of their concentrations at this site.

4.1.3. Component 5: Surface-exposed bitumen and hot-water bitumen extraction

Component 5 correlates more strongly with the IVOCs (r = 0.74) than with any other component and correlates strongly with LO-OOA (r = 0.72), weakly with rBC (r = 0.44), and poorly with HOA (r = 0.25), NO_y (r = 0.22), decane (r = 0.23), undecane (r = 0.20), and TRS (r = 0.26). We interpret this profile as emissions from surface-exposed bitumen which outgases IVOCs.

One possibility is that these emissions occur on mine faces, where previously unexposed bitumen is brought to the surface as a result of mining. Only a relatively small portion of the mine faces is actively

mined; those parts give rise to rBC and NO_y emissions from combustion engines in heavy haulers or generators powering equipment. The poor association of component 5 with TRS could be due to sulfur reducing bacteria found on the surface of bitumen. However, most of the variability of TRS at AMS 13 is attributed to composite or "dry" tailings ponds given their more conducive environment to microbial activity.

Component 5 does not correlate with CO_2 (r = -0.03) ~~and only poorly~~or with CH_4 (r = 0.12), which is somewhat at odds with the notion of mine faces as the main source of IVOCs. The mine faces give rise to substantial fugitive emissions of CO_2 and CH_4 (Johnson et al., 2016) – these emissions are likely captured by component 6 in this analysis (see S.I.). It is unclear to what extent these greenhouse gases are released relatively quickly from "hot spots" (i.e., from a small number of locations) through surface cracks and fissures or by slow release from new material that is exposed and then releases greenhouse gases during material handling, transport and processing (Johnson et al., 2016). IVOCs from surface-exposed bitumen are likely released by the latter mechanism and are temperature-dependent. If the mine faces are indeed the main IVOC source, the analysis results presented here suggest that the IVOCs emissions from surface-exposed bitumen on mine faces are decoupled from CH_4 emissions in time and appear as a distinct component and hence corroborate the "hot spots" or fast release hypothesis, though clearly, more work is needed to characterize greenhouse gas emissions from oil sands mine faces.

The association of IVOCs with component 5 may also be a result of fugitive emissions during the hot water-based extraction of bitumen sand slurries during the separation phase of bitumen treatment. Generally, bitumen is extracted in a weak alkaline environment by aeration of the solution to optimize the separation of sand and bitumen (Masliyah et al., 2004). Unrecovered bitumen and naphtha then end up in tailings. The recovered bitumen and naphtha are moved to upgrader facilities where they undergo further treatment (such as coking or hydrotreatment). The magnitude of fugitive emissions during these

downstream extraction processes could be large, considering the bitumen is heated and actively aerated. Future work should investigate IVOC fluxes near extraction plants and on mine faces.

Finally, it is conceivable that a "natural" background of IVOCs exists in the region (since bitumen can be found at or near the surface in many parts of the region); such a natural background would also be included in component 5. However, this "natural" bitumen would have been exposed at the surface for geological time scales and, unlike unexposed, buried bitumen, likely would have lost most of its volatile content over that period. Furthermore, the mine faces occupy large swaths of land in the region (as evident from satellite imagery). Thus, the IVOCs emissions are more likely due to anthropogenic activity than due to a natural phenomenon.

4.2. ~~Sources~~ Components not associated with IVOCs

4.2.1. Component 3: Biogenic emissions and respiration

Component 3 is strongly correlated with the monoterpenes α-pinene (r = 0.98), ß-pinene (r = 0.98) and limonene (r = 0.92) and is hence identified as a biogenic emissions source. This component is also weakly associated with CO_2 (r = 0.48).

At AMS 13, CO_2 and the monoterpenes exhibit a very similar diurnal cycle: they are present in higher concentrations during the night than during the day (Fig. 3) due to a decrease in the boundary layer height (BLH) at night coupled with plant respiration of CO_2 and non-photochemical emission of monoterpenes (Fares et al., 2013; Guenther et al., 2012). During the day, mixing ratios of CO_2 are lower due to plant uptake and photosynthesis, and mixing ratios of terpenes are lower due to higher mixing heights and vertical entrainment and due to oxidation by O_3 and OH (Fuentes et al., 1996). Hence, the PCA gives a *positive* correlation of monoterpenes with CO_2 even though the physical processes,

644 photosynthesis and respiration, work in opposite direction.

645 The bivariate polar plots (Fig. S-5A-C) show that the monoterpenes and CO_2 were observed in highest
646 concentrations when the wind speeds were low (< 1 m s^{-1}), consistent with formation of a stable
647 nocturnal boundary layer.

648 To corroborate this interpretation, the PCA was repeated with BLH estimated by a light detection and
649 ranging (LIDAR) instrument (Strawbridge et al., in prep.) added as a variable (Table S-9 in the S.I.). Since
650 BLH is not "emitted" by any source, it appears as a single variable component (r = 0.90). The only other
651 component that BLH (anti)correlates with is the biogenic component 3 (r = -0.35).

652 The dominant monoterpene species observed was α-pinene, followed by ß-pinene and limonene,
653 though occasionally there was twice as much ß-pinene than α-pinene in the sampled air. Some
654 variability of this ratio is expected since emission factors vary considerably between tree species (Geron
655 et al., 2000) which are not homogeneously distributed throughout the region (e.g., Fig. S1 of Rooney et
656 al. (2012)).

657 Simpson et al. (2010) observed enhancements of α-pinene and, to a greater extent, β-pinene over the
658 oil sands (up to 217 pptv and 610 pptv) compared to background levels of 20±7 and 84±24 pptv,
659 respectively, during mid-day overflights (which occurred between 11:00 and 13:00 local time). Similar
660 enhancements were also reported by Li et al. (2017) who observed emissions of biogenic hydrocarbons
661 in the four facilities sampled, three of which showed a higher β- than α-pinene concentration. The PCA
662 ~~analysis~~ (Table 5) showed no significant correlation of α- and β-pinene with any of the anthropogenic
663 ~~sources~~components, which implies that the biogenic source strength is simply too large for any
664 anthropogenic emissions of terpenes to be picked up in the analysis, especially considering that
665 terpenes are relatively short-lived.

666 The biogenic source shows poor anticorrelations with NO_y (r = -0.26) and~~,~~ NH_3 (r = -0.24)~~, and SO_2 (r~~

667 ~~= 0.15)~~. Many NO_y species (i.e., NO_2, HONO, peroxycarboxylic nitric anhydrides or PAN, and HNO_3) ~~and~~
668 ~~SO_2~~ deposit to the forest canopy (Hsu et al., 2016; Min et al., 2014; Fenn et al., 2015); at night, when
669 mixing heights are lower, their concentrations are expected to decrease faster than during the day and
670 are thus out of phase with the CO_2 and terpene concentrations. ~~In addition, there is a time-of-day~~
671 ~~observation bias for SO_2 and, to lesser extent, NO_y, which are found in upgrader plumes (see 4.2.2.).~~ The
672 poor anticorrelation with NH_3 likely arises because the NH_3 emissions from plants are mainly stomatal
673 and scale with temperature and are hence larger during the day than at night, anticorrelated with the
674 terpene source (Whaley et al., 2018).

675 **4.2.2 Component 4: Upgrader emissions**

676 Component 4 is strongly correlated with SO_2 (r = 0.97) and total sulfur (r = 0.93). By far the largest
677 source of SO_2 in the region are upgrader facilities, which emit as much as 6×10^7 kg annually according to
678 emission inventories (ECCC, 2013). Significant SO_2 emissions from upgrader facilities have recently been
679 confirmed by aircraft studies (Simpson et al., 2010; Howell et al., 2014; Liggio et al., 2016). Component 4
680 is also poorly correlated with NO_y (r = 0.21) but not with rBC (r = 0.05), consistent with a non-sooty (i.e.,
681 lean) combustion source such as upgrader stacks. Strong enhancements in SO_2 were only observed
682 intermittently as "spikes", which is expected when sampling emissions from relatively few and discrete
683 point sources.

684 Component 4 is ~~poorly anticorrelated~~not associated with CO_2 (r = -0.12), even though inventories
685 indicate that the upgrading facilities are the largest CO_2 source in the region (Furimsky, 2003; Englander
686 et al., 2013; Yeh et al., 2010). In this data set, the lack of correlation of component 4 with CO_2 (and to
687 some extent with PM_{10-1} as well) likely arises mainly from a sampling bias as stack emissions were only
688 observed during daytime, likely due to diurnal variability of the atmospheric boundary layer structure as
689 explained below.

690 Most of the variability in CO_2 concentration at AMS 13 is due to surface-based sources that originate
691 from large areas, especially biogenic processes (photosynthesis during the day and respiration at night,
692 component 3) and anthropogenic surface sources such as those captured by component 6 (section
693 4.2.3). Other anthropogenic pollutants, such as SO_2, NO_y, and CH_4, are not subject to large biogenically
694 driven processes and are less affected than CO_2.

695 In contrast to surface sources, emissions from the > 100 m tall stacks are comparatively undersampled
696 and observed mainly during daytime, when vertical mixing brings elevated plumes to the surface, yet
697 CO_2 concentrations are generally much lower than during the night due to uptake by vegetation. At
698 night, pollutants emitted from stacks are injected above the likely very shallow nocturnal surface layer
699 and were hence not observed at the surface. Vertical profile measurements of SO_2 stack plumes by a
700 Pandora spectral sun photometer at Fort McKay during daytime have shown considerable vertical
701 gradients and only occasional transport of SO_2 all the way to the surface (Fioletov et al., 2016).

702 The association of component 4 with CO_2 is negative because the stack emission source is observed only
703 during the day when the large biogenic sink dominates and effectively masks the relatively small
704 increase due to anthropogenic CO_2. In contrast, background concentrations of SO_2 are comparatively
705 low, and the increase in SO_2 concentrations is readily picked up the PCA.

706 It would be interesting to conduct a future study in winter when biogenic activities decrease; a
707 wintertime PCA ~~analysis~~ of surface measurements might be able to associate CO_2 enhancements with
708 upgraders, though boundary layer mixing heights would decrease as well, which would make a PCA
709 ~~analysis~~ using surface data even more challenging.

710 Component 4 does not correlate with PM_{10-1} volume (r = 0.09). It is clear that the emitted SO_2 will
711 contribute to secondary aerosol formation downwind, such that a correlation of stack emissions with
712 PM_{10-1} volume might be expected. However, these secondary contributions will likely mostly be in the

submicron aerosol fraction, which adds relatively little to PM_{10-1} volume. Further, PM_{10-1} volume is dominated by coarse particles from other primary sources, mostly wind-blown emission of sand from the mine surfaces, roadways and, perhaps, bioaerosol (component 7, see S.I.). These effects make PM_{10-1} volume from stacks appear comparatively small, such that the variability of the larger, surface-based sources likely masks the contribution of stacks emissions to PM_{10-1} variability.

The bivariate polar plot of component 4 (Fig. S-6D) shows that the largest magnitudes were observed when local winds were from the SE. The corresponding plot of SO_2 (Fig. S-6A) reveals two more distinct sources: a larger one from the E and a smaller one from the SSE. However, only two facilities (Sunrise and Firebag) are located to the E at relatively large distances of 37 km and 47 km respectively. The largest known upgraders and SO_2 sources in the area (i.e., upgraders located at the Mildred Lake and Suncor base plants) are located to the S and SE of AMS 13. Considering that the stack emissions are only observed intermittently, we speculate that there exists a mesoscale transport pattern in the Athabasca river valley which channel emissions, such that the local wind direction and speed may be misleading as to the true location of these sources. For more extensive data sets, such phenomena may very well average out but perhaps did not in this case.

4.3. Extended PCA with added secondary variables

The extended analysis (Table 7) qualitatively preserves the structure (with the exception of an added "Aged" component, # 6) of the original 10-component solution but allows an assessment of which components most result in formation of secondary products such as SOA, which has implications for health (Bernstein, 2004) and climate (Charlson et al., 1992). Secondary products vary considerably as a function of air mass chemical age (which depends, amongst other components, on time of day and synoptic conditions, including wind speed) and are hence expected to add considerable noise and scatter to the results leading to lower correlations. On the other hand, the distance between the

measurement site and sources is fixed, such that this variability should average out over time. This indeed appears to have happened in this data set in spite of the relatively low sample size.

The analysis indicates that the component with the strongest IVOC source (Component 5) also has the highest association with PM_1 (r = 0.70; Table 7). Aircraft measurements combined with a modelling study have required a group of IVOC hydrocarbons to explain the significant SOA formation and growth downwind of the oil sands region (Liggio et al., 2016). The association of IVOCs with PM_1 volume is consistent with the hypothesis that oxidation of IVOCs observed at AMS 13 leads to SOA generation and appears to have a significant impact on the variation in PM_1 mass.

The second component influencing PM_1 is that from stack emissions (Component 4 in the primary PCA; Component 2 in the secondary PCA) (Tables 5 and 7). It is well established that the oxidation of SO_2 to sulfate will lead to formation of fine particulate matter. This apparently occurs, at least partially, on the time scale between the point of emission and the AMS 13 site (assuming a wind speed of 3 m/s and a distance of 11 km, the transit time is 1 hour), though some fraction of SO_4^{2-}(p) is likely directly emitted.

5. Summary and conclusions

A PCA was applied to continuous measurements of 22 primary pollutant tracers at the AMS 13 ground site in the Athabasca oil sands during the 2013 JOSM intensive study to elucidate the origins of airborne analytically unresolved hydrocarbons that were observed by GC-ITMS. The analysis identified 10 components. Three components correlated with the IVOC signature and were tentatively assigned to mine faces and, potentially, hot-water bitumen extraction facilities, the mine hauler fleet, and wet tailings ponds emissions. All three are anthropogenic activities that involve the handling of raw bitumen, i.e., the unearthing, mining and transport of crude bitumen, and the disposal of processed material that contains residual bitumen in wet tailings ponds. The PCA results are consistent with our previous

interpretation that the unresolved hydrocarbons originate from bitumen~~, which was~~ based on the similarity of the chromatograms with those obtained in a head space vapor analysis of ground-up bitumen in the laboratory.

Liggio et al. (2016) showed that these hydrocarbons constitute a group of IVOCs in the saturation vapor concentration (C^*) range 10^5 µg m^{-3}< C^* < 10^7 µg m^{-3} that contribute significantly to secondary organic aerosol formation and growth downwind of the oil sands facilities. The correlation of LO-OOA with two of the three IVOC components in the main PCA ~~analysis~~ and with PM_1 in the extended analysis ~~corroborates~~ is consistent with the high SOA formation potential of IVOCs and suggests that further differentiation may be needed and stresses the need for IVOCs to be routinely monitored. In particular, direct measurements of emissions throughout the processing of raw bitumen are needed to pinpoint source contributions more accurately and aid in the development of potential mitigation strategies.

The PCA ~~analysis~~ in this study suffered from several limitations. For instance, PCA does not provide insight into emission factors of individual facilities, though it does capture what conditions change ambient concentrations the most. Further, the receptor nature of PCA did not always discern between large source areas that may have many individual point sources coming together at the point of observation. For example, component 1 contains an obvious tailings pond signature because of its high correlation~~s~~ with anthropogenic VOCs, methane and TRS, but also includes several combustion sources, making interpretation of this IVOC source location more challenging. A longer continuous data set with a greater number of variables would have perhaps been able to resolve these different sources, including the various tailings ponds, of which there are 19 in the region, all with slightly different emission profiles (Small et al., 2015) .

Another limitation is the bias of this (and most) ground site data set towards surface-based emissions and the undersampling of stack emissions. Facility stacks were only observed in the daytime because at

night the mixing height is so low that the stacks are emitting directly into the residual layer. These emissions could be quantified using aircraft based platforms (Howell et al., 2014; Li et al., 2017; Baray et al., 2018). The PCA struggled most with the allocation of greenhouse gases. Mixing ratios of CO_2, in particular, were difficult to reconcile in this analysis due to a high background and large attenuation by biogenic activity and boundary layer meteorology. Forests greatly affected CO_2 levels in the region because it is taken up during the day when plants are photosynthetically active and emitted at night when plants undergo cellular respiration. This CO_2 source and sink appears to dominate the PCA, effectively masking relatively small emissions from tailings ponds, facilities, and tail pipes in particular from the mine hauling fleet.

Finally, there is a need for improved monitoring methods for IVOCs. For instance, future studies should focus on characterizing the VOCs in the above mentioned volatility range using a greater mass and time resolution instrument, such as a time-of-flight mass spectrometer (TOF-MS) or higher resolution separation methods (e.g., multi-dimensional gas chromatography), and also include measurement of speciated aerosol organic composition by, for example, thermal desorption aerosol GC (TAG) analysis (Williams et al., 2006). Future studies should also investigate how IVOC volatility distributions vary with source type and chemical age.

Acknowledgments

Funding for this study was provided by Environment and Climate Change Canada and the Canada-Alberta Oil Sands Monitoring program. The GC-ITMS used in this work was purchased using funds provided by the Canada Foundation for Innovation and matching funds by the Alberta government. TWT, JAH, DKB, FVA and GRW acknowledge financial support from the Natural Sciences and Engineering Research Council of Canada (NSERC) Collaborative Research and Training Experience Program (CREATE) program Integrating Atmospheric Chemistry and Physics from Earth to Space (IACPES).

6. References

Government of Alberta, oil sands information portal: http://osip.alberta.ca, access: 23-FEB-2017, 2017.

Allen, E. W.: Process water treatment in Canada's oil sands industry: II. A review of emerging technologies, J. Environ. Eng. Sci., 7, 499-524, 10.1139/s08-020, 2008.

Baray, S., Darlington, A., Gordon, M., Hayden, K. L., Leithead, A., Li, S. M., Liu, P. S. K., Mittermeier, R. L., Moussa, S. G., O'Brien, J., Staebler, R., Wolde, M., Worthy, D., and McLaren, R.: Quantification of methane sources in the Athabasca Oil Sands Region of Alberta by aircraft mass balance, Atmos. Chem. Phys., 18, 7361-7378, 10.5194/acp-18-7361-2018, 2018.

Bari, M., and Kindzierski, W. B.: Fifteen-year trends in criteria air pollutants in oil sands communities of Alberta, Canada, Environ. Int., 74, 200-208, 10.1016/j.envint.2014.10.009, 2015.

Bari, M. A., Kindzierski, W. B., and Spink, D.: Twelve-year trends in ambient concentrations of volatile organic compounds in a community of the Alberta Oil Sands Region, Canada, Environ. Int., 91, 40-50, 10.1016/j.envint.2016.02.015, 2016.

Bari, M. A., and Kindzierski, W. B.: Ambient fine particulate matter (PM2.5) in Canadian oil sands communities: Levels, sources and potential human health risk, Sci. Tot. Environm., 595, 828-838, 10.1016/j.scitotenv.2017.04.023, 2017.

Bari, M. A., and Kindzierski, W. B.: Ambient volatile organic compounds (VOCs) in communities of the Athabasca oil sands region: Sources and screening health risk assessment, Environ. Pollut., 235, 602-614, 10.1016/j.envpol.2017.12.065, 2018.

Bernstein, D. M.: Increased mortality in COPD among construction workers exposed to inorganic dust, Eur. Resp. J., 24, 512-512, 10.1183/09031936.04.00044504, 2004.

Bond, T. C., Streets, D. G., Yarber, K. F., Nelson, S. M., Woo, J. H., and Klimont, Z.: A technology-based global inventory of black and organic carbon emissions from combustion, J. Geophys. Res., 109, D14203, 10.1029/2003JD003697, 2004.

Briggs, N. L., and Long, C. M.: Critical review of black carbon and elemental carbon source apportionment in Europe and the United States, Atmos. Environ., 144, 409-427, 10.1016/j.atmosenv.2016.09.002, 2016.

Buhamra, S. S., Bouhamra, W. S., and Elkilani, A. S.: Assessment of air quality in ninety-nine residences of Kuwait, Environ. Technol., 19, 357-367, 10.1080/09593331908616691, 1998.

Burtscher, H., Scherrer, L., Siegmann, H. C., Schmidtott, A., and Federer, B.: Probing aerosols by photoelectric charging, J. Appl. Phys., 53, 3787-3791, 10.1063/1.331120, 1982.

Bytnerowicz, A., Fraczek, W., Schilling, S., and Alexander, D.: Spatial and temporal distribution of ambient nitric acid and ammonia in the Athabasca Oil Sands Region, Alberta, J. Limnol., 69, 11-21, 10.3274/jl10-69-s1-03, 2010.

The facts on Canada's oil sands: http://www.capp.ca/publications-and-statistics/publications/296225, access: April 20, 2017, 2016.

Carslaw, D. C., and Ropkins, K.: openair - An R package for air quality data analysis, Environ. Modell. Softw., 27-28, 52-61, 10.1016/j.envsoft.2011.09.008, 2012.

Carslaw, D. C., and Beevers, S. D.: Characterising and understanding emission sources using bivariate polar plots and k-means clustering, Environ. Modell. Softw., 40, 325-329, 10.1016/j.envsoft.2012.09.005, 2013.

Cattell, R. B.: The Scree Test For The Number Of Factors, Multivariate Behavioral Research, 1, 245-276, 10.1207/s15327906mbr0102_10, 1966.

Chalaturnyk, R. J., Don Scott, J., and Ozum, B.: Management of oil sands tailings, Petroleum Science and Technology, 20, 1025-1046, 10.1081/lft-120003695, 2002.

Charlson, R. J., Schwartz, S. E., Hales, J. M., Cess, R. D., Coakley, J. A., Hansen, J. E., and Hofmann, D. J.: Climate forcing by anthropogenic aerosols, Science, 255, 423-430, 10.1126/science.255.5043.423 1992.

Chen, H., Karion, A., Rella, C. W., Winderlich, J., Gerbig, C., Filges, A., Newberger, T., Sweeney, C., and Tans, P. P.: Accurate measurements of carbon monoxide in humid air using the cavity ring-down spectroscopy (CRDS) technique, Atmos. Meas. Tech., 6, 1031-1040, 10.5194/amt-6-1031-2013, 2013.

Cho, S., Morris, R., McEachern, P., Shah, T., Johnson, J., and Nopmongcol, U.: Emission sources sensitivity study for ground-level ozone and PM2.5 due to oil sands development using air quality modelling system: Part II – Source apportionment modelling, Atmos. Environm., 55, 542-556, 10.1016/j.atmosenv.2012.02.025, 2012.

Cross, E. S., Hunter, J. F., Carrasquillo, A. J., Franklin, J. P., Herndon, S. C., Jayne, J. T., Worsnop, D. R., Miake-Lye, R. C., and Kroll, J. H.: Online measurements of the emissions of intermediate-volatility and semi-volatile organic compounds from aircraft, Atmos. Chem. Phys., 13, 7845-7858, 10.5194/acp-13-7845-2013, 2013.

de Gouw, J. A., Middlebrook, A. M., Warneke, C., Ahmadov, R., Atlas, E. L., Bahreini, R., Blake, D. R., Brock, C. A., Brioude, J., Fahey, D. W., Fehsenfeld, F. C., Holloway, J. S., Le Henaff, M., Lueb, R. A., McKeen, S. A., Meagher, J. F., Murphy, D. M., Paris, C., Parrish, D. D., Perring, A. E., Pollack, I. B., Ravishankara, A. R., Robinson, A. L., Ryerson, T. B., Schwarz, J. P., Spackman, J. R., Srinivasan, A., and Watts, L. A.: Organic Aerosol Formation Downwind from the Deepwater Horizon Oil Spill, Science, 331, 1295-1299, 10.1126/science.1200320, 2011.

Trends in atmospheric methane: www.esrl.noaa.gov/gmd/ccgg/trends_ch4/, access: April 11, 2017, 2017a.

Trends in atmospheric carbon dioxide: www.esrl.noaa.gov/gmd/ccgg/trends/, access: April 11, 2017, 2017b.

National pollutant release inventory (NPRI): http://open.canada.ca/data/en/dataset/e40099ae-b116-4c48-9475-f3806fe5a6a6, access: October 5, 2016, 2013.

ECCC: Joint oil sands monitoring program emissions inventory compilation report, Environment and Climate Change Canada, Downsview, 2016.

Englander, J. G., Bharadwaj, S., and Brandt, A. R.: Historical trends in greenhouse gas emissions of the Alberta oil sands (1970-2010), Environm. Res. Lett., 8, 044036, 10.1088/1748-9326/8/4/044036, 2013.

Fares, S., Schnitzhofer, R., Jiang, X., Guenther, A., Hansel, A., and Loreto, F.: Observations of Diurnal to Weekly Variations of Monoterpene-Dominated Fluxes of Volatile Organic Compounds from Mediterranean Forests: Implications for Regional Modeling, Environm. Sci. Technol., 47, 11073-11082, 10.1021/es4022156, 2013.

Fenn, M. E., Bytnerowicz, A., Schilling, S. L., and Ross, C. S.: Atmospheric deposition of nitrogen, sulfur and base cations in jack pine stands in the Athabasca Oil Sands Region, Alberta, Canada, Environ. Pollut., 196, 497-510, 10.1016/j.envpol.2014.08.023, 2015.

Fioletov, V. E., McLinden, C. A., Cede, A., Davies, J., Mihele, C., Netcheva, S., Li, S. M., and O'Brien, J.: Sulfur dioxide (SO_2) vertical column density measurements by Pandora spectrometer over the Canadian oil sands, Atmospheric Measurement Techniques, 9, 2961-2976, 10.5194/amt-9-2961-2016, 2016.

Fuentes, J. D., Wang, D., Neumann, H. H., Gillespie, T. J., DenHartog, G., and Dann, T. F.: Ambient biogenic hydrocarbons and isoprene emissions from a mixed deciduous forest, J. Atmos. Chem., 25, 67-95, 10.1007/BF00053286, 1996.

Furimsky, E.: Emissions of carbon dioxide from tar sands plants in Canada, Energy Fuels, 17, 1541-1548, 10.1021/ef0301102, 2003.

Geron, C., Rasmussen, R., Arnts, R. R., and Guenther, A.: A review and synthesis of monoterpene speciation from forests in the United States, Atmos. Environm., 34, 1761-1781, 10.1016/S1352-2310(99)00364-7, 2000.

Gordon, M., Li, S. M., Staebler, R., Darlington, A., Hayden, K., O'Brien, J., and Wolde, M.: Determining air pollutant emission rates based on mass balance using airborne measurement data over the Alberta oil sands operations, Atmos. Meas. Tech., 8, 3745-3765, 10.5194/amt-8-3745-2015, 2015.

Grimmer, G., Brune, H., Deutschwenzel, R., Dettbarn, G., Jacob, J., Naujack, K. W., Mohr, U., and Ernst, H.: Contribution of polycyclic aromatic-hydrocarbons and nitro-derivatives to the carcinogenic impact of diesel-engine exhaust condensate evaluated by implantation into the lungs of rats, Cancer Lett., 37, 173-180, 10.1016/0304-3835(87)90160-1, 1987.

Guenther, A. B., Jiang, X., Heald, C. L., Sakulyanontvittaya, T., Duhl, T., Emmons, L. K., and Wang, X.: The Model of Emissions of Gases and Aerosols from Nature version 2.1 (MEGAN2.1): an extended and updated framework for modeling biogenic emissions, Geosci. Model Dev., 5, 1471-1492, 10.5194/gmd-5-1471-2012, 2012.

Guo, H., Wang, T., and Louie, P. K. K.: Source apportionment of ambient non-methane hydrocarbons in Hong Kong: Application of a principal component analysis/absolute principal component scores (PCA/APCS) receptor model, Environ. Pollut., 129, 489-498, 10.1016/j.envpol.2003.11.006, 2004.

Hair, J. F., Anderson, R. E., Tatham, R. L., and Black, W. C.: Multivariate data analysis, in, 7th edition ed., Prentice-Hall, Upper Saddle River, NJ, pp. 108 -110, 1998.

Harrison, R. M., Smith, D. J. T., and Luhana, L.: Source apportionment of atmospheric polycyclic aromatic hydrocarbons collected from an urban location in Birmingham, UK, Environ. Sci. Technol., 30, 825-832, 10.1021/es950252d, 1996.

Helmig, D., Klinger, L. F., Guenther, A., Vierling, L., Geron, C., and Zimmerman, P.: Biogenic volatile organic compound emissions (BVOCs) I. Identifications from three continental sites in the U.S, Chemosphere, 38, 2163-2187, 10.1016/S0045-6535(98)00425-1, 1999.

922 Holowenko, F. M., MacKinnon, M. D., and Fedorak, P. M.: Methanogens and sulfate-reducing bacteria in
923 oil sands fine tailings waste, Canadian Journal of Microbiology, 46, 927-937, 10.1139/cjm-46-10-927,
924 2000.
925 Howell, S. G., Clarke, A. D., Freitag, S., McNaughton, C. S., Kapustin, V., Brekovskikh, V., Jimenez, J. L.,
926 and Cubison, M. J.: An airborne assessment of atmospheric particulate emissions from the processing
927 of Athabasca oil sands, Atmos. Chem. Phys., 14, 5073-5087, 10.5194/acp-14-5073-2014, 2014.
928 Hsu, Y. M., Bytnerowicz, A., Fenn, M. E., and Percy, K. E.: Atmospheric dry deposition of sulfur and
929 nitrogen in the Athabasca Oil Sands Region, Alberta, Canada, Sci. Tot. Environm., 568, 285-295,
930 10.1016/j.scitotenv.2016.05.205, 2016.
931 Jautzy, J., Ahad, J. M. E., Gobeil, C., and Savard, M. M.: Century-Long Source Apportionment of PAHs in
932 Athabasca Oil Sands Region Lakes Using Diagnostic Ratios and Compound-Specific Carbon Isotope
933 Signatures, Environm. Sci. Technol., 47, 6155-6163, 10.1021/es400642e, 2013.
934 Jautzy, J. J., Ahad, J. M. E., Gobeil, C., Smirnoff, A., Barst, B. D., and Savard, M. M.: Isotopic Evidence for
935 Oil Sands Petroleum Coke in the Peace-Athabasca Delta, Environm. Sci. Technol., 49, 12062-12070,
936 10.1021/acs.est.5b03232, 2015.
937 Jimenez, J. L., Canagaratna, M. R., Donahue, N. M., Prevot, A. S. H., Zhang, Q., Kroll, J. H., DeCarlo, P. F.,
938 Allan, J. D., Coe, H., Ng, N. L., Aiken, A. C., Docherty, K. S., Ulbrich, I. M., Grieshop, A. P., Robinson, A.
939 L., Duplissy, J., Smith, J. D., Wilson, K. R., Lanz, V. A., Hueglin, C., Sun, Y. L., Tian, J., Laaksonen, A.,
940 Raatikainen, T., Rautiainen, J., Vaattovaara, P., Ehn, M., Kulmala, M., Tomlinson, J. M., Collins, D. R.,
941 Cubison, M. J., E., Dunlea, J., Huffman, J. A., Onasch, T. B., Alfarra, M. R., Williams, P. I., Bower, K.,
942 Kondo, Y., Schneider, J., Drewnick, F., Borrmann, S., Weimer, S., Demerjian, K., Salcedo, D., Cottrell,
943 L., Griffin, R., Takami, A., Miyoshi, T., Hatakeyama, S., Shimono, A., Sun, J. Y., Zhang, Y. M., Dzepina,
944 K., Kimmel, J. R., Sueper, D., Jayne, J. T., Herndon, S. C., Trimborn, A. M., Williams, L. R., Wood, E. C.,

945 Middlebrook, A. M., Kolb, C. E., Baltensperger, U., and Worsnop, D. R.: Evolution of Organic Aerosols
946 in the Atmosphere, Science, 326, 1525-1529, 10.1126/science.1180353, 2009.
947 Johnson, M. R., Crosland, B. M., McEwen, J. D., Hager, D. B., Armitage, J. R., Karimi-Golpayegani, M., and
948 Picard, D. J.: Estimating fugitive methane emissions from oil sands mining using extractive core
949 samples, Atmos. Environm., 144, 111-123, 10.1016/j.atmosenv.2016.08.073, 2016.
950 Jolliffe, I. T., and Cadima, J.: Principal component analysis: a review and recent developments,
951 Philosophical Transactions of the Royal Society A: Mathematical, Physical and Engineering Sciences,
952 374, 10.1098/rsta.2015.0202, 2016.
953 Kaiser, H. F.: The varimax criterion for analytic rotation in factor-analysis, Psychometrika, 23, 187-200,
954 10.1007/bf02289233, 1958.
955 Kindzierski, W. B., and Ranganathan, H. K. S.: Indoor and outdoor SO2 in a community near oil sand
956 extraction and production facilities in northern Alberta, J. Environ. Eng. Sci., 5, S121-S129,
957 10.1139/s06-022, 2006.
958 Landis, M. S., Pancras, J. P., Graney, J. R., Stevens, R. K., Percy, K. E., and Krupa, S.: Chapter 18 - Receptor
959 Modeling of Epiphytic Lichens to Elucidate the Sources and Spatial Distribution of Inorganic Air
960 Pollution in the Athabasca Oil Sands Region, in: Developments in Environmental Science, edited by:
961 Percy, K. E., Elsevier, 427-467, 2012.
962 Landis, M. S., Pancras, J. P., Graney, J. R., White, E. M., Edgerton, E. S., Legge, A., and Percy, K. E.: Source
963 apportionment of ambient fine and coarse particulate matter at the Fort McKay community site, in
964 the Athabasca Oil Sands Region, Alberta, Canada, Sci. Tot. Environm., 584, 105-117,
965 10.1016/j.scitotenv.2017.01.110, 2017.
966 Lee, A. K. Y., Adam, M. G., Liggio, J., Li, S.-M., Li, K., Willis, M. D., Abbatt, J. P. D., Tokarek, T. W., Odame-
967 Ankrah, C. A., Huo, J. A., Osthoff, H. D., Strawbridge, K. B., and Brook, J. R.: A large contribution of
968 anthropogenic organonitrate to secondary organic aerosol in Alberta oil sands, in prep., 2018.

969 Li, S.-M., Leithead, A., Moussa, S. G., Liggio, J., Moran, M. D., Wang, D., Hayden, K., Darlington, A.,
970 Gordon, M., Staebler, R., Makar, P. A., Stroud, C. A., McLaren, R., Liu, P. S. K., Oâ€™Brien, J.,
971 Mittermeier, R. L., Zhang, J., Marson, G., Cober, S. G., Wolde, M., and Wentzell, J. J. B.: Differences
972 between measured and reported volatile organic compound emissions from oil sands facilities in
973 Alberta, Canada, Proceedings of the National Academy of Sciences, 114, E3756-E3765,
974 10.1073/pnas.1617862114, 2017.
975 Liggio, J., Li, S.-M., Hayden, K., Taha, Y. M., Stroud, C., Darlington, A., Drollette, B. D., Gordon, M., Lee, P.,
976 Liu, P., Leithead, A., Moussa, S. G., Wang, D., O'Brien, J., Mittermeier, R. L., Brook, J., Lu, G., Staebler,
977 R., Han, Y., Tokarek, T. W., Osthoff, H. D., Makar, P. A., Zhang, J., Plata, D., and Gentner, D. R.: Oil
978 Sands Operations as a Large Source of Secondary Organic Aerosols, Nature, 534, 91-94,
979 10.1038/nature17646, 2016.
980 Marey, H. S., Hashisho, Z., Fu, L., and Gille, J.: Spatial and temporal variation in CO over Alberta using
981 measurements from satellites, aircraft, and ground stations, Atmos. Chem. Phys., 15, 3893-3908,
982 10.5194/acp-15-3893-2015, 2015.
983 Markovic, M. Z., VandenBoer, T. C., and Murphy, J. G.: Characterization and optimization of an online
984 system for the simultaneous measurement of atmospheric water-soluble constituents in the gas and
985 particle phases, J. Environ. Monit., 14, 1872-1884, 10.1039/C2EM00004K, 2012.
986 Masliyah, J., Zhou, Z. J., Xu, Z. H., Czarnecki, J., and Hamza, H.: Understanding water-based bitumen
987 extraction from athabasca oil sands, Can. J. Chem. Eng., 82, 628-654, 10.1002/cjce.5450820403,
988 2004.
989 McLinden, C. A., Fioletov, V., Boersma, K. F., Krotkov, N., Sioris, C. E., Veefkind, J. P., and Yang, K.: Air
990 quality over the Canadian oil sands: A first assessment using satellite observations, Geophys. Res.
991 Lett., 39, 8, 10.1029/2011gl050273, 2012.

992 Miller, S. M., Matross, D. M., Andrews, A. E., Millet, D. B., Longo, M., Gottlieb, E. W., Hirsch, A. I., Gerbig,
993 C., Lin, J. C., Daube, B. C., Hudman, R. C., Dias, P. L. S., Chow, V. Y., and Wofsy, S. C.: Sources of carbon
994 monoxide and formaldehyde in North America determined from high-resolution atmospheric data,
995 Atmos. Chem. Phys., 8, 7673-7696, 10.5194/acp-8-7673-2008, 2008.
996 Min, K. E., Pusede, S. E., Browne, E. C., LaFranchi, B. W., and Cohen, R. C.: Eddy covariance fluxes and
997 vertical concentration gradient measurements of NO and NO2 over a ponderosa pine ecosystem:
998 observational evidence for within-canopy chemical removal of NOx, Atmos. Chem. Phys., 14, 5495-
999 5512, 10.5194/acp-14-5495-2014, 2014.
1000 Nara, H., Tanimoto, H., Tohjima, Y., Mukai, H., Nojiri, Y., Katsumata, K., and Rella, C. W.: Effect of air
1001 composition (N_2, O_2, Ar, and H_2O) on CO_2 and CH_4 measurement by wavelength-scanned cavity ring-
1002 down spectroscopy: calibration and measurement strategy, Atmos. Meas. Tech., 5, 2689-2701,
1003 10.5194/amt-5-2689-2012, 2012.
1004 Nimana, B., Canter, C., and Kumar, A.: Energy consumption and greenhouse gas emissions in the
1005 recovery and extraction of crude bitumen from Canada's oil sands, Appl. Energy, 143, 189-199,
1006 10.1016/j.apenergy.2015.01.024, 2015a.
1007 Nimana, B., Canter, C., and Kumar, A.: Energy consumption and greenhouse gas emissions in upgrading
1008 and refining of Canada's oil sands products, Energy, 83, 65-79, 10.1016/j.energy.2015.01.085, 2015b.
1009 Detailed facility information: http://www.ec.gc.ca/inrp-npri/donnees-
1010 data/index.cfm?do=facility_information&lang=En&opt_npri_id=0000002274&opt_report_year=2013
1011 , access: April 13, 2017, 2013.
1012 Odame-Ankrah, C. A.: Improved detection instrument for nitrogen oxide species, Ph.D., Chemistry,
1013 University of Calgary, http://hdl.handle.net/11023/2006, 10.5072/PRISM/26475, Calgary, 2015.

1014 Onasch, T. B., Trimborn, A., Fortner, E. C., Jayne, J. T., Kok, G. L., Williams, L. R., Davidovits, P., and
1015 Worsnop, D. R.: Soot Particle Aerosol Mass Spectrometer: Development, Validation, and Initial
1016 Application, Aerosol Sci. Technol., 46, 804-817, 10.1080/02786826.2012.663948, 2012.
1017 Paatero, P., and Tapper, U.: Positive matrix factorization: A non-negative factor model with optimal
1018 utilization of error estimates of data values, Environmetrics, 5, 111-126,
1019 doi:10.1002/env.3170050203, 1994.
1020 Parajulee, A., and Wania, F.: Evaluating officially reported polycyclic aromatic hydrocarbon emissions in
1021 the Athabasca oil sands region with a multimedia fate model, Proceedings of the National Academy
1022 of Sciences, 111, 3344-3349, 10.1073/pnas.1319780111, 2014.
1023 Paul, D., and Osthoff, H. D.: Absolute Measurements of Total Peroxy Nitrate Mixing Ratios by Thermal
1024 Dissociation Blue Diode Laser Cavity Ring-Down Spectroscopy, Anal. Chem., 82, 6695-6703,
1025 10.1021/ac101441z, 2010.
1026 Penner, T. J., and Foght, J. M.: Mature fine tailings from oil sands processing harbour diverse
1027 methanogenic communities, Canadian Journal of Microbiology, 56, 459-470, 10.1139/w10-029, 2010.
1028 Percy, K. E.: Ambient Air Quality and Linkage to Ecosystems in the Athabasca Oil Sands, Alberta, Geosci.
1029 Can., 40, 182-201, 10.12789/geocanj.2013.40.014, 2013.
1030 Peters, T. M., and Leith, D.: Concentration measurement and counting efficiency of the aerodynamic
1031 particle sizer 3321, J. Aerosol Sci., 34, 627-634, 10.1016/s0021-8502(03)00030-2, 2003.
1032 Quagraine, E. K., Headley, J. V., and Peterson, H. G.: Is biodegradation of bitumen a source of recalcitrant
1033 naphthenic acid mixtures in oil sands tailing pond waters?, J. Environ. Sci. Health Part A-Toxic/Hazard.
1034 Subst. Environ. Eng., 40, 671-684, 10.1081/ese-200046637, 2005.
1035 Rooney, R. C., Bayley, S. E., and Schindler, D. W.: Oil sands mining and reclamation cause massive loss of
1036 peatland and stored carbon, Proc. Natl. Acad. Sci. U.S.A., 109, 4933-4937, 10.1073/pnas.1117693108,
1037 2012.

RStudio Boston, M.: Integrated development environment for R, 2017.

Shahimin, M. F. M., and Siddique, T.: Sequential biodegradation of complex naphtha hydrocarbons under methanogenic conditions in two different oil sands tailings, Environ. Pollut., 221, 398-406, 10.1016/j.envpol.2016.12.002, 2017.

Siddique, T., Fedorak, P. M., and Foght, J. M.: Biodegradation of short-chain n-alkanes in oil sands tailings under methanogenic conditions, Environ. Sci. Technol., 40, 5459-5464, 10.1021/es060993m, 2006.

Siddique, T., Gupta, R., Fedorak, P. M., MacKinnon, M. D., and Foght, J. M.: A first approximation kinetic model to predict methane generation from an oil sands tailings settling basin, Chemosphere, 72, 1573-1580, 10.1016/j.chemosphere.2008.04.036, 2008.

Siddique, T., Penner, T., Semple, K., and Foght, J. M.: Anaerobic Biodegradation of Longer-Chain n-Alkanes Coupled to Methane Production in Oil Sands Tailings, Environm. Sci. Technol., 45, 5892-5899, 10.1021/es200649t, 2011.

Siddique, T., Penner, T., Klassen, J., Nesbo, C., and Foght, J. M.: Microbial Communities Involved in Methane Production from Hydrocarbons in Oil Sands Tailings, Environ. Sci. Technol., 46, 9802-9810, 10.1021/e53022024, 2012.

Simpson, I. J., Blake, N. J., Barletta, B., Diskin, G. S., Fuelberg, H. E., Gorham, K., Huey, L. G., Meinardi, S., Rowland, F. S., Vay, S. A., Weinheimer, A. J., Yang, M., and Blake, D. R.: Characterization of trace gases measured over Alberta oil sands mining operations: 76 speciated C2–C10 volatile organic compounds (VOCs), CO_2, CH_4, CO, NO, NO_2, NO_y, O_3 and SO_2, Atmos. Chem. Phys., 10, 11931-11954, 10.5194/acp-10-11931-2010, 2010.

Small, C. C., Cho, S., Hashisho, Z., and Ulrich, A. C.: Emissions from oil sands tailings ponds: Review of tailings pond parameters and emission estimates, Journal of Petroleum Science and Engineering, 127, 490-501, 10.1016/j.petrol.2014.11.020, 2015.

1062 Thurston, G. D., and Spengler, J. D.: A quantitative assessment of source contributions to inhalable
1063 particulate matter pollution in metropolitan Boston, Atmos. Environ., 19, 9-25, 10.1016/0004-
1064 6981(85)90132-5, 1985.
1065 Thurston, G. D., Ito, K., and Lall, R.: A source apportionment of U.S. fine particulate matter air pollution,
1066 Atmos. Environ., 45, 3924-3936, 10.1016/j.atmosenv.2011.04.070, 2011.
1067 Tokarek, T. W., Huo, J. A., Odame-Ankrah, C. A., Hammoud, D., Taha, Y. M., and Osthoff, H. D.: A gas
1068 chromatograph for quantification of peroxycarboxylic nitric anhydrides calibrated by thermal
1069 dissociation cavity ring-down spectroscopy, Atmos. Meas. Tech., 7, 3263-3283, 10.5194/amt-7-3263-
1070 2014, 2014.
1071 Tokarek, T. W., Brownsey, D. K., Jordan, N., Garner, N. M., Ye, C. Z., Assad, F. V., Peace, A., Schiller, C. L.,
1072 Mason, R. H., Vingarzan, R., and Osthoff, H. D.: Biogenic emissions and nocturnal ozone depletion
1073 events at the Amphitrite Point Observatory on Vancouver Island, Atmosphere-Ocean, 55, 121-132,
1074 10.1080/07055900.2017.1306687, 2017a.
1075 Tokarek, T. W., Brownsey, D. K., Jordan, N., Garner, N. M., Ye, C. Z., Assad, F. V., Peace, A., Schiller, C. L.,
1076 Mason, R. H., Vingarzan, R., and Osthoff, H. D.: Biogenic Emissions and Nocturnal Ozone Depletion
1077 Events at the Amphitrite Point Observatory on Vancouver Island, Atmosphere-Ocean, 1-12,
1078 10.1080/07055900.2017.1306687, 2017b.
1079 Wang, S. C., and Flagan, R. C.: Scanning electrical mobility spectrometer, Aerosol Sci. Technol., 13, 230-
1080 240, 10.1080/02786829008959441, 1990.
1081 Wang, X. L., Chow, J. C., Kohl, S. D., Percy, K. E., Legge, A. H., and Watson, J. G.: Characterization of
1082 PM2.5 and PM10 fugitive dust source profiles in the Athabasca Oil Sands Region, J. Air Waste Manag.
1083 Assoc., 65, 1421-1433, 10.1080/10962247.2015.1100693, 2015.

1084 Wang, X. L., Chow, J. C., Kohl, S. D., Percy, K. E., Legge, A. H., and Watson, J. G.: Real-world emission
1085 factors for Caterpillar 797B heavy haulers during mining operations, Particuology, 28, 22-30,
1086 10.1016/j.partic.2015.07.001, 2016.
1087 Warren, L. A., Kendra, K. E., Brady, A. L., and Slater, G. F.: Sulfur Biogeochemistry of an Oil Sands
1088 Composite Tailings Deposit, Front. Microbiol., 6, 14, 10.3389/fmicb.2015.01533, 2016.
1089 Watson, J., Chow, J., Wang, X., Zielinska, B., Kohl, S., and Gronstal, S.: Characterization of real-world
1090 emissions from nonroad mining trucks in the Athabasca Oil Sands Region during September, 2009,
1091 2013.
1092 WBEA: WBEA annual report 2013, Wood Buffalo Environmental Association, 2013.
1093 Whaley, C. H., Makar, P. A., Shephard, M. W., Zhang, L., Zhang, J., Zheng, Q., Akingunola, A., Wentworth,
1094 G. R., Murphy, J. G., Kharol, S. K., and Cady-Pereira, K. E.: Contributions of natural and anthropogenic
1095 sources to ambient ammonia in the Athabasca Oil Sands and north-western Canada, Atmos. Chem.
1096 Phys., 18, 2011-2034, 10.5194/acp-18-2011-2018, 2018.
1097 Williams, B. J., Goldstein, A. H., Kreisberg, N. M., and Hering, S. V.: An in-situ instrument for speciated
1098 organic composition of atmospheric aerosols: Thermal Desorption Aerosol GC/MS-FID (TAG), Aerosol
1099 Sci. Technol., 40, 627-638, 10.1080/02786820600754631, 2006.
1100 Wilson, N. K., Barbour, R. K., Chuang, J. C., and Mukund, R.: Evaluation of a real-time monitor for fine
1101 particle-bound PAH in air, Polycycl. Aromat. Compd., 5, 167-174, 10.1080/10406639408015168,
1102 1994.
1103 Yang, C., Wang, Z., Yang, Z., Hollebone, B., Brown, C. E., Landriault, M., and Fieldhouse, B.: Chemical
1104 Fingerprints of Alberta Oil Sands and Related Petroleum Products, Environmental Forensics, 12, 173-
1105 188, 10.1080/15275922.2011.574312, 2011.

Yeh, S., Jordaan, S. M., Brandt, A. R., Turetsky, M. R., Spatari, S., and Keith, D. W.: Land Use Greenhouse Gas Emissions from Conventional Oil Production and Oil Sands, Environm. Sci. Technol., 44, 8766-8772, 10.1021/es1013278, 2010.

Zhang, Y., Wang, Y., Chen, G., Smeltzer, C., Crawford, J., Olson, J., Szykman, J., Weinheimer, A. J., Knapp, D. J., Montzka, D. D., Wisthaler, A., Mikoviny, T., Fried, A., and Diskin, G.: Large vertical gradient of reactive nitrogen oxides in the boundary layer: Modeling analysis of DISCOVER-AQ 2011 observations, J. Geophys. Res.-Atmos., 121, 1922-1934, 10.1002/2015jd024203, 2016.

Supplementary information for

Principal component analysis of summertime ground site measurements in the Athabasca oil sands with a focus on analytically unresolved intermediate volatility organic compounds~~: Sources of IVOCs~~

Travis W. Tokarek[1], Charles A. Odame-Ankrah[1], Jennifer A. Huo[1], Robert McLaren[2], Alex K. Y. Lee[3, 4], Max G. Adam[4], Megan D. Willis[5], Jonathan P. D. Abbatt[5], Cristian Mihele[6], Andrea Darlington[6], Richard L. Mittermeier[6], Kevin Strawbridge[6], Katherine L. Hayden[6], Jason S. Olfert[7], Elijah. G. Schnitzler[8], Duncan K. Brownsey[1], Faisal V. Assad[1], Gregory R. Wentworth[5, a], Alex G. Tevlin[5], Douglas E. J. Worthy[6], Shao-Meng Li[6], John Liggio[6], Jeffrey R. Brook[6], and Hans D. Osthoff[1*]

[1] Department of Chemistry, University of Calgary, Calgary, Alberta, T2N 1N4, Canada

[2] Centre for Atmospheric Chemistry, York University, Toronto, Ontario M3J 1P3, Canada

[3] Department of Civil and Environmental Engineering, National University of Singapore, Singapore 117576, Singapore.

[4] NUS Environmental Research Institute, National University of Singapore, Singapore

[5] Department of Chemistry, University of Toronto, Toronto, Ontario, M5S 3H6, Canada

[6] Air Quality Research Division, Environment and Climate Change Canada, Toronto, Ontario, M3H 5T4, Canada

[7] Department of Mechanical Engineering, University of Alberta, Edmonton, Alberta, T6G 1H9, Canada

[8] Department of Chemistry, University of Alberta, Edmonton, Alberta, T6G 2G2, Canada

[a] Now at: Environmental Monitoring and Science Division, Alberta Environment and Parks, Edmonton, Alberta, T5J 5C6, Canada

* Corresponding author

Table of contents

Descriptions of instrumentation used

A Griffin 450 gas chromatograph equipped with a cylindrical ion trap mass spectrometer and electron impact ionization (GC-ITMS) was used to quantify selected VOCs including o-xylene, decane, undecane, 1,2,3- and 1,2,4-trimethylbenzene (TMB), and several monoterpenes (i.e., α-pinene, ß-pinene and limonene). The GC-ITMS primary responsibility was the quantification of monoterpenes. The remaining VOCs quantified were chosen because (a) they sufficiently resolved on the analytical column, and (b) response factors could be determined, either because the compounds of interest were part of the VOC standard used in the field (such as the aromatics o-xylene, 1,2,3- and 1,2,4-TMB, see below) or relative response factors were determined post-campaign. Operation, calibration and performance of this instrument have been described elsewhere (Tokarek et al., 2017; Liggio et al., 2016). The GC-ITMS sampled from a 3.6 m long stainless-steel inlet with an o.d. of 0.635 cm from a height of 5 m above ground. A 1 m long section of the inlet was heated to 110 °C and optimized to remove interference due to O_3 while avoiding decomposition of alkenes (Tokarek et al., 2017). The GC oven was programmed as follows: hold at 40 °C for 3.00 min, heat at 1.5 °C min^{-1} to 70° C (reached at 23.00 min), heat at 5° C min^{-1} to 200 °C (reached at 49.00 min) and hold for 4 min (total 53.00 min). This was followed by a 5 min recovery time to allow the oven and pre-concentration trap to cool back to 40 °C. The ion trap mass spectrometer was set to an *m/z* range of 50-425. After data reduction, the GC-ITMS generated 10-minute average concentrations of each VOC quantified every hour.

During the campaign, the GC-ITMS was calibrated in the field using an IONICON VOC standard (Table S-1) containing (in addition to VOCs that the GC-ITMS did not detect) α-pinene and o-xylene at mixing ratios of ~ 1 ppmv and an uncertainty of 5% and 6%, respectively. A commercial calibrator assembly (IONICON, GCU Standard) was used to deliver diluted calibration mixtures. The instrument responses to the VOC standards were linear ($R^2 > 0.99$). The GC-ITMS was calibrated for other VOCs offline relative to α-pinene. In the field, there was no noticeable carry-over (i.e., memory effects) of IVOCs, which was

occasionally evaluated by flooding the inlet with purified, VOC-free air.

Matrices of ions plotted against retention times for the total ion chromatograms (shown in Figure 2 in the main manuscript) are shown in Fig. S-1. In both cases, the greatest intensity is with masses are associated with alkanes (i.e., *m/z* 55, 57, 67, 69, etc.).

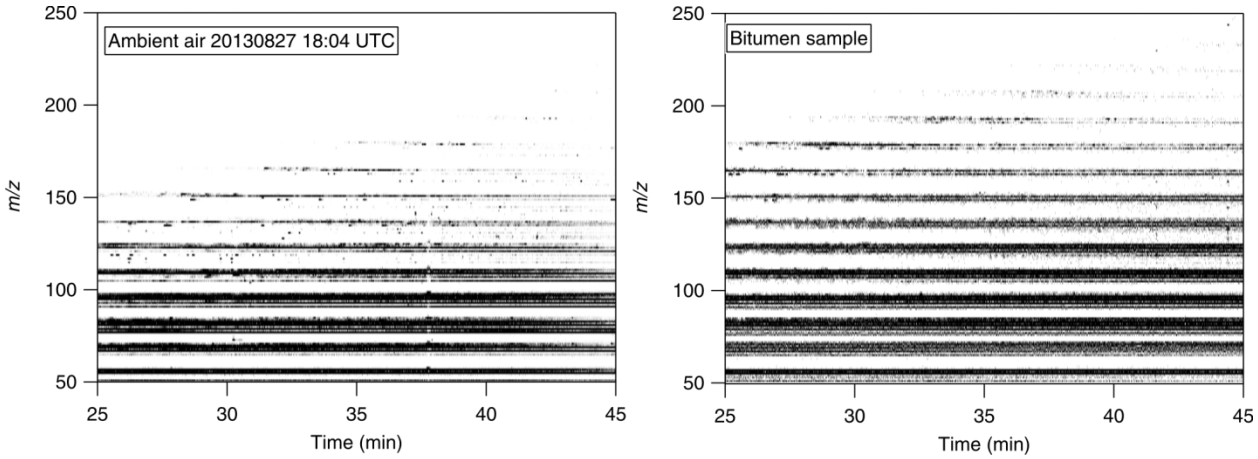

Figure S-1. Scatter of ions as a function of retention time for the total ion chromatograms shown in Figure 2 of the main manuscript. Darker pixels represent a higher intensity than lighter pixels.

Mixing ratios of carbon monoxide (CO), carbon dioxide (CO_2) and methane (CH_4) in ambient air were quantified using a commercial cavity ring-down spectrometer (Picarro G2401) (Nara et al., 2012; Chen et al., 2013). Ambient air was sampled from a height of 10 m through 0.635 cm outer diameter (o.d.) perfluoroalkoxyalkane (PFA) Teflon™ tubing and a 47 mm diameter, 1 µm pore filter at a flow rate of ~0.5 L min^{-1}. A scrubber ($MgClO_4$) was installed at the base of the sample line to remove water from the air. Operating procedures developed for Canada's greenhouse gas network of monitors across all stations in Canada by the Climate Division of ECCC were followed (ECCC, 2013b).The cavity ring-down spectrometer was calibrated every few days with calibrated standard gas mixtures (Scott-Marrin); a target background mixture (CO_2 at a mixing ratio of 379.5 parts-per-million by volume (ppmv), CH_4 at 1.976 ppmv and CO at 198.4 parts-per-billion by volume (ppbv)) and a working mixture (CO_2 = 452.15

ppmv, CH_4 = 2.988 ppmv, CO = 494.5 ppbv). The estimated precision of 1 min data was ±0.12 ppmv, ±0.6 ppbv, and ±1.89 ppbv for CO_2, CH_4 and CO respectively, while the estimated accuracy was < 1 ppmv, < 3 ppbv, and < 4 ppbv, respectively.

Mixing ratios of total odd nitrogen ($NO_y \equiv NO + NO_2 + \Sigma PAN + \Sigma AN + HNO_3 + HONO + 2N_2O_5 + ClNO_2 + ...$) were measured by a chemiluminescence analyzer equipped with a heated Molybdenum converter (Thermo 42i) as described elsewhere (Tokarek et al., 2014; Odame-Ankrah, 2015).

The total sulfur (TS) measurements were conducted using a thermal oxidizer (Thermo Scientific Model CON101) to convert TS to SO_2 and detected using a pulsed-fluorescence analyzer (Thermo Scientific, Model 43iTLE). SO_2 was measured directly with a second analyzer (Thermo Scientific, Model 43iTLE). Total reduced sulfur (TRS) mixing ratios were calculated by subtracting mixing ratios of SO_2 from TS.

Concentrations of particle-surface bound polycyclic aromatic hydrocarbons (pPAH) were measured using a photoelectric aerosol sensor (EcoChem Analytics, Model PAS 2000CE) (Wilson et al., 1994; Burtscher et al., 1982).

Two soot-particle aerosol mass spectrometers (SP-AMS, Aerodyne Research, Inc.) (Onasch et al., 2012) measured non-refractory PM_1 components. Both SP-AMS were high resolution time-of-flight aerosol mass spectrometers (HR-ToF-AMS) fitted with a diode pumped Nd:YAG 1064 nm laser vaporizer; one SP-AMS had its oven removed to measure black carbon containing particles only using the laser. Direct calibrations of rBC using mono-disperse "Regal Black" (Cabot Corp. R400) particles were carried out three times during the 2013 JOSM intensive study. Positive Matrix Factorization (PMF) was performed to identify the potential sources of organic aerosol as described in the companion study (Adam et al., in prep). Factors associated with primary aerosol, i.e., hydrocarbon-like organic aerosol (HOA), a less oxidized oxygenated organic aerosol factor (LO-OOA) and measured refractory black carbon (rBC) were added as variables for PCA analysis. Mass spectra associated with LO-OOA exhibited H/C, O/C and N/C

ratios of ~1.62, ~0.36, and ~0.004, respectively; while the O/C and N/C ratios are similar to HOA, the H/C ratio of LO-OOA more resembles the more oxidized OOA factor (MO-OOA) (Adam et al., in prep.).

Particle volumes were calculated (assuming spherical particle shapes) from sub- and super-micron size distributions acquired using a scanning mobility particle sizer (SMPS, TSI with a differential mobility analyzer model 3081 and condensation particle counter model 3776; PM_1) and a 0.071 cm impactor over the size range of 13.6 nm to 736.5 nm and an Aerodynamic Particle Sizer (APS, TSI 3321; PM_{10-1}) over the size range 1.04 µm to 10.4 µm, respectively. Both instruments were operated at ambient relative humidity. The SMPS sampled through conductive silicon tubing to minimize wall losses due to wall charges. The APS was operated from a container located on top of the trailer and sampled from a 1.6 m tall, ½ o.d. aluminum tube whose tip was bent into a U-shape.

An ambient ion monitor – ion chromatograph (AIM-IC) (Markovic et al., 2012) was used to measure hourly averaged gas-phase NH_3 and $PM_{2.5}$ particle-phase (i.e., of particles < 2.5 µm diameter) NH_4^+ concentrations. High time-resolution particle-phase NH_4^+ measurements made by the SP-AMS were scaled by interpolated phase ratios observed by AIM-IC to calculate gas-phase NH_3 concentrations at high time resolution. This approach assumes the same phase ratios for $PM_{2.5}$ as for PM_1.

Determination of optimum PCA solution

The full component pattern (before component removal, with rotation, i.e., showing 22 components for 22 variables) obtained for this data set is shown in Table S-2. A common challenge in PCA is the determination of the maximum number of components to retain in the analysis. Several criteria are used for this purpose: the latent root criterion, where only components with eigenvalues greater than 1 are considered significant, the 5% variance criterion, where the last component selected accounts for only a small portion (<5%) of the variance, the 95% cumulative percentage of variance criterion, where the extracted components account for at least 95% of the total variance, and the Scree test. In the latter, the eigenvalues are plotted against the number of components in the order of extraction (Fig. S-2); to avoid including too many components with unique variance, the number of acceptable components is located at the point where this plot becomes horizontal. The latent root criterion is most commonly used, but tends to extract too few components when the number of variables is < 20 (Hair et al., 1998). The Scree test, on the other hand, often requires "some art in administering it" (Cattell, 1966), i.e., is subjective, though generally results in the inclusion of two or three more components than the latent root criterion (Hair et al., 1998).

The maximum component number for each criterion are summarized in Table S-9. The Scree test plot (Fig. S-1) shows two plateaus where the slope becomes approximately horizontal: The first is located at N = 5 and the second at N = 12. The latent root criterion and the <5% variance method suggests a 7-component solution, whereas the >95% percentage of variance criterion suggests using a 10-component solution. Hair et al. (1998) recommend to examine component solutions with differing numbers of components to evaluate which best represents the structure of the variables. In the following, solutions are presented in ascending order of extracted components.

5-component solution

As a first attempt at interpretation of the PCA, the first cut-off of the Scree test criterion was chosen (N = 5 variables). The results (after Varimax rotation) are presented in Table S-3.

The 5-component solution accounts for a cumulative variance of 81.0 % after rotation. Communalities for the analysis, i.e., the fraction of total pollutant observations accounted for by the PCA (Otto, 2007), are greater than 70% for 18 variables. The lowest communalities were obtained for gas-phase ammonia (0.40), CO (0.48) and PM_{10-1} (0.51). TRS and the IVOCs were also relatively poorly represented (0.63 and 0.73, respectively). All eigenvalues are greater than 1.

The component accounting for most of the variance of the data, component 1, is strongly associated with all of the anthropogenic VOCs (with correlations of $r > 0.8$) and TRS ($r = 0.76$), weakly associated with CH_4 ($r = 0.62$), HOA ($r = 0.44$), LO-OOA ($r = 0.59$), IVOCs ($r = 0.47$), and CO ($r = 0.53$), and poorly associated with NO_y and TS ($r = 0.25$ and $r = 0.28$, respectively). Component 1 is consistent with tailings ponds emissions with potentially small contributions from nearby facilities (interpreted from weak and poor correlations with rBC ($r = 0.33$) and NO_y ($r = 0.25$)), which would otherwise remain unexplained.

Component 2 is strongly associated with the combustion tracers NO_y ($r = 0.83$), rBC ($r = 0.89$) and pPAH ($r = 0.83$) and weakly associated with IVOCs ($r = 0.61$), gas-phase ammonia ($r = 0.34$), undecane ($r = 0.31$), and CH_4 (0.38), but poorly and not ~~significantly~~ with CO or CO_2 ($r = 0.19$ and 0.06, respectively); this component is identified as mine fleet emissions. Component 3 is strongly associated ($r > 0.9$) with the biogenic VOCs and weakly ($r = 0.55$) associated with CO_2 and is identified as a biogenic component. Component 4 is strongly associated with SO_2 and TS ($r = 0.93$ and 0.91, respectively) and is consistent with emissions from upgrader facilities. These four components persisted, with little variation, in all solutions with a greater number of selected components (see below).

Component 5 is strongly associated with CO_2 ($r = 0.71$), and weakly associated with PM_{10-1} ($r = 0.57$), CH_4 ($r = 0.53$) and CO ($r = 0.40$). We are not aware of a source type that would fit this profile, i.e., combine

this particular set of pollutants without also being associated with NO_y (r = 0.02). This suggests that this component is an artifact arising from an insufficient number of components used in the analysis and motivates the inclusion of more components.

6-component solution

A 6-component solution is shown in Table S-4. Satisfying the percentage of variance criterion of the last component accounting for less than 5% of the variance (4.6% in this case, Table S-2) was selected. This solution accounts for a total variance of 85.23%. The first four components are essentially unchanged from the 5-component solution (with the exception of LO-OOA in component 2 becoming more poorly correlated (r = 0.22)). Component 5 is strongly associated with IVOCs (r = 0.70) and weakly associated with LO-OOA (r = 0.60), and TRS (r = 0.56). Component 6 is strongly associated with PM_{10-1} (r = 0.81) and weakly associated with CO_2 (r = 0.62), CH_4 (r = 0.41), HOA (r = 0.30) and NH_3 (r = 0.36) and, unlike the 5-component solution, not associated with CO.

7-component solution

Next, the latent root criterion gives a 7-component solution. The PCA results (after Varimax rotation) are presented in Table S-5. The seven components account for a cumulative variance of 88.7% after rotation. Communalities for the analysis are all greater than 60%, with the lowest communality obtained for CO (0.61). All eigenvalues are greater than 1.

Components 1 through 4 have the same associations with similar r values as those in the 5-component analysis, with the only significant exception a poorer association (r = 0.20) of component 2 with gas-phase ammonia.

The identifications of components 5 through 7 of the 7-component solution are murky at best. Component 5 is weakly associated with TRS (r = 0.56) and IVOCs (r = 0.66). Component 6 is strongly

associated with PM_{10-1} volume (r = 0.89), and weakly with CO_2 (r = 0.54), and CH_4 (r = 0.36) and appears to be combination of a dust component with a source of greenhouse gases, whereas component 7 is strongly associated with gas-phase ammonia (r = 0.82) and poorly associated with CO (r = 0.29). Both appear to be amalgamations of distinct sources and suggest that too few components were selected. Hair et al. (1998) note that the latent root criterion has a tendency to extract a conservative number of components if the number of variables is < 20, close to the 22 variables in this analysis, consistent with what is observed here. Hence, the 7-component solution is sub-optimal.

8-component solution

An 8-component solution is presented in Table S-6. Not satisfying any criterion, it is included here for the sake of completeness. Owing to the inclusion of an additional component, the cumulative variance improved to 91.6%. The greatest improvement was seen for CO, gas-phase ammonia, as well as the IVOCs, whose communalities increased from 0.61, 0.91, and 0.80 (for the 7-component solution) to 0.96, 0.96 and 0.84, respectively.

The main effect of the inclusion of an additional component was the separation of component 7 into two distinct components: one of these was strongly associated with gas-phase ammonia (r = 0.92), and the other was strongly associated with CO (r = 0.85). A considerable fraction of the CO observed in the region is generated as a byproduct of the photochemical oxidation of hydrocarbons (Shephard et al., 2015); component 8 appears to capture this source, whereas component 1 captures the anthropogenic emissions. The area near the oil sands mining operations is enriched in ammonia, which originates from multiple sources: it is used as a floating agent to separate and recover bitumen from tar and is generated during bitumen upgrading (called hydrotreating) in which N is removed as NH_3, and can be present as a contaminant in tailing ponds. Other sources, such as agricultural activities, biological decay processes, and smoldering fires are relatively minor in the region (Bytnerowicz et al., 2010). The poor

association of component 2 with ammonia (r = 0.22) may capture the use of ammonia as a floating agent, whereas component 8 embodies the remaining sources.

Component 5 is strongly associated with IVOCs (r = 0.71), and weakly associated with LO-OOA (r = 0.65) and TRS (r = 0.40). It is unclear if these variables originate from the same source or are forced together as a result of having chosen too few components. Considering that component 7 is split when an additional component is used (see below), the latter is more likely. Component 6 remains strongly associated with PM_{10-1} volume (r = 0.89), and weakly associated with CO_2 (r = 0.53), and CH_4 (r = 0.35) and is difficult to interpret. Because of the unclear classification of components 5 through 8, the 8-component solution is rejected.

9-component solution

A 9-component solution is presented in Table S-7. Components 1 through 8 describe sources that are qualitatively similar to those provided by the 8-component solution. Component 9 is strongly associated with TRS (r = 0.71) and poorly associated with o-xylene (r = 0.30); its profile is consistent with tailings ponds emission, where the presence of naphtha as a diluent gives rise to BTEX emissions and bacteria produce reduced sulfur compounds (Small et al., 2015; Warren et al., 2016). Component 6 is strongly associated with PM_{10-1} (r = 0.89) and weakly associated with CO_2 (r = 0.54) and CH_4 (r = 0.41). We have decided to reject this solution on the basis that < 95 % cumulative variance is observed.

10-component solution

Next, a 10-component solution with cumulative variance of 95.5%, satisfying the 95% criterion, was considered. With this solution, all communalities are >0.85 (Table 3). Component 6 is strongly associated with CO_2 (r = 0.77) and weakly associated with CH_4 (r = 0.59) but is not associated with other combustion tracers and is identified as inactive open-pit mines (see main text). Component 7 is strongly correlated

253 with PM_{10-1} (r = 0.93) and is identified as wind-blown dust. Component 8 and 9 are strongly associated
254 with a single variable each, gas-phase ammonia (r = 0.94) and CO (r = 0.87), respectively. Component 10
255 is strongly associated with TRS (r = 0.71) and weakly associated with o-xylene (r = 0.32). Overall, this
256 component is most consistent with a tailings ponds source, where the presence of naphtha as diluent
257 gives rise to BTEX emissions, and sulfur-reducing bacteria are at work (Small et al., 2015; Warren et al.,
258 2016). Overall, the 10-component solution was judged to be optimal.
259
260 **11-component solution**
261 The 11-component analysis is presented in Table S-8. Component 10 is now strongly associated with LO-
262 OOA (r = 0.72) and weakly with rBC (r = 0.34)~~,~~ and has a low eigenvalue of 0.87. This solution is therefore
263 rejected as we believe it contains too many components.
264

Discussion of low-eigenvalue components

Component 6: A non-combustion source of CO_2 and CH_4

Component 6 of the analysis has a strong association with the greenhouse gases CO_2 ($r = 0.77$) and a weak association with CH_4 ($r = 0.59$) but is not associated with tracers of combustion (i.e., NO_y, pPAH, rBC) or naphtha (i.e., anthropogenic VOCs).

A significant amount of carbon is stored in bitumen, which, on geological time scales, conduces formation of CO_2 and CH_4 (i.e., natural gas) reservoirs and pools. When bitumen is mined, substantial emissions of CO_2 and, in particular, of CH_4 occur (Johnson et al., 2016). It is unclear, though, to what extent these greenhouse gases are released from "hot spots" (i.e., from a small number of locations) through surface cracks and fissures in the mine faces, or from new material that is exposed and then releases greenhouse gases during material handling, transport and processing (Johnson et al., 2016). The PCA analysis presented here would be more consistent with the "hot spots" hypothesis since component 6 is not associated with NOy, PAHs, or CO, which are expected to be emitted by the Diesel machinery involved in surface mining (i.e., active disturbance of the bitumen).

Another potential source contribution to component 6 is the degradation of peat and surface soil. Peatland soils, as they occur in the boreal forest surrounding the AMS 13 site, have long been recognized as important contributors to greenhouse gas fluxes and may also be contributing to component 6 (Miller et al., 2014; Gorham, 1991; Warner et al., 2017). The fixation and/or release of CO_2 as well as consumption and/or production of CH_4 through root, anaerobic and aerobic microbial respiration are dependent on soil conditions such as water table position, temperature, soil pH, and plant community composition (Yavitt et al., 2005; Oertel et al., 2016; Whalen, 2005). Emissions from peat and surface soil that was stripped as part of surface mining is expected to release between

288 1.1×10^{10} and 4.7×10^{10} kg stored carbon (Rooney et al., 2012), though it is unclear on what time scale this
289 release will occur. Some of this historical peat material is used for land reclamation. However, a
290 preliminary assessment of greenhouse gas fluxes from such a site gave no indication of significant
291 emissions, at least in the short term (Nwaishi et al., 2016). The bivariate polar plot shows that
292 component 6 is associated with no particular wind direction but with relatively low wind speeds (<
293 1.5 m/s; Figure S-7C), consistent with a dispersed surface source. Further, when variables associated
294 with secondary processes were added to the analysis (Table 7), component 6 anticorrelates with O_x ($r = -0.41$).
295 Dry deposition is a significant O_3 and NO_2, and therefore O_x, loss process (Wesely and Hicks,
296 2000; Zhang et al., 2002).

297 Overall, we have too little information to constrain soil fluxes for this data set. Considering the large CH_4
298 and CO_2 concentrations observed in this study, it is more likely that anthropogenic sources dominate
299 over natural soil emissions (Thompson et al., 2017). Future field campaigns at AMS 13 would benefit
300 from N_2O measurements to constrain contributions of natural sources to greenhouse gas
301 concentrations, such as those produced by microbes in water-logged soil.

302

303 **Component 7: Wind-blown dust**

304 Component 7 is correlated with PM_{10-1} (r = 0.93) and poorly with CO_2 (r = 0.25), ~~CH_4 (r = 0.11),~~ HOA (r =
305 0.23), and LO-OOA (r = 0.25). In the Athabasca oil sands region, surface mining has created large
306 portions of land whose surface is void of vegetation and is covered by sand and soil particles, which are
307 readily suspended by wind and vehicle traffic. Other mining activities add to the PM_{10-1} emissions,
308 including combustion processes, tailings sands, and mine haul roads, though the contributions of each of
309 these to the overall PM_{10-1} burden is uncertain (Wang et al., 2015). Recently, Phillips-Smith et al.
310 investigated metal species found in $PM_{2.5}$ aerosol at AMS 13 and found haul road dust and soil from

mine faces to be important sources of $PM_{2.5}$ (Phillips-Smith et al., 2017) and, likely, PM_{10-1} as well. The very poor associations of this component with CO_2 and CH_4 and lack of association with NO_y ($r = 0.02$) suggest contributions of open mine face soil in addition to dust suspended by vehicles travelling on unpaved roads.

The size range captured by PM_{10-1} may also include bioaerosol, including bacteria, fungal spores and plant pollen, which constitute the "natural" background aerosol over vegetated continental regions, typically contributing a few μg m^{-3} of aerosol mass (Huffman et al., 2010). Considering the large PM_{10-1} volumes observed in this work (Table 3), the contribution of bioaerosol is likely minor.

Component 8: Ammonia

Component 8 is a single variable component strongly associated with NH_3 ($r = 0.94$) but with no other variables~~: the second largest correlation coefficient is that of rBC ($r = 0.13$)~~.

Bytnerowicz et al. (2010) reported larger concentrations of NH_3 in the oil sands region than the provincial average. More recently, Shephard et al. (2015) reported enhancements of NH_3 in the general area as judged from satellite observations. Both studies hence suggest the existence of anthropogenic sources, though Shephard et al. (2015) speculated that biomass burning can contribute to the ammonia burden in the region. A recent modelling study by Whaley et al. (2018) estimated that around half of near-surface NH_3 during the study was likely from bi-directional exchange (i.e., re-emission from soil and plants).

In the oil sands, NH_3 is used as a floating agent for the separation and recovery of bitumen from tar, during bitumen upgrading in a process called "hydrotreating", and in tailing ponds, which, on occasion, have been contaminated with NH_3 to such a degree that they outgas it (Bytnerowicz et al., 2010).

Ammonia is also used for flue gas de-sulfurization by Syncrude; emission inventories (NPRI, 2013; ECCC, 2013a) suggest their fugitive emissions are the largest anthropogenic source in the region, though it is not clear if all sources are accurately inventoried.

The lack of association of ammonia with other variables in this component and the bivariate polar plots (Figure S-9) are consistent with an NH_3-specific source profile, such as fugitive emissions from one or more point sources that emit independently from other activities (i.e., ammonia storage tanks) and natural emissions from soil and trees (Whaley et al., 2018).

Component 9: Incomplete hydrocarbon oxidation

Component 9 is another single variable component and strongly correlates with CO (r = 0.87). ~~The variables with the next largest correlation coefficients are CH_4 (r = 0.17), 1,2,3- and 1,2,4-TMB (both r = 0.18), and o-xylene (r = 0.16).~~

The conventional interpretation of CO is as a byproduct of incomplete VOC oxidation, as it is found in fossil fuel combustion exhaust or in biomass burning plumes. Component 9, however, is not associated with NO_y (r = -0.08) or CO_2 (r = 0.05), which rules out this conventional interpretation.

Recently, Marey et al. (2015) examined the spatial distribution of CO in Northern Alberta using a combination of satellite and ground station data and found that most CO is derived from anthropogenic sources, biomass burning and the photochemical oxidation of methane and other VOCs. During the 2013 JOSM study, there was no obvious (i.e., tracer) evidence for fire emissions impacting the measurements at AMS 13 (Phillips-Smith et al., 2017), though an impact from distant sources (such as fires located 1,000s of km upwind in British Columbia or Washington State) cannot be entirely ruled out. We therefore interpret component 9 as a VOC oxidation product component.

Component 10: Dry tailings

Component 10 is strongly associated with TRS (r = 0.71) and weakly with o-xylene (r = 0.32)~~. There are poor correlations with CH_4 (r = 0.14~~ and poorly with~~) and~~ IVOCs (r= 0.20). This component is qualitatively similar to component 1, in that the presence of o-xylene suggests emission of naphtha, and the presence of TRS ~~and CH_4~~ suggests anaerobic sulfur reducing bacteria and methanogens as they occur in tailings ponds (Holowenko et al., 2000; Percy, 2013; Quagraine et al., 2005). However, the absence of correlations with NO_y, rBC, and CO suggests that this source is not in spatial proximity with a continuously operating combustion source. The much poorer correlations of o-xylene, CH_4, and IVOCs than for component 1 suggests that this component is much more "aged", i.e., emits less naphtha and bitumen.

As part of the reclamation process, tailings ponds in the Alberta oil sands region are converted into "composite tailings", which consist of a consolidated alkaline, saline mixture of processed sand, residual bitumen, clay fines, and gypsum ($CaSO_4$). This mixture settles and releases water, forming shallow pools of surface water (Figure 4J). Due to intensive microbial activity, composite tailings deposits are strong sources of H_2S and, likely, other reduced sulfur species (Warren et al., 2016; Bradford et al., 2017). Composite tailings are a source consistent with the emission profile of component 10. The association with TRS is explained by its production from biological activity and the presence of IVOCs by outgassing from the residual bitumen. Syncrude (the company operating closest to AMS 13) has been undertaking a pilot scale wetland reclamation project in the Athabasca Oil Sands Region to allow the development of a fen wetland above composite tailings (Bradford et al., 2017). Component 10 is hence interpreted as a dry tailings pond component, though the confidence in this interpretation is somewhat marginal as judged, for example, from the low eigenvalue of 0.74.

Bivariate polar plots

Bivariate polar plots map a surface using wind direction and wind speed and then model pollutant concentrations. While PCA is good at showing the temporal distribution of sources, bivariate polar plots help to show the spatial distribution of sources.

Figure S-3 shows a sample of variables associated with component 1. This component appears to dominate when winds are from the SSE and E and of moderate wind speeds (2-3 m/s).

Figure S-4 shows a sample of dominant variables associated with component 2. This component appears to dominate when winds are from the E at low wind speeds (1-2 m/s). The map appears to track the location of the Athabasca river and highway 63, corroborating that this source is from vehicular emissions.

Figure S-5 shows a sample of dominant variables associated with component 3. This component appears to dominate when winds are stagnant and local. This is unsurprising because biogenic emissions are expected to be emitted in great concentrations locally since our site is surrounded on all sides by forest.

Figure S-6 shows a sample of dominant variables associated with component 4 (or with component 2 in the secondary processes PCA). This component appears to dominate when winds are moderate (2-3 m/s) and from the SE and E.

Figure S-7 shows a sample of dominant variables associated with component 5. This component appears to dominate when winds are from the E at moderate wind speeds (2-3 m/s).

Figure S-8 shows a sample of dominant variables associated with component 6. This component appears to dominate when winds are stagnant and local. This suggests that this source is biogenic and may be due to emissions from trees.

Figure S-9 shows a sample of dominant variables associated with component 7. This component appears to dominate when winds are from the SE and E at moderate wind speeds (1-3 m/s).

Figure S-10 shows a sample of dominant variables associated with component 8. This component does

not appear to have a specific direction associated with it and is observed in all directions. This component is observed when winds are at moderate to high speeds (2-4 m/s).

Figure S-11 shows a sample of dominant variables associated with component 9. This component is observed when winds are from the S, SE, and E. This component is observed when winds are at low to moderate speeds (1-3 m/s).

Figure S-12 shows a sample of dominant variables associated with component 10. This component is observed when winds are from the SSE. This component is observed when winds are around 1.5 m/s. This source is very likely a point source due to its consistency with wind direction and speed.

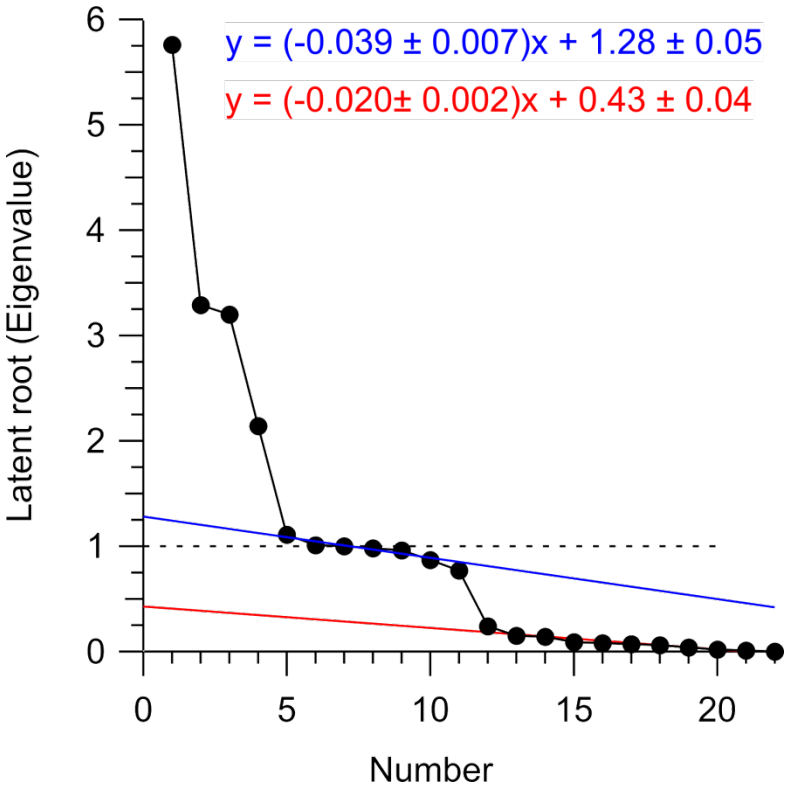

Figure S-2. Scree plot used to consider the number of components to retain. Dashed line represents the latent root criterions (eigenvalues > 1). Blue line represents the first instance of eigenvalues becoming horizontal. Red line represents the second instance of eigenvalues becoming horizontal.

Table S-1. Ionimed Analytical GCU Standard.

Compound	Volume mixing ratio (ppmv)	Uncertainty (%)
Formaldehyde	1.01	±8
Methanol	1.01	±8
Acetonitrile	1.01	±6
Acetaldehyde	1.01	±5
Ethanol	1.01	±8
Acrolein	0.98	±5
Acetone	1.02	±5
Isoprene	0.99	±5
Crotonaldehyde	0.92	±6
2-Butanone	1.01	±5
Benzene	1.01	±5
Toluene	1.02	±5
o-xylene	1.03	±6
Chlorobenzene	1.02	±5
α-pinene	0.93	±5
1,2, Dichlorobenzene	1.03	±7
1,2,4-Trichlorobenzene	1.01	±9

418 **Table S-2.** The component pattern after Varimax rotation. Correlations greater than 0.30 or less than -0.30 are bolded.

	1	2	3	4	5	6	7	8	9	10	11	12	13	14	15	16	17	18	19	20	21	22
Anthropogenic VOCs																						
o-xylene	**0.89**	0.07	0.03	0.10	0.09	0.06	-0.03	0.11	0.15	0.06	0.26	0.11	0.00	0.04	-0.08	0.24	0.00	-0.01	-0.02	0.00	-0.01	0.00
1,2,3 - TMB	**0.94**	0.15	0.07	0.06	0.05	0.08	-0.01	0.06	0.17	0.01	-0.01	0.02	-0.04	0.01	-0.08	-0.14	0.03	0.00	-0.09	0.00	-0.07	0.00
1,2,4 - TMB	**0.94**	0.13	0.01	0.11	0.08	0.05	-0.02	0.09	0.17	0.04	0.12	0.03	-0.01	0.02	-0.06	0.03	0.01	0.00	-0.04	0.00	0.09	0.00
decane	**0.91**	0.22	-0.02	0.15	0.05	0.00	0.04	0.15	0.05	0.15	0.07	-0.02	0.04	-0.01	0.07	-0.03	-0.03	0.02	0.16	0.00	-0.01	0.00
undecane	**0.85**	0.27	-0.08	0.23	0.08	-0.03	0.06	0.05	0.00	0.20	0.01	-0.10	0.09	0.00	0.26	-0.05	-0.02	0.02	0.02	0.00	0.00	0.00
Biogenic VOCs																						
α-pinene	-0.03	-0.08	**0.98**	-0.11	0.02	0.05	-0.08	0.02	0.01	0.00	-0.01	0.02	0.00	0.00	-0.01	0.01	-0.08	-0.01	0.00	0.09	0.00	0.00
ß-pinene	-0.02	-0.08	**0.97**	-0.12	0.01	0.05	-0.08	0.01	0.01	0.01	0.01	-0.02	0.00	-0.02	0.02	0.00	-0.10	0.01	0.01	-0.09	0.00	0.00
limonene	0.08	-0.02	**0.92**	-0.08	0.06	0.23	-0.11	0.08	0.02	0.07	-0.05	0.02	-0.03	0.03	-0.02	0.00	0.23	0.00	-0.01	0.00	0.00	0.00
Combustion tracers																						
NO_y	0.26	**0.80**	-0.25	0.21	0.03	-0.05	0.10	0.19	-0.04	0.07	0.04	0.01	**0.34**	0.00	0.04	0.00	-0.01	-0.01	0.01	0.00	0.00	0.00
rBC	**0.31**	**0.80**	0.03	0.05	0.08	0.07	0.11	0.24	0.12	**0.34**	-0.03	0.02	-0.02	-0.05	0.02	-0.01	0.00	0.22	0.01	0.00	0.00	0.00
CO	**0.41**	0.18	0.04	0.02	0.08	0.07	0.05	0.03	**0.88**	0.06	0.00	0.02	0.00	0.01	0.00	0.00	0.00	0.00	0.00	0.00	0.00	0.00
CO_2	0.10	0.09	**0.46**	-0.12	0.23	**0.82**	-0.14	-0.03	0.07	0.00	-0.05	0.02	-0.01	0.01	0.00	0.00	0.00	0.00	0.00	0.00	0.00	0.00
Aerosol species																						
pPAH	0.07	**0.94**	-0.08	-0.11	0.02	0.06	0.14	0.00	0.09	-0.15	0.00	0.01	-0.14	-0.07	-0.02	0.00	0.00	-0.10	0.00	0.00	0.00	0.00
PM_{10-1}	0.18	0.13	0.07	0.10	**0.94**	0.16	-0.03	0.04	0.07	0.10	0.08	0.02	0.00	0.01	0.00	0.00	0.00	0.00	0.00	0.00	0.00	0.00
HOA	**0.41**	**0.74**	0.02	0.11	0.21	0.11	-0.04	0.13	0.15	0.19	0.10	0.05	0.01	**0.35**	0.00	0.01	0.01	-0.01	0.00	0.00	0.00	0.00
LO-OOA	**0.45**	0.17	0.13	0.25	0.19	0.01	-0.04	0.28	0.10	0.73	0.16	0.02	0.01	0.03	0.01	0.00	0.00	0.00	0.00	0.00	0.00	0.00
Sulfur																						
TS	0.25	0.04	-0.16	**0.94**	0.07	-0.05	-0.02	0.02	0.01	0.09	0.14	0.00	0.01	0.01	0.01	0.00	0.00	0.00	0.00	0.00	0.00	0.01
SO_2	0.11	0.02	-0.15	**0.98**	0.04	-0.04	-0.03	-0.02	0.01	0.05	-0.05	-0.01	0.01	0.01	0.00	0.00	0.00	0.00	0.00	0.00	0.00	-0.01
TRS	**0.57**	0.05	-0.08	0.11	0.14	-0.05	0.03	0.16	-0.01	0.13	**0.77**	0.02	0.00	0.01	0.00	0.00	0.00	0.00	0.00	0.00	0.00	0.00
Other																						
IVOCs	**0.34**	**0.34**	0.12	-0.03	0.05	-0.02	-0.02	**0.84**	0.04	0.18	0.13	0.01	0.01	0.01	0.00	0.00	0.00	0.00	0.00	0.00	0.00	0.00
NH_3	0.01	0.19	-0.23	-0.04	-0.03	-0.09	**0.95**	-0.01	0.04	-0.01	0.01	0.00	0.01	0.00	0.00	0.00	0.00	0.00	0.00	0.00	0.00	0.00
CH_4	**0.60**	**0.39**	0.10	-0.05	0.14	0.44	0.00	0.06	0.16	0.08	0.09	**0.46**	0.01	0.03	-0.02	0.01	0.00	0.00	0.00	0.00	0.00	0.00
Eigenvalues	5.76	3.29	3.20	2.14	1.11	1.01	1.00	0.98	0.96	0.87	0.77	0.24	0.15	0.14	0.09	0.08	0.07	0.06	0.04	0.02	0.01	0.00
% of variance	26.17	14.97	14.55	9.75	5.06	4.60	4.53	4.46	4.34	3.94	3.51	1.09	0.69	0.63	0.42	0.37	0.33	0.28	0.17	0.08	0.06	0.00
% cum. var.	26.17	41.14	55.69	65.43	70.49	75.09	79.62	84.07	88.42	92.36	95.87	96.97	97.66	98.29	98.71	99.08	99.41	99.69	99.86	99.94	100.0	100

Table S-3. The pattern after Varimax rotation with 5 components selected.

	1	2	3	4	5	Communalities
Anthropogenic VOCs						
o-xylene	**0.94**	0.08	0.03	0.09	0.15	0.93
1,2,3 - TMB	**0.90**	0.14	0.04	0.01	0.23	0.89
1,2,4 - TMB	**0.95**	0.14	-0.01	0.09	0.18	0.97
decane	**0.91**	0.27	-0.03	0.16	0.05	0.93
undecane	**0.82**	**0.31**	-0.10	0.26	0.05	0.84
Biogenic VOCs						
α-pinene	-0.03	-0.05	**0.94**	-0.15	0.04	0.91
ß-pinene	-0.02	-0.06	**0.94**	-0.15	0.03	0.90
limonene	0.07	0.02	**0.94**	-0.10	0.18	0.93
Combustion tracers						
NO_y	0.25	**0.83**	-0.29	0.22	0.02	0.89
rBC	**0.33**	**0.89**	0.04	0.07	0.13	0.92
CO	**0.53**	0.19	-0.02	-0.08	**0.40**	0.48
CO_2	0.07	0.06	**0.55**	-0.13	**0.71**	0.83
Aerosol species						
pPAH	0.01	**0.83**	-0.20	-0.20	0.27	0.84
PM_{10-1}	0.21	0.19	0.15	0.29	**0.57**	0.51
HOA	**0.44**	**0.75**	0.03	0.15	**0.32**	0.88
LO-OOA	**0.59**	**0.37**	0.28	0.41	-0.06	0.74
Sulfur						
TS	0.28	0.04	-0.18	**0.91**	0.01	0.94
SO_2	0.10	0.01	-0.18	**0.93**	0.05	0.91
TRS	**0.76**	0.10	-0.04	0.17	-0.13	0.63
Other						
IVOCs	**0.47**	**0.61**	0.28	0.03	-0.25	0.73
NH_3	0.02	**0.34**	**-0.47**	-0.21	-0.14	0.40
CH_4	**0.62**	**0.38**	0.12	-0.09	**0.53**	0.84
Eigenvalues	6.42	3.79	3.56	2.34	1.70	
% of variance	29.20	17.25	16.20	10.63	7.74	
Cumulative variance	29.20	46.45	62.65	73.28	81.01	

Table S-4. The pattern after Varimax rotation with 6 components selected.

	1	2	3	4	5	6	Communalities
Anthropogenic VOCs							
o-xylene	**0.92**	0.04	0.01	0.08	0.24	0.13	0.93
1,2,3 - TMB	**0.94**	0.16	0.08	0.07	0.06	0.05	0.92
1,2,4 - TMB	**0.95**	0.13	0.00	0.11	0.16	0.08	0.97
decane	**0.88**	0.23	-0.02	0.18	0.28	0.00	0.94
undecane	**0.79**	0.28	-0.09	0.29	0.25	0.00	0.85
Biogenic VOCs							
α-pinene	-0.02	-0.09	**0.96**	-0.12	0.04	0.01	0.95
ß-pinene	-0.02	-0.10	**0.96**	-0.12	0.05	0.01	0.94
limonene	0.09	-0.01	**0.95**	-0.09	0.04	0.15	0.95
Combustion tracers							
NO_y	0.22	**0.81**	-0.27	0.23	0.25	0.00	0.89
rBC	**0.31**	**0.85**	0.07	0.08	0.28	0.10	0.92
CO	**0.64**	0.29	0.09	0.02	-0.23	0.09	0.56
CO_2	0.17	0.12	**0.57**	-0.17	-0.23	**0.62**	0.84
Aerosol species							
pPAH	0.09	**0.90**	-0.10	-0.14	-0.10	0.05	0.87
PM_{10-1}	0.19	0.14	0.03	0.12	0.17	**0.81**	0.76
HOA	**0.44**	**0.73**	0.04	0.13	0.22	**0.30**	0.88
LO-OOA	**0.46**	0.22	0.17	**0.32**	**0.60**	0.21	0.79
Sulfur							
TS	0.25	0.02	-0.18	**0.92**	0.12	0.06	0.97
SO_2	0.10	0.03	-0.15	**0.97**	-0.02	0.02	0.98
TRS	**0.62**	-0.04	-0.17	0.06	**0.56**	0.14	0.75
Other							
IVOCs	**0.31**	**0.43**	0.17	-0.06	**0.70**	0.02	0.80
NH_3	0.06	**0.41**	**-0.36**	-0.11	-0.11	**-0.36**	0.46
CH_4	**0.68**	**0.42**	0.15	-0.10	0.00	**0.41**	0.84
Eigenvalues	6.09	3.60	3.47	2.25	1.76	1.58	
% of variance	27.70	16.38	15.78	10.22	7.98	7.18	
Cumulative variance	27.70	44.07	59.85	70.08	78.06	85.23	

Table S-5. The pattern after Varimax rotation with 7 components selected.

	1	2	3	4	5	6	7	Commu-nalities
Anthropogenic VOCs								
o-xylene	**0.93**	0.07	0.01	0.08	0.21	0.12	-0.05	0.93
1,2,3 - TMB	**0.94**	0.18	0.08	0.06	0.03	0.03	-0.03	0.93
1,2,4 - TMB	**0.96**	0.15	0.00	0.11	0.14	0.07	-0.02	0.98
decane	**0.88**	0.26	-0.02	0.18	0.26	0.00	0.01	0.94
undecane	**0.79**	**0.30**	-0.09	0.28	0.23	0.00	0.03	0.85
Biogenic VOCs								
α-pinene	-0.03	-0.09	**0.96**	-0.11	0.04	0.00	-0.05	0.96
ß-pinene	-0.02	-0.10	**0.96**	-0.11	0.06	0.01	-0.05	0.95
limonene	0.09	0.01	**0.95**	-0.08	0.03	0.12	-0.13	0.95
Combustion tracers								
NO_y	0.22	**0.83**	-0.28	0.22	0.20	-0.02	0.06	0.91
rBC	**0.31**	**0.85**	0.07	0.08	0.25	0.11	0.13	0.92
CO	**0.62**	0.22	0.13	0.03	-0.21	0.19	0.29	0.61
CO_2	0.17	0.17	**0.56**	-0.18	-0.28	**0.54**	-0.27	0.84
Aerosol species								
pPAH	0.08	**0.89**	-0.10	-0.15	-0.14	0.03	0.15	0.88
PM_{10-1}	0.18	0.12	0.06	0.13	0.18	**0.89**	0.01	0.89
HOA	**0.44**	**0.76**	0.03	0.12	0.16	0.27	-0.03	0.89
LO-OOA	**0.46**	0.23	0.18	**0.33**	**0.59**	0.25	0.01	0.81
Sulfur								
TS	0.25	0.04	-0.18	**0.92**	0.12	0.06	-0.02	0.97
SO_2	0.10	0.04	-0.15	**0.97**	-0.02	0.02	-0.03	0.98
TRS	**0.62**	-0.03	-0.16	0.07	**0.56**	0.19	0.02	0.77
Other								
IVOCs	**0.32**	**0.48**	0.16	-0.07	**0.66**	0.00	-0.05	0.80
NH_3	0.01	0.20	-0.26	-0.06	0.00	-0.05	**0.89**	0.91
CH_4	**0.68**	**0.45**	0.15	-0.11	-0.05	**0.36**	-0.10	0.85
Eigenvalues	6.09	3.65	3.42	2.23	1.61	1.46	1.03	
% of variance	27.70	16.60	15.57	10.14	7.33	6.66	4.70	
Cumulative variance	27.70	44.30	59.86	70.01	77.34	84.00	88.70	

Table S-6. The pattern after Varimax rotation with 8 components selected.

	1	2	3	4	5	6	7	8	Communalities
Anthropogenic VOCs									
o-xylene	**0.93**	0.08	0.03	0.07	0.14	0.13	-0.03	0.11	0.93
1,2,3 - TMB	**0.91**	0.19	0.09	0.06	-0.01	0.02	-0.04	0.21	0.93
1,2,4 - TMB	**0.95**	0.16	0.01	0.11	0.09	0.07	-0.03	0.18	0.98
decane	**0.90**	0.26	-0.01	0.17	0.19	0.01	0.03	0.08	0.95
undecane	**0.82**	**0.30**	-0.07	0.28	0.15	0.01	0.06	0.03	0.87
Biogenic VOCs									
α-pinene	-0.04	-0.10	**0.97**	-0.11	0.06	0.00	-0.05	0.00	0.96
ß-pinene	-0.02	-0.10	**0.96**	-0.11	0.06	0.00	-0.04	-0.01	0.96
limonene	0.07	0.00	**0.95**	-0.08	0.06	0.11	-0.14	0.05	0.95
Combustion tracers									
NO_y	0.25	**0.83**	-0.26	0.22	0.19	-0.01	0.10	-0.08	0.92
rBC	0.28	**0.83**	0.06	0.07	**0.33**	0.10	0.09	0.17	0.93
CO	**0.42**	0.18	0.04	0.01	0.07	0.11	0.06	**0.85**	0.96
CO_2	0.13	0.19	**0.58**	-0.17	-0.28	**0.53**	-0.27	0.10	0.86
Aerosol species									
pPAH	0.06	**0.91**	-0.08	-0.14	-0.11	0.03	0.16	0.06	0.89
PM_{10-1}	0.18	0.12	0.07	0.12	0.16	**0.89**	0.01	0.06	0.89
HOA	**0.42**	**0.75**	0.03	0.12	0.21	0.26	-0.06	0.15	0.89
LO-OOA	**0.46**	0.19	0.15	**0.30**	**0.65**	0.24	-0.04	0.15	0.87
Sulfur									
TS	0.28	0.03	-0.18	**0.92**	0.09	0.07	-0.01	-0.02	0.97
SO_2	0.11	0.04	-0.15	**0.97**	-0.01	0.02	-0.04	0.03	0.98
TRS	**0.72**	-0.03	-0.13	0.06	**0.40**	0.23	0.11	-0.20	0.80
Other									
IVOCs	**0.35**	**0.43**	0.13	-0.09	**0.71**	0.00	-0.07	0.01	0.84
NH_3	0.01	0.22	-0.24	-0.05	-0.05	-0.04	**0.92**	0.05	0.96
CH_4	**0.65**	**0.47**	0.17	-0.11	-0.08	**0.35**	-0.10	0.16	0.86
Eigenvalues	5.99	3.58	3.40	2.20	1.52	1.43	1.03	1.00	
% of variance	27.23	16.28	15.44	10.01	6.90	6.52	4.70	4.53	
Cumulative variance	27.23	43.51	58.95	68.96	75.86	82.37	87.08	91.61	

Table S-7. The pattern after Varimax rotation with 9 components selected.

	1	2	3	4	5	6	7	8	9	Communalities
Anthropogenic VOCs										
o-xylene	**0.89**	0.09	0.03	0.09	0.11	0.11	-0.05	0.16	**0.30**	0.95
1,2,3 - TMB	**0.93**	0.16	0.08	0.05	0.05	0.05	-0.02	0.17	-0.02	0.94
1,2,4 - TMB	**0.94**	0.15	0.01	0.11	0.11	0.08	-0.02	0.18	0.12	0.98
decane	**0.91**	0.22	-0.03	0.16	0.25	0.04	0.05	0.03	0.03	0.97
undecane	**0.85**	0.25	-0.10	0.25	0.24	0.06	0.10	-0.05	-0.08	0.94
Biogenic VOCs										
α-pinene	-0.04	-0.09	**0.97**	-0.10	0.05	0.00	-0.06	0.02	0.02	0.97
ß-pinene	-0.03	-0.10	**0.97**	-0.11	0.05	0.00	-0.05	0.00	0.02	0.96
limonene	0.09	-0.01	**0.94**	-0.09	0.08	0.13	-0.13	0.03	-0.06	0.95
Combustion tracers										
NO_y	0.26	**0.82**	-0.26	0.22	0.22	0.00	0.11	-0.09	0.02	0.92
rBC	**0.31**	**0.79**	0.04	0.05	**0.41**	0.12	0.12	0.12	-0.10	0.94
CO	**0.42**	0.19	0.05	0.02	0.08	0.10	0.06	**0.87**	-0.02	0.98
CO_2	0.16	0.17	**0.56**	-0.18	-0.22	**0.56**	-0.25	0.06	-0.17	0.86
Aerosol species										
pPAH	0.06	**0.93**	-0.07	-0.12	-0.11	0.01	0.14	0.09	0.03	0.93
PM_{10-1}	0.16	0.11	0.06	0.12	0.17	**0.89**	0.02	0.06	0.10	0.89
HOA	**0.41**	**0.75**	0.03	0.13	0.23	0.25	-0.06	0.16	0.08	0.90
LO-OOA	**0.46**	0.14	0.13	0.28	0.70	0.26	-0.01	0.10	0.05	0.90
Sulfur										
TS	0.25	0.04	-0.17	**0.93**	0.08	0.06	-0.02	0.00	0.13	0.99
SO_2	0.11	0.03	-0.15	**0.97**	0.01	0.02	-0.03	0.01	-0.05	0.99
TRS	**0.59**	0.05	-0.09	0.11	0.24	0.14	0.04	-0.04	**0.71**	0.96
Other										
IVOCs	**0.32**	**0.41**	0.12	-0.09	**0.70**	-0.01	-0.08	0.02	0.20	0.84
NH_3	0.01	0.21	-0.24	-0.05	-0.04	-0.04	**0.93**	0.04	0.01	0.97
CH_4	**0.65**	**0.47**	0.16	-0.10	-0.06	**0.36**	-0.10	0.17	0.07	0.86
Eigenvalues	5.84	3.44	3.37	2.19	1.58	1.47	1.03	0.95	0.74	
% of variance	26.54	15.63	15.30	9.98	7.19	6.66	4.69	4.31	3.38	
Cumulative variance	26.54	42.17	57.47	67.44	74.63	81.29	85.98	90.29	93.67	

428 **Table S-8.** The factor pattern after Varimax rotation with 11 factors selected.

	Factor 1	Factor 2	Factor 3	Factor 4	Factor 5	Factor 6	Factor 7	Factor 8	Factor 9	Factor 10	Factor 11	Commu-nalities
Anthropogenic VOCs												
o-xylene	**0.88**	0.08	0.03	0.10	0.13	0.07	-0.04	0.17	0.11	0.04	**0.32**	0.95
1,2,3 - TMB	**0.94**	0.16	0.07	0.05	0.11	0.05	-0.01	0.18	0.06	-0.01	-0.02	0.96
1,2,4 - TMB	**0.94**	0.15	0.01	0.11	0.08	0.08	-0.02	0.18	0.09	0.03	0.13	0.99
decane	**0.92**	0.24	-0.02	0.15	0.00	0.05	0.04	0.04	0.13	0.16	0.05	0.97
undecane	**0.87**	0.29	-0.08	0.22	-0.06	0.09	0.05	-0.05	0.03	0.22	-0.05	0.96
Biogenic VOCs												
α-pinene	-0.03	-0.08	**0.98**	-0.11	0.04	0.01	-0.08	0.02	0.02	0.00	0.00	0.98
ß-pinene	-0.02	-0.08	**0.98**	-0.12	0.02	0.02	-0.07	0.00	0.00	0.02	0.01	0.98
limonene	0.08	-0.02	**0.93**	-0.08	0.24	0.05	-0.11	0.03	0.09	0.06	-0.05	0.95
Combustion tracers												
NO_y	0.27	**0.83**	-0.26	0.21	-0.04	0.03	0.10	-0.08	0.18	0.07	0.01	0.92
rBC	**0.30**	**0.81**	0.04	0.04	0.09	0.07	0.12	0.12	0.23	**0.34**	-0.05	0.95
CO	**0.41**	0.19	0.04	0.02	0.08	0.08	0.05	**0.87**	0.03	0.06	-0.01	0.99
CO_2	0.09	0.08	**0.48**	-0.12	**0.77**	0.25	-0.14	0.05	-0.04	-0.01	-0.09	0.95
Aerosol species												
pPAH	0.06	**0.93**	-0.07	-0.12	0.07	0.02	0.14	0.10	-0.02	-0.20	0.01	0.95
PM_{10-1}	0.18	0.14	0.08	0.10	0.17	**0.94**	-0.03	0.07	0.04	0.09	0.08	1.00
HOA	**0.40**	**0.77**	0.03	0.11	0.14	0.20	-0.07	0.16	0.09	0.19	0.13	0.92
LO-OOA	**0.45**	0.19	0.13	0.25	0.03	0.19	-0.04	0.11	0.27	**0.72**	0.16	0.98
Sulfur												
TS	0.26	0.05	-0.16	**0.93**	-0.05	0.07	-0.02	0.01	0.02	0.08	0.13	0.26
SO_2	0.12	0.03	-0.15	**0.98**	-0.04	0.04	-0.03	0.01	-0.02	0.05	-0.05	0.12
TRS	**0.58**	0.06	-0.08	0.10	-0.04	0.14	0.03	-0.03	0.16	0.13	**0.74**	0.58
Other												
IVOCs	**0.34**	**0.37**	0.13	-0.03	-0.01	0.05	-0.03	0.03	**0.82**	0.18	0.12	1.00
NH_3	0.01	0.20	-0.24	-0.04	-0.08	-0.03	**0.94**	0.04	-0.02	-0.01	0.01	1.00
CH_4	**0.59**	**0.40**	0.10	-0.06	**0.59**	0.10	0.00	0.17	0.05	0.07	0.15	0.93
Eigenvalues	5.75	3.43	3.24	2.13	1.12	1.10	0.99	0.96	0.93	0.87	0.79	
% var.	26.14	15.61	14.72	9.66	5.11	4.99	4.51	4.35	4.22	3.95	3.60	
% Cum. var.	26.14	41.74	56.46	66.12	71.23	76.22	80.73	85.09	89.31	93.26	96.86	

Table S-9. The pattern with mixing height included after Varimax rotation with 10 components.

	1	2	3	4	5	6	7	8	9	10	Commu-nalities
Anthropogenic VOCs											
o-xylene	**0.89**	0.04	0.03	0.10	0.29	0.10	-0.01	-0.06	0.17	0.16	0.95
1,2,3 - TMB	**0.94**	0.17	0.10	0.04	-0.04	0.01	-0.03	-0.04	0.17	0.06	0.95
1,2,4 - TMB	**0.94**	0.13	0.03	0.10	0.11	0.09	-0.02	-0.06	0.18	0.07	0.98
decane	**0.92**	0.25	0.03	0.15	0.11	0.11	0.01	0.04	0.03	-0.04	0.97
undecane	**0.87**	**0.31**	-0.05	0.23	-0.03	0.17	0.03	0.10	-0.05	-0.11	0.96
Biogenic VOCs											
α-pinene	-0.02	-0.08	**0.96**	-0.10	0.03	0.01	-0.05	-0.11	0.01	0.02	0.96
ß-pinene	-0.01	-0.08	**0.96**	-0.11	0.04	0.02	-0.05	-0.12	-0.01	0.02	0.96
limonene	0.11	0.02	**0.95**	-0.08	0.04	0.02	-0.11	-0.06	0.03	0.12	0.96
Combustion tracers											
NO_y	0.21	**0.86**	-0.25	0.21	0.11	0.06	0.10	0.01	-0.08	-0.02	0.92
rBC	0.29	**0.89**	0.12	0.02	0.10	0.19	0.03	0.09	0.10	-0.01	0.95
CO	**0.43**	0.20	0.04	0.01	0.00	0.08	0.02	0.05	**0.86**	0.07	0.98
CO_2	0.15	0.17	**0.56**	-0.13	-0.12	0.13	-0.14	-0.12	0.08	**0.68**	0.91
Aerosol species											
pPAH	0.01	**0.86**	-0.09	-0.13	-0.08	-0.03	0.23	-0.18	0.12	0.17	0.90
PM_{10-1}	**0.31**	0.22	0.05	0.15	0.12	**0.88**	0.04	-0.01	0.08	0.10	0.97
HOA	**0.45**	**0.79**	0.02	0.14	0.16	0.15	-0.02	-0.02	0.16	0.10	0.93
LO-OOA	**0.52**	**0.30**	0.21	0.26	**0.37**	**0.36**	-0.17	0.27	0.04	-0.18	0.88
Sulfur											
TS	0.27	0.06	-0.16	**0.93**	0.10	0.10	-0.03	0.04	-0.01	-0.02	1.00
SO_2	0.11	0.05	-0.14	**0.97**	-0.06	0.06	-0.05	0.05	0.01	-0.05	0.99
TRS	**0.64**	0.01	-0.12	0.11	**0.63**	0.20	0.09	-0.04	-0.09	0.12	0.91
Other											
IVOCs	0.28	**0.50**	0.22	-0.07	**0.66**	0.08	-0.13	0.04	0.06	-0.18	0.87
NH_3	0.00	0.22	-0.20	-0.07	-0.03	0.03	**0.92**	0.11	0.02	-0.06	0.96
CH_4	**0.64**	**0.43**	0.15	-0.07	0.09	0.10	0.00	-0.07	0.17	**0.50**	0.92
Mixing height	-0.04	-0.07	**-0.35**	0.07	0.01	0.00	0.12	**0.90**	0.04	-0.07	0.96
Eigenvalues	6.06	3.81	3.51	2.16	1.19	1.12	1.03	1.02	0.94	0.92	
% var.	26.35	16.57	15.27	9.39	5.19	4.86	4.48	4.42	4.08	3.98	
% Cum. var.	26.35	42.92	58.19	67.58	72.77	77.63	82.11	86.53	90.61	94.60	

Table S-10. Criteria for number of components extracted by PCA.

Criterion	Number of components extracted	% Variance explained (after rotation)
Scree test 1	5	81.0%
< 5% variance	6	85.2%
Latent root	7	88.7%
≥ 95% cumulative variance	10	95.5%
Scree test 2	11	96.9%

Table S-11. Association of IVOCs with relevant components.

# of components in solution	Oil sands surface mining facilities (Component 1)	Mine fleet and operations (Component 2)	Mine face (Component 5)
5	0.47	0.61	n/a
6	0.31	0.43	n/a
7	0.32	0.48	0.66
8	0.35	0.43	0.71
9	0.32	0.41	0.70
10	0.31	0.39	0.74
11	0.34	0.37	n/a

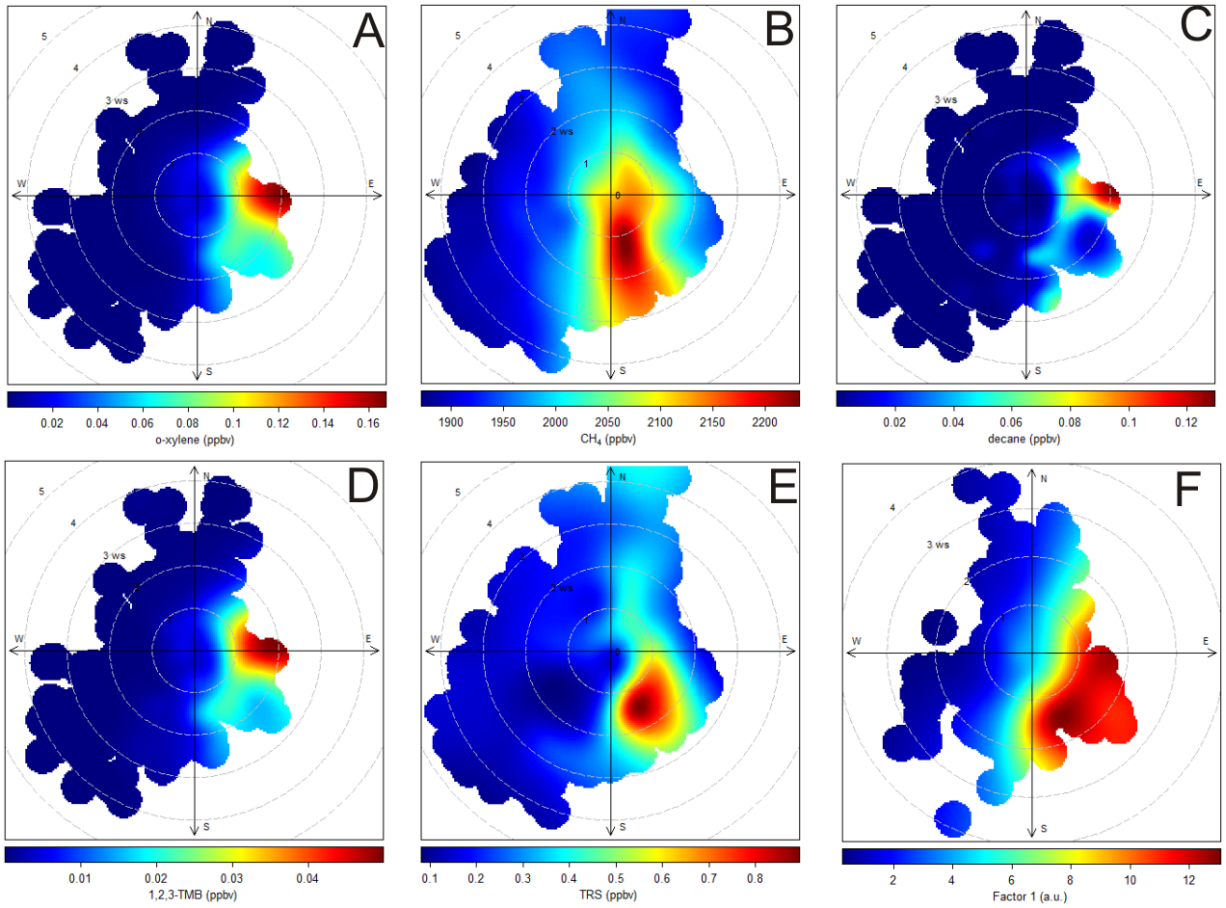

Figure S-3. Bivariate polar plots associated with component 1 for the optimum primary pollutant solution (Table 5.). **(A)** o-xylene, **(B)** CH_4, **(C)** decane, **(D)** 1, 2, 3-TMB, **(E)** TRS, **(F)** and component 1.

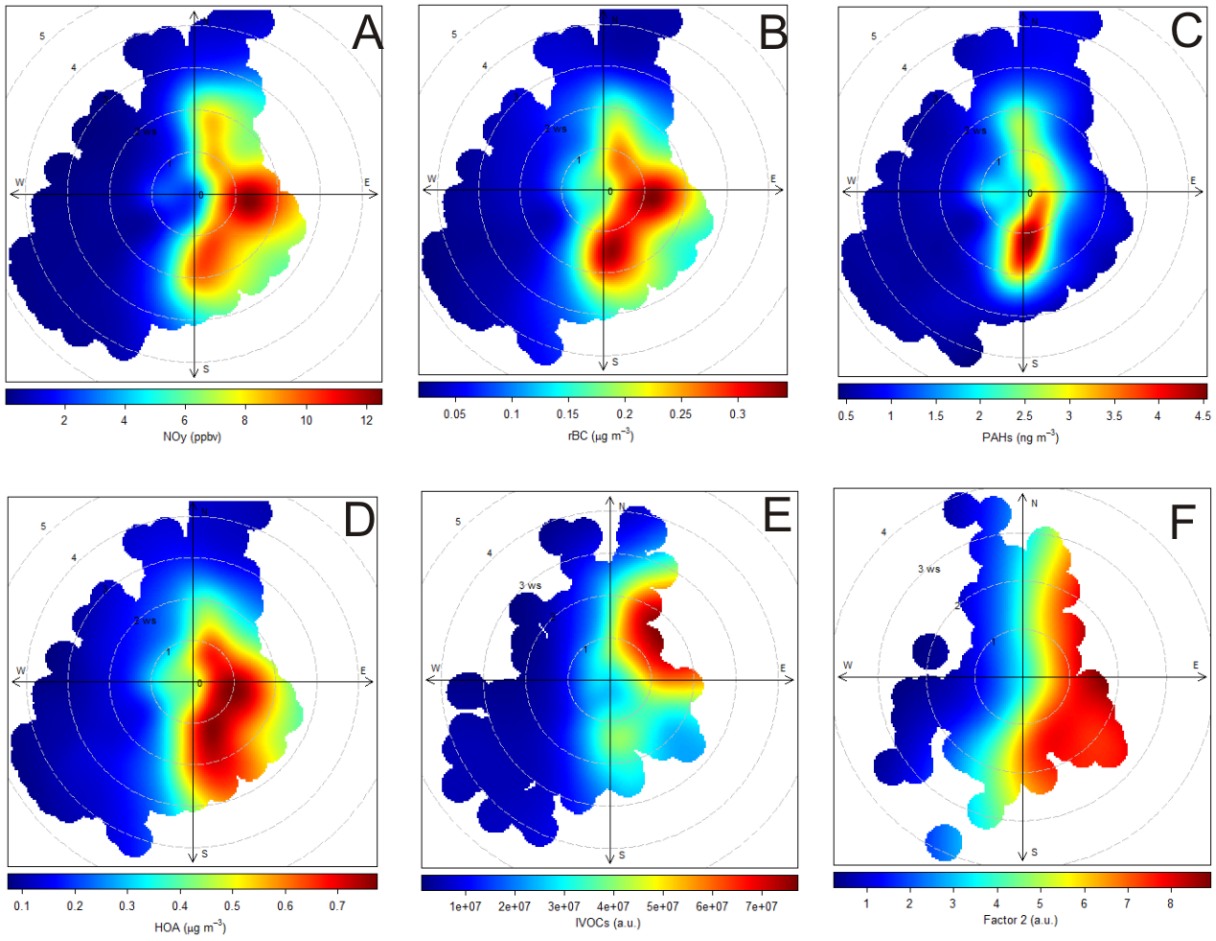

Figure S-4. Bivariate polar plots associated with component 2 for the optimum primary pollutant solution (Table 5.). **(A)** NO_y, **(B)** rBC, **(C)** PAHs, **(D)** HOA, **(E)** IVOCs, **(F)** and component 2.

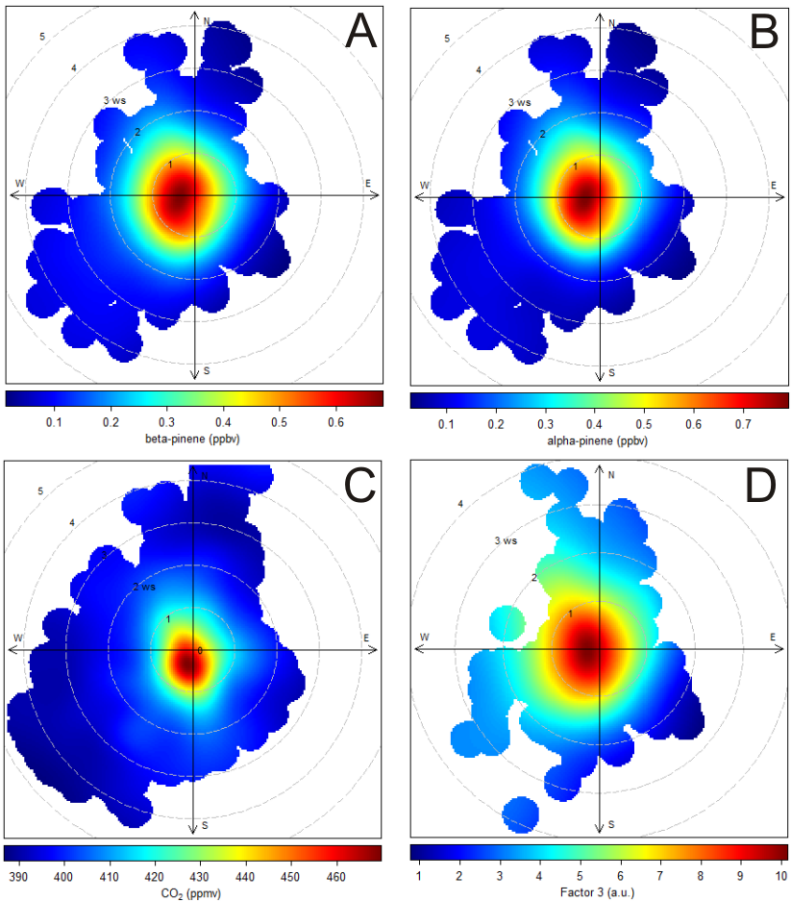

Figure S-5. Bivariate polar plots associated with component 3 for the optimum primary pollutant solution (Table 5.). **(A)** ß-pinene, **(B)** α-pinene, **(C)** CO_2, **(D)** and component 3.

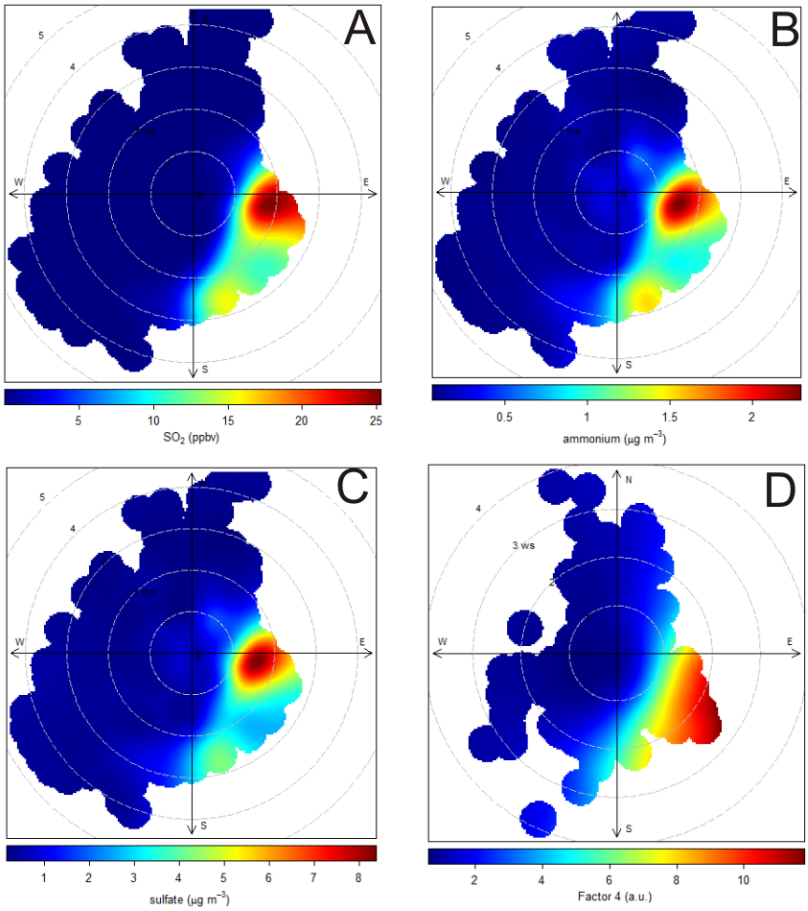

Figure S-6. Bivariate polar plots associated with component 4 for the optimum secondary pollutant solution (Table 7). **(A)** SO_2, **(B)** $NH_4^+{}_{(p)}$, **(C)** $SO_4^{2-}{}_{(p)}$, **(D)** and component 4.

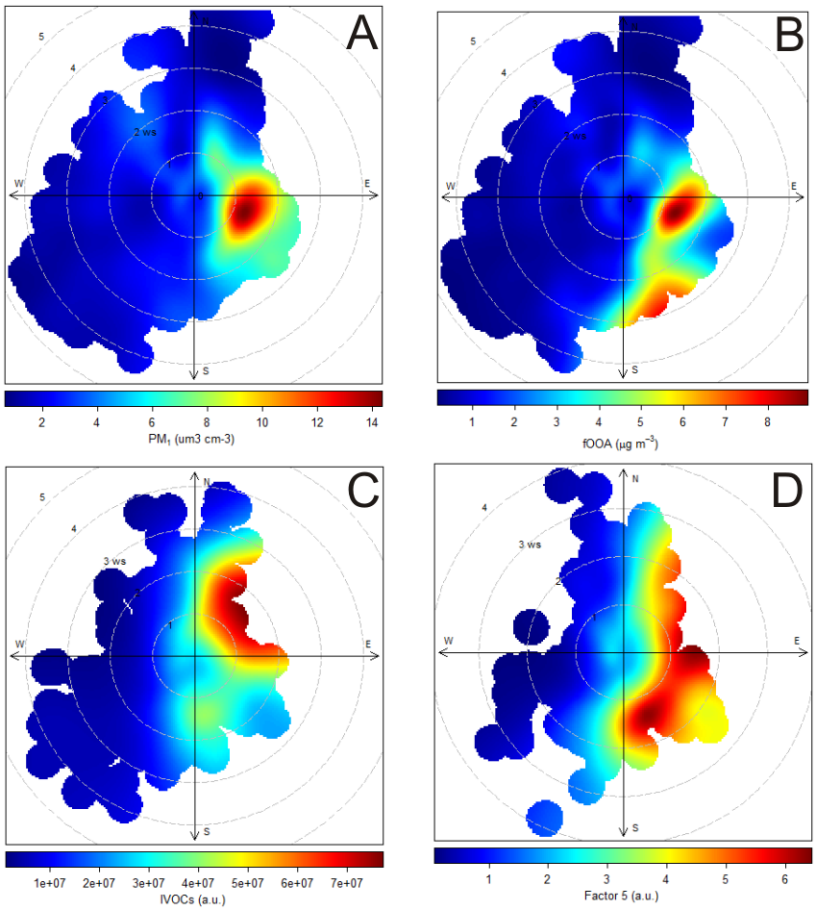

Figure S-7. Bivariate polar plots associated with component 5 for the optimum secondary pollutant solution (Table 7). **(A)** PM_1 (11-component solution), **(B)** LO-OOA, **(C)** IVOCs, and **(D)** component 5.

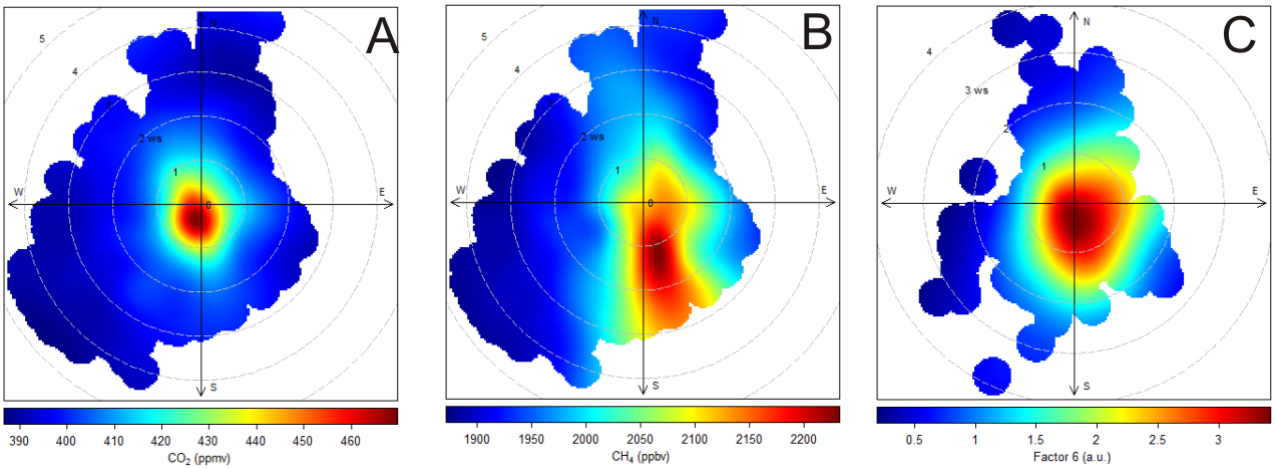

Figure S-8. Bivariate polar plots associated with component 6 for the optimum primary pollutant solution (Table 5). **(A)** CO_2, **(B)** CH_4, and **(C)** component 6.

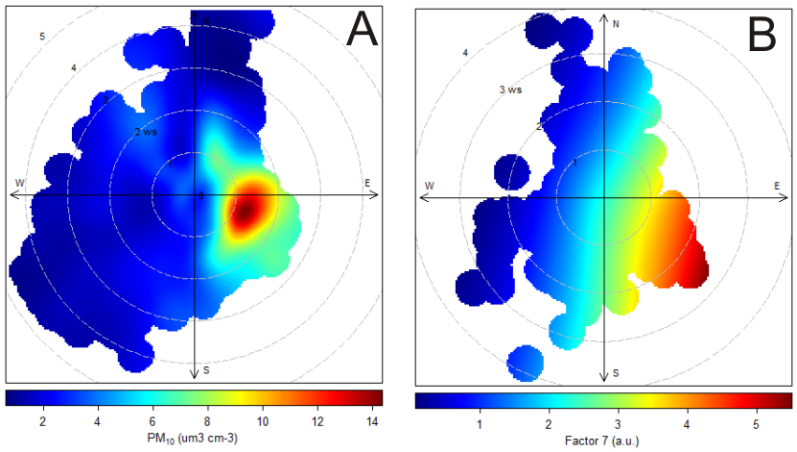

Figure S-9. Bivariate polar plots associated with component 7 for the optimum primary pollutant solution (Table 5). **(A)** PM_{10-1}, **(B)** and component 7.

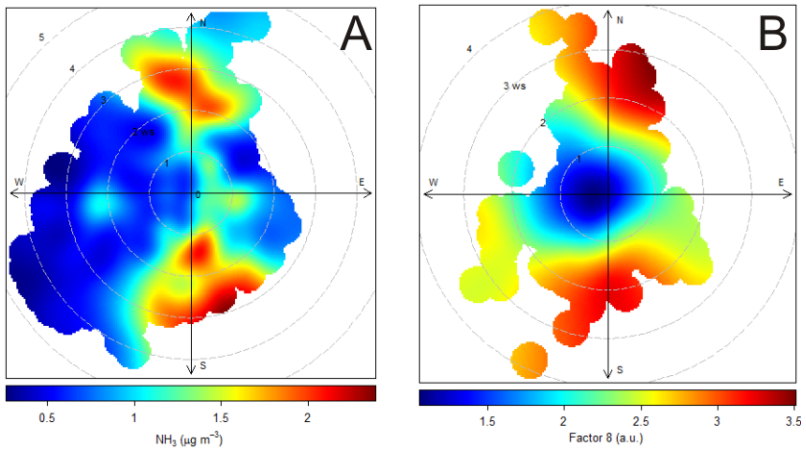

Figure S-10. Bivariate polar plots associated with component 8 for the optimum primary pollutant solution (Table 5). **(A)** NH_3, **(B)** and component 8.

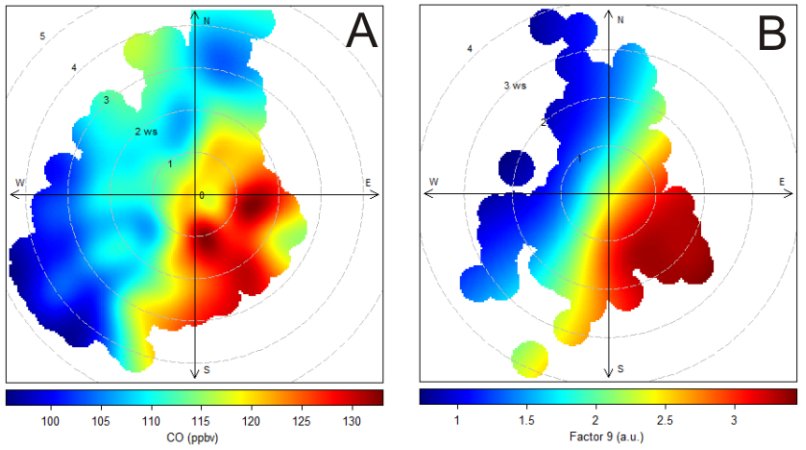

Figure S-11. Bivariate polar plots associated with component 9 for the optimum primary pollutant solution (Table 5). **(A)** CO, and **(B)** component 9.

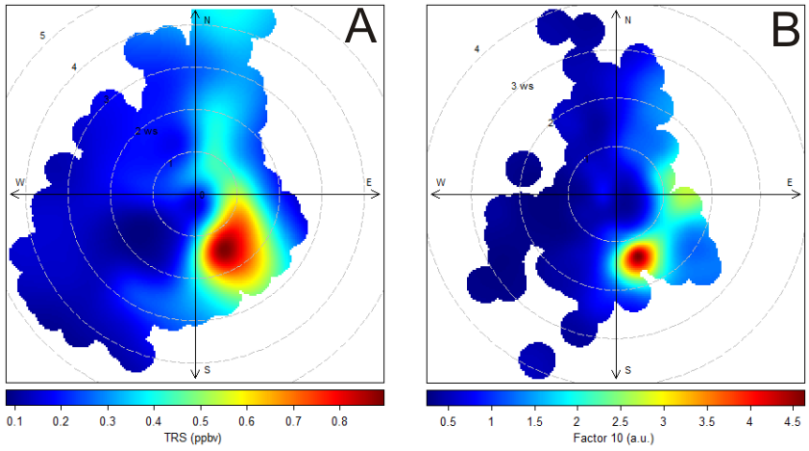

Figure S-12. Bivariate polar plots associated with component 10 for the optimum primary pollutant solution (Table 5). **(A)** TRS, **(B)** and component 10.

References

Bradford, L. M., Ziolkowski, L. A., Goad, C., Warren, L. A., and Slater, G. F.: Elucidating carbon sources driving microbial metabolism during oil sands reclamation, Journal of Environmental Management, 188, 246-254, 10.1016/j.jenvman.2016.11.029, 2017.

Burtscher, H., Scherrer, L., Siegmann, H. C., Schmidtott, A., and Federer, B.: Probing aerosols by photoelectric charging, J. Appl. Phys., 53, 3787-3791, 10.1063/1.331120, 1982.

Bytnerowicz, A., Fraczek, W., Schilling, S., and Alexander, D.: Spatial and temporal distribution of ambient nitric acid and ammonia in the Athabasca Oil Sands Region, Alberta, J. Limnol., 69, 11-21, 10.3274/jl10-69-s1-03, 2010.

Cattell, R. B.: The Scree Test For The Number Of Factors, Multivariate Behavioral Research, 1, 245-276, 10.1207/s15327906mbr0102_10, 1966.

Chen, H., Karion, A., Rella, C. W., Winderlich, J., Gerbig, C., Filges, A., Newberger, T., Sweeney, C., and Tans, P. P.: Accurate measurements of carbon monoxide in humid air using the cavity ring-down spectroscopy (CRDS) technique, Atmos. Meas. Tech., 6, 1031-1040, 10.5194/amt-6-1031-2013, 2013.

ECCC: National pollutant release inventory (NPRI): http://open.canada.ca/data/en/dataset/e40099ae-b116-4c48-9475-f3806fe5a6a6, access: October 5, 2016, 2013a.

ECCC: Measurement instrumentation: carbon dioxide: https://www.ec.gc.ca/mges-ghgm/default.asp?lang=En&n=7903528C-1, access: April 25, 2017, 2013b.

Gorham, E.: Northern peatlands - role in the carbon-cycle and probable responses to climatic warming, Ecol. Appl., 1, 182-195, 10.2307/1941811, 1991.

Hair, J. F., Anderson, R. E., Tatham, R. L., and Black, W. C.: Multivariate data analysis, in, 7th edition ed., Prentice-Hall, Upper Saddle River, NJ, pp. 108 -110, 1998.

509 Holowenko, F. M., MacKinnon, M. D., and Fedorak, P. M.: Methanogens and sulfate-reducing bacteria in
510 oil sands fine tailings waste, Canadian Journal of Microbiology, 46, 927-937, 10.1139/cjm-46-10-927,
511 2000.
512 Huffman, J. A., Treutlein, B., and Pöschl, U.: Fluorescent biological aerosol particle concentrations and
513 size distributions measured with an Ultraviolet Aerodynamic Particle Sizer (UV-APS) in Central
514 Europe, Atmos. Chem. Phys., 10, 3215-3233, 10.5194/acp-10-3215-2010, 2010.
515 Johnson, M. R., Crosland, B. M., McEwen, J. D., Hager, D. B., Armitage, J. R., Karimi-Golpayegani, M., and
516 Picard, D. J.: Estimating fugitive methane emissions from oil sands mining using extractive core
517 samples, Atmos. Environm., 144, 111-123, 10.1016/j.atmosenv.2016.08.073, 2016.
518 Liggio, J., Li, S.-M., Hayden, K., Taha, Y. M., Stroud, C., Darlington, A., Drollette, B. D., Gordon, M., Lee, P.,
519 Liu, P., Leithead, A., Moussa, S. G., Wang, D., O'Brien, J., Mittermeier, R. L., Brook, J., Lu, G., Staebler,
520 R., Han, Y., Tokarek, T. W., Osthoff, H. D., Makar, P. A., Zhang, J., Plata, D., and Gentner, D. R.: Oil
521 Sands Operations as a Large Source of Secondary Organic Aerosols, Nature, 534, 91-94,
522 10.1038/nature17646, 2016.
523 Marey, H. S., Hashisho, Z., Fu, L., and Gille, J.: Spatial and temporal variation in CO over Alberta using
524 measurements from satellites, aircraft, and ground stations, Atmos. Chem. Phys., 15, 3893-3908,
525 10.5194/acp-15-3893-2015, 2015.
526 Markovic, M. Z., VandenBoer, T. C., and Murphy, J. G.: Characterization and optimization of an online
527 system for the simultaneous measurement of atmospheric water-soluble constituents in the gas and
528 particle phases, J. Environ. Monit., 14, 1872-1884, 10.1039/C2EM00004K, 2012.
529 Miller, S. M., Worthy, D. E. J., Michalak, A. M., Wofsy, S. C., Kort, E. A., Havice, T. C., Andrews, A. E.,
530 Dlugokencky, E. J., Kaplan, J. O., Levi, P. J., Tian, H. Q., and Zhang, B. W.: Observational constraints on
531 the distribution, seasonality, and environmental predictors of North American boreal methane
532 emissions, Glob. Biogeochem. Cycle, 28, 146-160, 10.1002/2013gb004580, 2014.

Nara, H., Tanimoto, H., Tohjima, Y., Mukai, H., Nojiri, Y., Katsumata, K., and Rella, C. W.: Effect of air composition (N_2, O_2, Ar, and H_2O) on CO_2 and CH_4 measurement by wavelength-scanned cavity ring-down spectroscopy: calibration and measurement strategy, Atmos. Meas. Tech., 5, 2689-2701, 10.5194/amt-5-2689-2012, 2012.

NPRI: Detailed facility information: http://www.ec.gc.ca/inrp-npri/donnees-data/index.cfm?do=facility_information&lang=En&opt_npri_id=0000002274&opt_report_year=2013, access: April 13, 2017, 2013.

Nwaishi, F., Petrone, R. M., Macrae, M. L., Price, J. S., Strack, M., and Andersen, R.: Preliminary assessment of greenhouse gas emissions from a constructed fen on post-mining landscape in the Athabasca oil sands region, Alberta, Canada, Ecol. Eng., 95, 119-128, 10.1016/j.ecoleng.2016.06.061, 2016.

Odame-Ankrah, C. A.: Improved detection instrument for nitrogen oxide species, Ph.D., Chemistry, University of Calgary, http://hdl.handle.net/11023/2006, 10.5072/PRISM/26475, Calgary, 2015.

Oertel, C., Matschullat, J., Zurba, K., Zimmermann, F., and Erasmi, S.: Greenhouse gas emissions from soils A review, Chem Erde-Geochem., 76, 327-352, 10.1016/j.chemer.2016.04.002, 2016.

Onasch, T. B., Trimborn, A., Fortner, E. C., Jayne, J. T., Kok, G. L., Williams, L. R., Davidovits, P., and Worsnop, D. R.: Soot Particle Aerosol Mass Spectrometer: Development, Validation, and Initial Application, Aerosol Sci. Technol., 46, 804-817, 10.1080/02786826.2012.663948, 2012.

Percy, K. E.: Ambient Air Quality and Linkage to Ecosystems in the Athabasca Oil Sands, Alberta, Geosci. Can., 40, 182-201, 10.12789/geocanj.2013.40.014, 2013.

Phillips-Smith, C., Jeong, C. H., Healy, R. M., Dabek-Zlotorzynska, E., Celo, V., Brook, J. R., and Evans, G.: Sources of Particulate Matter in the Athabasca Oil Sands Region: Investigation through a Comparison of Trace Element Measurement Methodologies, Atmos. Chem. Phys. Discuss., 2017, 1-34, 10.5194/acp-2016-966, 2017.

Quagraine, E. K., Headley, J. V., and Peterson, H. G.: Is biodegradation of bitumen a source of recalcitrant naphthenic acid mixtures in oil sands tailing pond waters?, J. Environ. Sci. Health Part A-Toxic/Hazard. Subst. Environ. Eng., 40, 671-684, 10.1081/ese-200046637, 2005.

Rooney, R. C., Bayley, S. E., and Schindler, D. W.: Oil sands mining and reclamation cause massive loss of peatland and stored carbon, Proc. Natl. Acad. Sci. U.S.A., 109, 4933-4937, 10.1073/pnas.1117693108, 2012.

Shephard, M. W., McLinden, C. A., Cady-Pereira, K. E., Luo, M., Moussa, S. G., Leithead, A., Liggio, J., Staebler, R. M., Akingunola, A., Makar, P., Lehr, P., Zhang, J., Henze, D. K., Millet, D. B., Bash, J. O., Zhu, L., Wells, K. C., Capps, S. L., Chaliyakunnel, S., Gordon, M., Hayden, K., Brook, J. R., Wolde, M., and Li, S. M.: Tropospheric Emission Spectrometer (TES) satellite observations of ammonia, methanol, formic acid, and carbon monoxide over the Canadian oil sands: validation and model evaluation, Atmospheric Measurement Techniques, 8, 5189-5211, 10.5194/amt-8-5189-2015, 2015.

Small, C. C., Cho, S., Hashisho, Z., and Ulrich, A. C.: Emissions from oil sands tailings ponds: Review of tailings pond parameters and emission estimates, Journal of Petroleum Science and Engineering, 127, 490-501, 10.1016/j.petrol.2014.11.020, 2015.

Thompson, R. L., Sasakawa, M., Machida, T., Aalto, T., Worthy, D., Lavric, J. V., Myhre, C. L., and Stohl, A.: Methane fluxes in the high northern latitudes for 2005-2013 estimated using a Bayesian atmospheric inversion, Atmos. Chem. Phys., 17, 3553-3572, 10.5194/acp-17-3553-2017, 2017.

Tokarek, T. W., Huo, J. A., Odame-Ankrah, C. A., Hammoud, D., Taha, Y. M., and Osthoff, H. D.: A gas chromatograph for quantification of peroxycarboxylic nitric anhydrides calibrated by thermal dissociation cavity ring-down spectroscopy, Atmos. Meas. Tech., 7, 3263-3283, 10.5194/amt-7-3263-2014, 2014.

Tokarek, T. W., Brownsey, D. K., Jordan, N., Garner, N. M., Ye, C. Z., Assad, F. V., Peace, A., Schiller, C. L., Mason, R. H., Vingarzan, R., and Osthoff, H. D.: Biogenic Emissions and Nocturnal Ozone Depletion

581 Events at the Amphitrite Point Observatory on Vancouver Island, Atmosphere-Ocean, 1-12,
582 10.1080/07055900.2017.1306687, 2017.
583 Wang, X. L., Chow, J. C., Kohl, S. D., Percy, K. E., Legge, A. H., and Watson, J. G.: Characterization of
584 PM2.5 and PM10 fugitive dust source profiles in the Athabasca Oil Sands Region, J. Air Waste Manag.
585 Assoc., 65, 1421-1433, 10.1080/10962247.2015.1100693, 2015.
586 Warner, D. L., Villarreal, S., McWilliams, K., Inamdar, S., and Vargas, R.: Carbon Dioxide and Methane
587 Fluxes From Tree Stems, Coarse Woody Debris, and Soils in an Upland Temperate Forest, Ecosystems,
588 10.1007/s10021-016-0106-8, 2017.
589 Warren, L. A., Kendra, K. E., Brady, A. L., and Slater, G. F.: Sulfur Biogeochemistry of an Oil Sands
590 Composite Tailings Deposit, Front. Microbiol., 6, 14, 10.3389/fmicb.2015.01533, 2016.
591 Wesely, M. L., and Hicks, B. B.: A review of the current status of knowledge on dry deposition, Atmos.
592 Environm., 34, 2261-2282, 10.1016/S1352-2310(99)00467-7, 2000.
593 Whalen, S. C.: Biogeochemistry of methane exchange between natural wetlands and the atmosphere,
594 Environ. Eng. Sci., 22, 73-94, 10.1089/ees.2005.22.73, 2005.
595 Whaley, C. H., Makar, P. A., Shephard, M. W., Zhang, L., Zhang, J., Zheng, Q., Akingunola, A., Wentworth,
596 G. R., Murphy, J. G., Kharol, S. K., and Cady-Pereira, K. E.: Contributions of natural and anthropogenic
597 sources to ambient ammonia in the Athabasca Oil Sands and north-western Canada, Atmos. Chem.
598 Phys., 18, 2011-2034, 10.5194/acp-18-2011-2018, 2018.
599 Wilson, N. K., Barbour, R. K., Chuang, J. C., and Mukund, R.: Evaluation of a real-time monitor for fine
600 particle-bound PAH in air, Polycycl. Aromat. Compd., 5, 167-174, 10.1080/10406639408015168,
601 1994.
602 Yavitt, J. B., Williams, C. J., and Wieder, R. K.: Soil chemistry versus environmental controls on
603 production of CH_4 and CO_2 in northern peatlands, Eur. J. Soil Sci., 56, 169-178, 10.1111/j.1365-
604 2389.2004.00657.x, 2005.

605 Zhang, L. M., Brook, J. R., and Vet, R.: On ozone dry deposition - with emphasis on non-stomatal uptake
606 and wet canopies, Atmos. Environm., 36, 4787-4799, 10.1016/s1352-2310(02)00567-8, 2002.
607
608